The Analysis Of Bolted Plate Splices.

THE ANALYSIS

OF

BOLTED PLATE SPLICES

by

John William Fisher

A Dissertation

Presented to the Graduate Faculty

of Lehigh University

in Candidacy for the Degree of

Doctor of Philosophy

Lehigh University

1964

Approved and recommended for acceptance as a dissertation in partial fulfillment of the requirements for the degree of Doctor of Philosophy.

Jan 6, 1964
(Date)

Lynn S. Beedle
Professor in Charge

Accepted. Jan 20, 1964
(Date)

Special Committee directing the
doctoral work of John W. Fisher

Professor Theodore V. Galambos
Chairman

Professor William J. Eney

Professor Alan S. Pense

Professor Clarence A. Shook

Professor Lynn S. Beedle

ACKNOWLEDGEMENTS

The author wishes to express his appreciation for the helpful suggestions and criticisms made by a number of the research personnel at Fritz Engineering Laboratory while various parts of the development presented in this dissertation were in preparation. In particular he thanks his colleagues on the Large Bolted Connections Project, Messrs. P. O. Ramseier, R. J. Christopher and J. J. Wallaert.

The supervision, encouragement, and critical review of this work by Dr. Lynn S. Beedle, Professor in charge of the dissertation, are sincerely appreciated. The interest of Professors Theodore V. Galambos, William J. Eney, Alan S. Pense, and Clarence A. Shook, Chairman and members of the special committee directing the author's doctoral work, is gratefully acknowledged.

The dissertation covers parts of the research project on large bolted connections being conducted at Fritz Engineering Laboratory, Department of Civil Engineering, Lehigh University. Professor William J. Eney is head of the Department and of the Laboratory.

The project is sponsored financially by the Pennsylvania Department of Highways, the U. S. Department of Commerce - Bureau of Public Roads and the American Institute of Steel Construction. Technical guidance has been provided by the Research Council on Riveted and Bolted Structural Joints through an advisory committee under the chairmanship of Dr. J. L. Rumpf.

The manuscript was typed by Miss Grace Mann and Miss Valerie Austin

and the drawings were prepared by Messrs. R. Sopko, H. A. Izquierdo and R. J. Weiss. Their help has been invaluable. The author is also appreciative of the encouragement and help provided by his wife Nelda.

TABLE OF CONTENTS

A B S T R A C T

In this dissertation a theoretical solution is developed for the unequal distribution of load among the mechanical fasteners of bolted double-lap tension splices which act in a non-linear manner. To accomplish this solution, mathematical models have been developed which establish the relationship between deformation and load throughout the elastic and inelastic regions for the component parts of the connections.

The solution has been used to make a number of hypothetical studies in order to ascertain the relative importance of a number of parameters on the ultimate strength of the connections. Among the variables studied were joint length, pitch, variation in fastener diameter, and variation in the relative proportions of the bolt shear area and net tensile area.

The theoretical solution has been compared with test results of eight full-size connections using 7/8-inch A325 bolts and A7 steel plate and seven full-size connections using 7/8-inch A325 bolts and A440 steel plate. The maximum deviation between the theoretical solution and the test results was 4%.

The results of the theoretical studies show that the average shear strength decreases with increasing joint length for both A7 and

A440 steel joints. However, the higher yield strength steels effect a better redistribution of the bolt forces with increasing joint length. Fastener diameter was found to have no significant effect on the average shear strength. The fastener pitch was found to have no appreciable effect on the shear strength other than its interaction with joint length. The total joint length, and not the number of fasteners (governed by pitch), was the most important variable insofar as the average shear strength was concerned.

The study of the variation in the relative proportions of the bolt shear and the net tensile areas showed that the "balanced design" concept has no meaning. A joint can only be in balance for a specified length which corresponds to a specific ratio of the bolt shear area and net tension area.

It has shown that the average shear stress at failure for A325 bolts is the same when installed in compact joints of A7 or A440. With increasing joint length, a decrease in the bolt shear strength was evident. This decrease was greatest for the A7 steel joints. In both steels the decrease was dependent on the relative proportions of the bolt shear area and net tension area.

INTRODUCTION

1.1 CRITERION FOR BEARING-TYPE CONNECTIONS

In recent years high-strength steels have continued to be developed for structural applications. Progress in the use of high-strength steels has been a function of the connecting methods employed. Mechanical fasteners, whether rivets or bolts, are integral elements in the connecting process.

Riveted joints of considerable size have been used for many years in the construction of large steel bridge structures. Early work with riveted joints showed that rivets had an ultimate shear strength which was about 75% of their tensile strength[1]. Since the tensile strength of A141 steel rivets (58 to 62 ksi) was about equal to the ultimate strength of A7 steel plates, it was reasonable that the allowable shear stress should be set at approximately 75% of the allowable tensile stress. As a result, the "tension-shear ratio" and "balanced design" concepts came into being and were accepted by the profession. The "tension-shear ratio" is the ratio of the tensile stress on the net section of the plate to the shear stress on the nominal area of the fastener. The concept of balanced design meant that the ultimate strength of the fasteners in shear should equal the tensile capacity of the net section of the main material.

The introduction of the A325 bolt as a replacement for the A141 steel rivet was first made on the basis of one bolt for one rivet[2]. Since the shear strength of the bolt was greater than the rivet, the A325 bolted joint was no longer in "balance". Tests were subsequently conducted on compact bolted joints to determine the proper ratio of the shear area and net tension area for balanced design[3]. It was shown in these studies that the proper tension-shear ratio was 1 to 1.10 for A325 bolts in A7 steel joints. The corresponding ratio for A141 steel rivets in A7 steel has been 1 to 0.75.

The balanced design concept was also used in tests to determine the relative proportions of shear and net areas when A325 bolts were used to connect A440 steel plates[4]. From this work the balanced design concept yielded a tension-shear ratio of 1 to 1 for A325 bolts in A440 steel joints. The results of these investigations implied that when the A325 bolt was installed in A7 steel, an allowable design stress of 22 ksi should be used. When the bolt was installed in A440 steel, balanced design would yield an allowable shear stress of 27.5 ksi.

This result, incidentally, poses an interesting question in design philosophy: How can different allowable shear stresses in a fastener be justified because the fastener is used in different materials? These aspects have been reviewed and discussed in Ref. 5. This examination showed that:

(1) the concept of balanced design leads to inconsistent allowable bolt stresses for different plate materials for the same bolt;

(2) the A325 bolt behaves similarly under shear in a compact joint regardless of the type of connected material; and

(3) the balanced design concept has no meaning in long joints because the bolts unbutton before the plate material can attain its full strength.

A more logical criterion for design would result if the factor of safety were fixed against the shear strength of the fastener[5]. Clearly this proposed philosophy is more logical and consistent and would result in a more uniform factor of safety as well as safe and economical construction.

Certain limitations remain, some as a result of the differing philosophy and others from the lack of knowledge. Among these are the behavior of A7 and A440 steel joints of considerable length connected with A325 bolts; the behavior and performance of constructional alloy steel joints fastened with A325 bolts; and the behavior and performance of joints fastened with new or different structural fasteners such as the A490 bolt. As a result of these questions, a need existed for a theoretical approach that would enable one to ascertain the relative significance of varying these and other parameters such as variations in the relative proportions of the bolt shear area and net tensile area; the effect of fastener pitch; the effect of bolt diameter; and the particularly significant influence of joint length as it interrelates with all of these variables.

1.2 BEHAVIOR OF DOUBLE-LAP BUTT JOINTS

The behavior of mechanically fastened double-lap butt joints, whether they are riveted or bolted is basically the same. From tests reported in Refs. 1, 3, 4 and 6 the following descriptions of the joint behavior have evolved. Two distinct phases are involved: one, before slip, in which the principal load transfer mechanism is one of friction between the faying surfaces, and the other in which the principal load transfer mechanism is one of bearing. Figure 1 shows the behavior of a typical joint under load. The regions corresponding to the two major load transfer phases are also indicated in Figure 1. The load transfer is due to friction prior to major slip. After slip the load transfer mechanism is primarily due to bearing.

Both riveted and bolted joints generally exhibit each of these load transfer mechanisms. In riveted joints one can seldom predict when the load transfer mechanism is going to change. The tests reported in Refs. 1, 3 and 6 have shown that the two phases do exist. However, it is well known that the clamping force in the rivet cannot be predicted reliably and in fact may not exist.

The behavior of a bolted joint during its loading history was described in some detail by Rumpf[7]. The load history was divided into phases which included (a) complete interaction of the connected parts; (b) partial slip; (c) complete slip; (d) partial bearing; (e) complete bearing and (f) bolt shear and unbuttoning.

Only a summary of the phases which make up the loading history

of a mechanically fastened joint is given here. A more detailed description is given in Ref. 7. Phases a, b and c fall under the category of load transfer by friction and phases d, e and f fall under the category of load transfer by bearing.

1. Load Transfer by Friction

After bolts or rivets are installed in a joint, a clamping force is present which compresses the connected plies. The magnitude of the clamping force may vary considerably as in a riveted joint, or it may be relatively uniform as in a bolted joint. Under initial loading there is usually no relative displacement of the faying surfaces, and the joint behaves much like a solid piece of metal. The plates undergo shear deformations due to the frictional forces acting on the faying surface; however, these deformations are very small and have no influence on the joint behavior.

A theoretical and experimental study on the frictional load transfer in bolted joints[8] has shown that higher frictional stresses exist at the joint ends because of the strain compatibility condition. For example at one end of the joint the main plate is carrying a high load while the adjacent lap plates have relatively low loads. As a result, there is a relative displacement of certain discreet points on the faying surfaces near the ends of the joint. When the load is increased, the slip zone proceeds inward from the ends of the joint. Eventually, the slip zones cover the entire faying surface with a resulting maximum static frictional resistance. Any increase in load

cannot be balanced and large relative displacements occur until the fasteners come into bearing with the sides of the holes.

The above description covers phases a, b and c and describes the frictional load transfer mechanism.

Even with all holes in perfect alignment, some of the bolts may be touching the sides of the holes. As a result, "complete" slip does not occur, and as additional load is applied gradual slipping occurs until all bolts are in complete bearing. Generally the plate accelerations are so large that the only way to stop the slip is for one plate to encounter bolts which are bearing against the other plate.

2. Load Transfer by Bearing

After slip has occurred, several of the fasteners are in bearing, being in contact with the main plate on one side of the fasteners and with the lap plates on the other. Unless some of the holes are misaligned, the end fasteners come into bearing first because the greatest differential elongations have occurred there. Generally, both the fastener and the plate are elastic at this point.

Before coming into bearing the only force acting on the fastener was its initial tension. As the fastener comes into contact it tends to shear, bend, and deform by bearing with a resulting relaxation in its initial tension. In addition, the plate tends to deform locally at its points of contact with the fastener. As load is applied the end fasteners and holes deform until succeeding fasteners come into bearing.

When the joint has more than two fasteners in a line, the plate deformations influence the load partition among the mechanical fasteners.

Once all fasteners are in bearing, additional load causes further plate deformations which impose compatible deformations in the fasteners. The deformations result in additional bolt forces. The deformations are dependent on the difference in the elongations of the lap plate and the main plate between any two rows of fasteners as elastic and inelastic analysis have shown. If the plate material were perfectly rigid, each fastener would deform the same amount and presumably would carry an equal share of the load.

Irrespective of whether the plate or the fasteners deform permanently first, eventually the accumulated differential strains between the main plate and the lap plate exceed the deformation capacity of the fasteners and failure is precipitated. If the joint is reasonaly compact, the fasteners all will have approached their maximum load carrying capacity. As one or more end bolts fracture, the load cannot be redistributed as all are carrying a maximum, and all fasteners shear nearly simultaneously. For longer joints the accumulated differential deformations cause the end fasteners to fail but their load is redistributed to the other fasteners. A reloading is required and a sequential type of failure occurs progressing inward from the ends of the joint. This phenomenon of sequential failure of the fasteners is called "unbuttoning".

If the plate strength at the net section is considerably less than the shear strength of the fasteners, failure will invariably occur by tearing of the plate for compact and intermediate length joints. This behavior will depend on the relative proportions of the shear and tensile areas. The fasteners in this case have sufficient deformation capacity unless the joint has considerable length. When the plate strength at the net section is considerably larger than the shear strength of the fasteners, the perfectly rigid case is approached.

After slip has occurred and the joint is in bearing, undoubtedly some load transfer is taking place by frictional forces. However, as the fasteners undergo permanent deformation at their shear planes, a relaxation in the initial clamping force occurs. Observations and measurements made during testing of large bolted connections have shown that the bolts experienced a loss in preload after major slip had occurred and the fasteners were in bearing[9]. All bolts except those in the end rows at the lap plate end tended to show a continuous decrease in their internal bolt tension until practically no clamping force existed near the ultimate load.

1.3 SUMMARY OF THEORETICAL STUDIES

An extensive review of previous theoretical studies of mechanically fastened joints was given in Ref. 7. This review is summarized briefly here and extended to include other studies.

Most of the past theoretical studies of mechanically fastened joints have considered only the elastic or linear range of behavior between load and deformation. The first known study was Arnovlevic[10] in 1909. This was followed by the work of Batho[11], Bleich[12], Hrennikoff[13] and Vogt[14]. These studies showed that the end fasteners carried the greatest percentage of load and that not much was gained in the elastic range by adding additional fasteners because the interior fasteners were practically useless.

Vogt[14] was among the first to propose an extension of the elastic studies into the inelastic and non-linear region. This analysis was restricted since it considered the non-linear deformations to occur in the fasteners and holes alone. The combined load-deformation characteristics of the fastener and hole were assumed to be represented by two linear relationships. This work was followed by an extensive study on aluminum riveted joints by Francis[15]. He considered the behavior of double shear joints in the elastic range and beyond. Equilibrium and compatibility conditions were formulated and the partition of load was determined. Also described was a semi-graphical construction which facilitated the solution of the load partition in the inelastic regions.

Rumpf[7] adapted the methods described by Francis[15] to bolted bearing-type joints of A7 steel and A325 bolts. The solution was found to be applicable to the region from the slip load up to the ultimate load. Excellent correlation between the theoretical values and the experi-

mental data was obtained.

The semi-graphical construction used by Francis[15] and Rumpf[7] is convenient to use when only short joints are analyzed. However, the solution remains as an interative type and usually several trials are required before the solution is obtained. When longer joints are involved the analysis can become extremely tedious and time consuming, if not impossible to use.

1.4 SUMMARY OF EXPERIMENTAL STUDIES

A considerable amount of experimental work has been conducted on bolted and riveted joints. In general, most of these tests were on small scale specimens; only a few large tests have been conducted. The tests of riveted joints have been summarized by DeJonge[16]. The summaries given hereafter are for tests on large butt-splice specimens connected by rivets or bolts.

In 1940, Davis, Woodruff and Davis[1] reported on an extensive series of tests of large riveted joints. These tests were conducted in connection with the design and construction of the San Francisco-Oakland Bay Bridge. They reported instances in which premature fastener failure occurred in joints of considerable length connected with 7/8-in. rivets. They pointed out that excessive deformation caused the end fasteners to fail.

In 1957, a demonstration test of a compact A242 high-strength steel specimen connected by nine A325 and nine A354BD bolts was performed at Northwestern University[17]. The joint was proportioned such that plate failure occurred.

The University of Washington[18] reported an unbuttoning failure in a connection having thirteen rows of A325 bolts. Several other compact specimens were tested and failed by a shearing of the bolts.

Static tension tests of large compact butt joints conducted at Lehigh University[3] showed that the end fasteners had a tendency to fail prematurely. However, these tests were conducted on specimens with lengths no greater than 14-inches. As a result, the average shear stress at first bolt failure was not greatly affected by the joint length.

Because of the premature failure of the end fasteners, additional tests were conducted at Lehigh University on long bolted connections[6]. In these tests the net tension area was 10% greater than the bolt shear area. All joints were fabricated of A7 steel and most were connected by 7/8-in. A325 bolts. In longer joints the end fasteners sheared before all bolts could develop their full shearing strength. In the short connections the average shear strength was about 90% of the strength of a single bolt, but bolts in the longest connection developed only 60% of the strength of a single bolt. Limited tests of bolted lap joints provided information on the behavior of bolts in single shear.

In addition, several tests of riveted connections provided a basis for comparing bolted and riveted connections.

More recently, tests of structural joints of A440 steel connected by A325 high-strength bolts were conducted at Lehigh University[4]. The joints had from 4 to 16 fasteners in a line. These tests showed that the shear strength of bolts in compact A440 joints did not differ significantly from the compact A7 steel joints. For the longer joints, the decrease in shear strength was not nearly as great as was experienced in A7 steel joints.

The tests reported in Refs. 3, 4 and 6 are compared with theory in Art. 4.

1.5 OBJECTIVE OF THIS STUDY

The continued introduction of new materials such as high-strength steels and low alloy-bolts and rivets, makes it desirable to have a general theoretical solution for the behavior of mechanically fastened joints. Such a solution should have the capability of examining a wide range of parameters that might influence the strength of a joint.

Among the variables to be studied are:

(1) the effect of bolt diameter;

(2) the effect of fastener pitch;

(3) the effect of variations in the relative proportions of the bolt shear and the net tensile area; and

(4) the influence of joint length which interacts with each of these variables.

This study will attempt to broaden the theoretical analysis of the static behavior of bolted double-lap tension splices which act in a non-linear manner. Suitable mathematical models are developed which establish the relationship between deformation and load throughout the elastic and inelastic regions for the component parts of the joints.

For the complex problem involved, the application of the electronic computer to the general analysis will greatly simplify and improve the computational effort which becomes almost prohibitive by the manual and graphical methods now employed. This will enable a comprehensive study of the many variables that effect the joint performance and behavior. The computer is well suited for this problem because its logic and information processes are particularly useful when called upon to assist in making choices between large amounts of information and alternate solutions.

2. DEVELOPMENT OF THEORETICAL SOLUTION

2.1 SCOPE OF INVESTIGATION

This investigation is concerned primarily with developing a solution for joints in which the mechanical fasteners are in a state of double shear.

The theoretical work of Francis[15] and Rumpf[7] is used as a foundation. Analytical expressions are developed for the load-deformation behavior of plate material and of the mechanical fasteners. These expressions are general in that they accommodate a range of parameters such as varying types of steel and different geometric configurations.

The theoretical solution of the load partition is based on the assumption that (1) the mechanical fasteners transmit all the applied load by shear and bearing once major slip has occurred; (2) the frictional forces may be neglected in the region for which the solution is intended (between major slip and the ultimate load). The validity of these assumptions will be discussed later.

2.2 EQIULIBRIUM AND COMPATIBILITY RELATIONSHIPS

The type of connection dealt with is a double shear symmetrical butt joint as shown in Fig. 2. The inner plate, hereafter called the main plate, is the principal member. The outer plates are denoted as

the lap plates. The longitudinal line of holes parallel to the axial load is called a line and the space between each hole is called a pitch. The transverse series of holes is called a row and the space between transverse holes is called the gage.

The lap plates are assumed to be of the same thickness and material. However, the main plate may be of different material and may have any thickness. The hole pattern is assumed to be completely filled and the bolts are assumed to be of the same size and material. For purposes of analysis, the joint is divided into gage strips as shown in Fig. 3. It is assumed that all gage strips are identical in behavior.

As was pointed out in Art. 2.1, the fasteners are assumed to transmit all applied load by shear once major slip has occurred. Such an assumption can be satisfied only if perfectly aligned holes are present. The solution would be valid equally for a joint erected in bearing and for a joint which was slipped into bearing.

The analysis consists basically of considering the joint as a statically indeterminate structure. Very similar analyses were used in Refs. 10, 12, 13 and 14, for elastic conditions alone. The analysis given here is equally applicable to the inelastic case and is made possible through a consideration of the non-linear behavior of the components.

The solution of the problem follows the method of ordinary mechanics. Two basic conditions must be formulated. One satisfies the condition of equilibrium (statics) and the other insures that continuity (or compatibility) will be maintained throughout the elastic and inelastic ranges. These conditions coupled with the initial value considerations such as the ultimate strength of the plate or the ultimate strength of the critical fastener yield the solution to the problem.

The equilibrium conditions can be visualized with the aid of Fig. 4. The load per gage strip in the main plate between bolts i and i+1 is equal to the total load on this strip, P_G, minus the sum of the loads on all bolts ($\sum R_i$) proceding the part of the joint considered. Hence between i and i+1

$$P_{i,\ i+1} = P_G - \sum_{i=1}^{i} R_i \tag{1}$$

The load per gage strip in the lap plates between bolts i and i+1 is equal to the sum of the loads transmitted to the lap plate by all the bolts preceding the part of the joint being considered. Hence,

$$Q_{i,\ i+1} = \sum_{i=1}^{i} R_i \tag{2}$$

The compatibility conditions described hereafter consider the joint in the slipped position so that the fasteners are in contact with

the plate. The inner and outer plates have already moved an amount equal to the hole clearance.

The compatibility equations that correspond to the equilibrium equation described by Eqs. 1 and 2 will be formulated by considering Fig. 5. As load is applied to the slipped joint the deformations are considered within the joint at points i and i+1 (Fig. 5). Due to the applied load, the main plate will have elongated so that the distance between the main plate holes is $p + e_{i,i+1}$. The lap plate will have elongated and its distance will be given by $p + e'_{i,i+1}$. The distance p is the fastener pitch as shown in Fig. 2. The elongations $e_{i,i+1}$ and $e'_{i,i+1}$ refer to the main plate and lap plate respectively. They are the elongations between points i and i+1. Hereafter, a primed symbol will be associated with the lap plates. An equation can be formulated by considering the total length of the lap and main plates between points i and i+1 and the deformations of the fasteners. From Fig. 5 it can be seen that

$$\Delta_i + p + e'_{i,i+1} = \Delta_{i+1} + p + e_{i,i+1} \tag{3}$$

or

$$\Delta_i + e'_{i,i+1} = \Delta_{i+1} + e_{i,i+1} \tag{4}$$

where Δ_i and Δ_{i+1} are the deformations of the i and i+1 fasteners. They include the effects of shear, bending, and bearing of the fastener and the localized effect of bearing on the plates. Further discussion

of these parameters is given in Article 2.4, where the load-deformation relationship of single fasteners is developed. It is assumed that the deformations of the fastener Δ_i are the same whether considered at the hole edge (fastener surface) or the centerline of the fastener.

Because of inelastic behavior the circular holes change to oval ones and allow movement of the fasteners. Rumpf has shown[7] that this is taken into account by the plate deformation relationship. The elongation needed is that occurring from the edge of one hole to the corresponding edge of the next hole.

If the plate elongations are expressed as functions of load in the segments of the joint between fasteners, and the fastener deformations as functions of the fastener loads, Eq. 4 can be written as

$$f\left[R_i\right] + \Psi\left[Q_{i,i+1}\right] = f\left[R_{i+1}\right] + \emptyset\left[P_{i,i+1}\right] \tag{5}$$

where $f\left[R_i\right]$, $f\left[R_{i+1}\right]$ are bolt deformations, $\emptyset\left[P_{i,i+1}\right]$ is the main plate elongation and $\Psi\left[Q_{i,i+1}\right]$ is the lap plate elongation. Finally Eqs. 1 and 2 can be substituted into Eq. 5 and the compatibility equations are finally expressed as functions of the unknown bolt forces. Hence,

$$f\left[R_i\right] + \Psi\left[\sum_{i=1}^{i} R_i\right] = f\left[R_{i+1}\right] + \emptyset\left[P_G - \sum_{i=1}^{i} R_i\right] \tag{6}$$

In the elastic or inelastic range of load for a joint having n fasteners in line, Eq. 6 can be written for each section of the joint,

giving n-1 simultaneous equations. These, with the equation of equilibrium

$$P_G - \sum_{i=1}^{n} R_i = 0 \qquad (7)$$

may be solved to give the loads acting on the fasteners if the relationship between load and elongation for the various components is known. With this information the total load acting on the joint may be determined for a given deformation, and finally the load at failure may be determined.

The two basic load-deformation relationships required, then, are that of the plate with holes and that of the fastener. These become the standard "coupons" which will be the basis for predicting joint behavior. These coupons and the analytical models describing them are the subject of Arts. 2.3 and 2.4

2.3 TENSILE STRESS-STRAIN RELATIONSHIPS FOR PLATE MATERIALS

1. Plates in Tension

A plate in tension having one or more holes is an integral part of a mechanically fastened joint. As was indicated in Art. 2.2 the true nature of the load-deformation relationships for the bolt and plates must be known if Eqs. 6 and 7 are to be solved. These relationships must first be established by experiments.

The "standard plate calibration coupon" which yields the load-deformation relationship for the connected plate is shown in Fig. 6. The results of this coupon test are needed to relate the behavior of portions of the gage strips shown in Fig. 3 when subjected to tensile loads. The "plate calibration coupon" should be cut from the same material used to fabricate the actual test connections. Its geometrical properties should also be similar; the thickness, gage, pitch, and hole diameter must be the same as used in the test connections or prototype connections.

If a ductile polycrystalline metal bar is loaded continuously and the resulting stresses are plotted as a function of the strain the characteristic stress-strain relationship shown in Fig. 7 is observed.* This curve is characteristic of most steels with structural applications. The material first stretches elastically until the load reaches a certain value at which permanent deformations start to develop. After a short transition curve from the elastic to the plastic range of strains, a relatively flat plateau exists during which the bar continues to stretch without any appreciable change in load. When the strain is about ten times the yield strain the material begins to strain-harden and additional strain produces an increase in load. This increase continues until the ultimate tensile strength is reached. Thereafter, the material begins to neck and finally ruptures.

---

* The data is plotted to two different longitudinal scales to more clearly describe the behavior in the plastic region.

When the "standard plate calibration coupon" is loaded continuously and the average stresses at the net section are plotted as a function of the average strain occurring between the two holes, the stress-strain relationship shown in Fig. 8 is observed. The material first stretches elastically until the load reaches a certain value at which permanent deformation starts to develop around the holes. However, unlike the standard flat bar coupon, the test curve indicates that this flat plateau does not exist. Strain-hardening begins almost immediately and additional strain is accompanied by an increase in load. This continues until the ultimate tensile strength of the material is reached at the net section. The material has necked considerably at the net section and the specimen ruptures almost invariably at the ultimate load.

The presence of holes in a steel plate influences the stress-strain relationship as can be seen by comparing the results of the "standard plate calibration coupon" with the stress-strain relationship of the standard flat bar coupon. This comparison is made in Fig. 9. Elastic studies have shown that the effect of the stress concentration at the holes is not uniformly distributed around the hole, but occurs at discreet points on the boundary of the hole[19] as shown schematically in Fig. 10a. The contour lines of radial stress computed according to elastic theory are shown. In Fig. 10b the stresses perpendicular to line A-A are shown and compared with the stresses in the bar some distance from the hole. As a result of the stress concentrations around the hole first yield starts at these points of maximum stress situated on the boundary. As the tensile stress is increased, yielding spreads

and very soon tends to progress along two comparatively narrow strips symmetrically situated with respect to the axis of load, and at an angle of approximately 45 degrees with the direction of the load[19,20] as shown in Fig. 11a.

For many pitches and gages, the yield strips which form symmetrically about adjacent holes will overlap as indicated in Fig. 11b. Because of this, there is interference of the slip bands. The necessity for compatibility at grain boundaries requires that slip occur on several slip systems. This causes severe deformation of the crystal lattice of each grain which results in the stress rising continuously with increasing strain.

A number of investigators have developed analytical models for the plain plate. Hollomon[21] developed an expression for the relationship between true stress and natural strain. Nadai[22] proposed an analytical expression for the conventional stress-strain curve for use in studies of plastic buckling. Later Ramberg and Osgood[23] suggested a slightly different analytical expression. Unfortunately, none of these analytical models are suitable for the "standard plate calibration coupon" as they are unable to account for the variations in material properties or plate geometry and they do not fit the test data.

The semi-graphical solution used by Francis[15] and Rumpf[7] utilized the actual stress-strain relationship for the "standard plate calibration coupon". For long joints the semi-graphical analysis be-

comes extremely tedious and time consuming, if not impossible to use. There is a need therefore to develop an "analytical model" which will describe the stress-strain behavior of the plate calibration coupon throughout the elastic and inelastic ranges. Ideally this model should account for variations in material properties and the plate geometry.

2. Development of Stress-Strain Relationship

In order to establish the behavior of the plate element in a bolted joint, the stress-strain relationship of the material was determined from a "standard plate calibration coupon" as shown in Fig. 6. The data from such a test was plotted in Fig. 8. The response of the plate calibration coupon can be idealized as shown in Fig. 12. Under initial loading the material remains elastic and the strain increases in a linear manner until point B is reached. Above point B the strain ceases to increase linearly with the applied stress.

The primary criterion in the choice of a suitable analytical model which will define the stress-strain relationship of the plate calibration coupon is the degree of correlation between the observed test data and the corresponding values calculated from the analytical expression. If possible, it is desirable to obtain a single general relationship which will take into account the physical and geometrical factors which influence the stress-strain relationship.

Among the variables influencing the stress-strain relationship of the plate calibration coupon are:

(1) the width or gage of the plate g;

(2) the hole diameter d;

(3) the spacing or pitch of adjacent holes p;

(4) the ultimate tensile strength of the coupon σ_u;

(5) the yield point of the coupon σ_y;

(6) the speed of testing the plate calibration coupon; and

(7) the different types or grades of steel.

The relative proportions of the net plate area to the gross plate area, governed by the dimensions g and d, may be expected to influence the shape of the stress-strain curve (see Fig. 8). In a plate having a large width, g, the hole, if small, could be expected to have little influence on the average stress-strain relationship. However, with increasing plate width g, the restraint to necking is greater as one would expect.

When the hole spacing, p, is close, interference can be expected between the slip bands. As was pointed out earlier this will also influence the stress-strain curve. As the holes become farther apart, their effect on the deformation occurring between the two holes is probably decreased. Hence, one would expect the plate calibration coupon to approach the behavior of the standard coupon without holes.

In a bolted or riveted joint, the variables g, d, and p will be limited to practical ranges. Minimum gage and pitch distances are usually specified. If not, a relative minimum can be estimated from the dimensions of the fasteners. The maximum dimensions of pitch and gage, if not specified, can be estimated from practical considerations.

Residual stresses and stress concentrations in the vicinity of the holes will cause nonlinearity to occur in the plate calibration coupon before the yield point of the standard bar coupon is reached. Observations of the test data indicated that the point of deviation from linearity was approximately equal to the static yield point of the standard coupon test. Hence, the influence of residual stress and stress concentrations can be accounted for by using this lower yield value.

The ultimate strength of the perforated plates at the net section is usually higher than the coupon ultimate strength of the main plate. It is well known from early experimental work that the "ultimate strength" of a cylindrical bar having a short circumferential groove is considerably higher than the ultimate strength of a round bar because of the prevention of normal necking in the constricted portion[20]. It is to be expected that a similar behavior will occur in a flat plate having a hole. The free lateral contraction which must accompany an axial extension cannot develop and a higher ultimate strength results.

This behavior was reported in Ref. 24 in work on riveted joints. It was found, particularly at the smaller gage or rivet spacings, that the strength was greater than one normally would expect on the basis of the joint geometry. The cause was attributed to the "reinforcement" or bi-axial stress effect created by the closely spaced holes. As the gage is increased, this effect is less noticeable. Additional information on this behavior is given in Ref. 25 when discussing the "efficiency coefficient".

The ratio of the ultimate strength of the plate calibration coupon is compared with the mean ultimate strength of the same material given by standard laboratory bar coupon tests in Fig. 13. The ratio is seen to be greater with the A440 steel. In general, the behavior of these test specimens was similar to the behavior reported by other investigators.

The dynamic stress-strain relationship is used because the analytical model is needed to aid in predicting the ultimate strength of the bolted joints. Generally these joints fail when load is being applied and the effect of speed of testing is present in the test results.

The following assumptions were made relative to the development of a suitable analytical relationship based in part upon the above mentioned influencing factors:

(1) Stress is proportional to strain when the strain is less than the yield strain.

(2) The average computed elastic strain is based on the gross section area.

(3) The deviation from linearity in the plate calibration coupon can be approximated by the static yield point of the standard bar coupon.

(4) The stress-strain relationship beyond the elastic limit is based on the dynamic stress-strain measurements of the plate calibration coupon.

(5) At $\epsilon_y < \epsilon < \epsilon_{ult}$, the stress σ increases at a decreasing rate as the stress approaches the ultimate strength.

(6) The average computed stress beyond the elastic limit is calculated using the initial net area as the reference point.

3. A General Stress-Strain Relationship

Hooke's law applies for the initial elastic region and can be expressed as

$$\sigma = \epsilon E \tag{8}$$

where $\epsilon < \epsilon_y$ and $\sigma = P/A_g$.

In the elastic range, the effect of holes on stretch can usually be ignored[26]. Neglecting the non-uniformity of strain because of the holes, the average strain between the holes is approximately

$$\epsilon = \frac{e}{P} = \frac{P}{A_g E} \tag{9}$$

where p = pitch or distance between the centerline of holes and

A_g = gross cross-sectional area

P = load

e = total deformation between the holes

This expression is applicable until yielding commences on the net section area, at which time the stress is less than the yield point on the gross area.

As yielding commences on the net section of the plate, the linear relationship between stress and strain is no longer valid. A relationship must be developed that follows a path from B to C as in Fig. 12. Furthermore, it should fit the boundary conditions so that at $\sigma = \sigma_y$, $\epsilon = \epsilon_y$ and at $\sigma = \sigma_{ult}$, $\epsilon = \epsilon_{ult}$.

The following expression was selected:

$$\sigma = \epsilon_y E + K (1 - \underline{e}^{-\alpha \epsilon_p)^{\beta}} \tag{10}$$

where $\epsilon_y < \epsilon < \epsilon_{ult}$ and $\sigma_y < \sigma < \sigma_{ult}$.

σ = average stress on the net area

α, β, K = empirical parameters

$\underline{e}$ = base of natural logarithm

ϵ_p = inelastic strain = $\epsilon - \epsilon_y$

Equation 10 was selected after several other analytical models were investigated including those reported in Refs. 21, 22 and 23. This equation was observed to exhibit the following characteristics:

1. As the inelastic strain approached zero, the stress approached the yield stress, σ_y, which was the limit of Eq. 8.
2. With appropriate values of α and β the term $\underline{e}^{-\alpha \epsilon}$ approached zero as the strain approached the ultimate strain ϵ_{ult}.

3. The equation satisfied the experimentally observed behavior in that the stress σ increased at a decreasing rate as the ultimate stress, σ_{ult}, was approached.

Taken together Eqs. 8 and 10 describe the complete relationship between stress and strain from Point A to Point C in Fig. 12.

4. Evaluation of the Parameters which Influence the Stress-Strain Relationship

For Eq. 10 to be general and represent the stress-strain relationship for steels having differing yield points and ultimate strengths, it is to be expected that the parameters α, β and K may be functions of these values. As was discussed earlier, other variables which may influence the stress-strain relationship are the hole diameter and the gage or plate width. In effect they relate the net area at the hole to the gross plate area.

The parameters α, β and K were initially evaluated by regression analysis. Equation 10 was first linearized as

$$\log \sigma = \log \epsilon_y E + \log K + \beta \log (1 - e^{-\alpha\epsilon}) \qquad (11)$$
$$= \log \gamma + \beta \log (1 - e^{-\alpha\epsilon})$$

where

$$\log \gamma = \log \epsilon_y E + \log K$$

The least square normal equations that will minimize the sum of squared residuals for N sets of data (values of stress and strain from the plate calibration coupon) are:

$$\sum \log \sigma = N \log \gamma + \beta \sum \log (1 - \underline{e}^{-\alpha \epsilon}) \tag{12}$$

$$\sum (\log \sigma)(\log (1 - \underline{e}^{-\alpha \epsilon})) = \log \gamma \sum \log (1 - \underline{e}^{-\alpha \epsilon}) + \beta \sum (\log (1 - \underline{e}^{-\alpha \epsilon}))^2 \tag{13}$$

The coefficients $\log \gamma$ and β were determined by simultaneous solution of Eqs. 12 and 13. Several values of α were assumed for the analyses made on each plate calibration coupons' data. A comparison of the test data for each coupon (Fig. 14) indicated that this parameter would differ from coupon to coupon. Because the parameter α cannot be arrived at explicitly from the regression analysis, it was necessary to repeat the analysis for several values until the best correlation was obtained.

After obtaining the values of α, β and K from the test data for A7 and A440 steel having large variation in the plate width and hole diameter, the final analysis was made by evaluating these coefficients in terms of the known boundary conditions.

The coefficient K was evaluated from the boundary condition at $\epsilon = \epsilon_{ult}$, $\sigma = \sigma_{ult}$. Therefore, from Eq. 10

$$\sigma = \sigma_{ult} = \sigma_y + K (1 - \underline{e}^{-\alpha \epsilon})^{\beta} \tag{14}$$

which yields $\sigma_u = \sigma_y + K.$ (15)

Therefore $K = \sigma_u - \sigma_y$ where σ_u = ultimate tensile strength at the net section of a perforated plate and σ_y = yield point at the net section.

The parameter α which varied from plate to plate was finally evaluated as a function of the geometry and material properties. It was evaluated from the regression coefficient as

$$\alpha = (\sigma_u - \sigma_y) \left(\frac{g}{g - d}\right) \tag{16}$$

where g = the width of the specimen

d = diameter of the hole.

The ratio g/(g - d) is in effect a ratio of the gross area to the net area, and α could be written as $(\sigma_u - \sigma_y) \frac{A_g}{A_n}$.

The parameter β was found to be a constant common to all materials and conditions. It was evaluated from the regression analysis as being

$$\beta = 3/2 \tag{17}$$

The final general relationship for stress-strain applicable to both A7 and A440 steel and various specimen geometries was found to have the form:

$$\sigma = \sigma_y + (\sigma_u - \sigma_y) \left[1 - \underline{e}^{-(\sigma_u - \sigma_y)\left(\frac{g}{g - d}\right)\frac{e}{p}} \right]^{3/2} \tag{18}$$

where

p = pitch or distance center to center of the holes

e = total deformation in the pitch

$e/p = \epsilon_p$ = plastic strain

This equation is applicable for values

$$\sigma_y < \sigma < \sigma_{ult}.$$

For stresses lower than the yield point, Eq. 8 is applicable. Equation 18 takes into account variations in the material properties (σ_u, σ_y) and variation in the geometrical configuration of the plate calibration coupon (g, p, d).

5. Comparison of Theory and Experimental Data

The special plate calibration coupon tests were conducted by testing a plate of the same material used in the large joints. The plates tested had a width equal to the gage distance g, a thickness of one inch, and two holes drilled a distance p on center as shown in Fig. 6. The tension-elongation data was recorded for the material with the distance between the hole centers as gage length, which was equal to the pitch length in the large joints. A more complete discussion of the testing procedure and results is given in Refs. 4 and 7.

Equations 8 and 18 are compared with the test data for A7 steel in Fig. 15. The average stress on the net section is plotted as a function of the average strain for the material between the hole centers. Each plot corresponds to a different plate calibration test. The principal difference between the different specimens was the gage width g. Also shown in each plot is the static yield point, σ_y, which was determined from the standard bar coupon tests. This value was

reached at the net section at $(\sigma_y)_{net}$. In addition, the average stress on the net section at which the static yield value is reached on the gross section is indicated $(\sigma_y)_{gross}$. The standard coupon ultimate strength is indicated as $(\sigma_u)_{coup}$. For all cases, the strength of the perforated plate was higher than the coupon ultimate strength. The static yield point, σ_y, was determined from coupon tests. Its mean value was 28.2 ksi for A7 steel.

In these tests d was maintained constant at 0.94 in. The gage g varied from 2.92 to 7.50 inches. It will be noted that the theoretical line is in excellent agreement with the test data.

A similar comparison is made with A440 steel test data in Fig. 16. The static yield point of the A440 material was found to be 43.0 ksi. The gage g varied from 3.32 to 6.94 inches and the hole diameter was again constant at 0.94 inches. Again the theoretical line is in excellent agreement with the test data.

In the comparisons made in Figs. 15 and 16, the pitch p was constant and equal to 3.5 in. A special series of tests was performed for an earlier study and was used to evaluate the effect of pitch. The pitch p was varied from 2.6 to 6 inches, while maintaining the hole diameter and gage width constant. The results of the theoretical lines are compared in Figs. 17 and 18 with the test data. The agreement in all cases is good.

A comparison of Figs. 17 and 18 does indicate that a "yield plateau" is approached as the pitch between the holes is increased.

Figure 19 is a schematic of the elastic and initial plastic region for the plate calibration coupon. The smooth transition curve between the initial yield on the net section, $(\sigma_y)_{net}$, and the onset of yielding on the gross section $(\sigma_y)_{gross}$ is to be expected as discussed earlier. For the larger pitches, the holes should have less influence on the average strain and one would expect a yield plateau similar to those encountered with the standard bar coupon. As the distance between adjacent holes is decreased, the slip line interference will become more pronounced with a resulting decrease in the length of the yield plateau for the gross section area between the holes. An examination of Figs. 17 and 18 indicates that this was the case.

A summary is presented in Figs. 20 and 21 where the total load acting on the plate calibration specimen is plotted as a function of the deformation e. The agreement between the theoretical and experimental results clearly shows the applicability of Eqs. 8 and 18 to the stress-strain relationships of A7 and A440 steel plates with fastener holes.

2.4 SHEAR DEFORMATION RELATIONSHIP FOR MECHANICAL FASTENERS

1. The Behavior of Mechanical Fasteners

In the development of load-deformation relationships for mechanical fasteners, it is generally assumed that the deformation

of the fastener would include the effects of shearing, bending and bearing of the fastener as well as the localized deformation of the main and lap plates.

If a single fastener joint is loaded as shown in Fig. 22, the relative movement of points a and b is influenced by the shear, bending and bearing of the fastener. Figure 23 shows a deformed bolt illustrating this behavior. The connected members will also deform and the relative movement of a and b, if measured at the edges of the plate, will be greater as a result of the compression of the members behind the fastener. For the elastic case Coker[27] has shown that the longitudinal compressive stress in the plate dies away at a distance of about twice the hole diameter from the edge of the hole. Hence, the bearing deformations in the plate are localized. In the side view of the joint, they are indicated by the dark edges. In measuring the relative movement of a and b, the deformation of the fastener and plate are combined. There is no reason to separate them.

Two types of control or "coupon" tests can be conducted to determine the load-deformation relationship. In one type the bolts are subjected to double shear by plates loaded in tension as indicated in Fig. 24a. In the other control test the bolts are subjected to double shear by applying a compressive load to the plates (Fig. 24b). As long as the shear jig plate is reasonably stiff and nothing other than local yielding due to bearing occurs, any plate elongations other than those due to bearing are negligible.

The load-deformation relationship for the two types of control tests are shown in Fig. 25 for a typical bolt lot. These calibration tests have shown that single bolts tested in plates loaded in tension had approximately 5 to 10% less shear strength than bolts loaded by plates in compression.

When single bolts are loaded by plates in tension, the bearing condition near the shear planes causes a "prying" action and results in an additional tensile component which reduces the bolt shear strength. The catenary action resulting from the deformations will also contribute to the tensile force component. This action in an actual joint is shown in Fig. 26. The tendency for the lap plates to bend apart at the free ends is evident. It would appear that the tension type test of individual bolts best simulates the action in a large joint.

The compression type test does not represent the prototype joint except in an approximate way. Tests have indicated[15,28] that if the prying action is minimized in the tension test, the shear strength is increased to that observed in the compression tests. This condition probably exists a few rows from the lap plate end where the prying action no longer exists. The relative merits of the two types of control tests are discussed in greater detail in Ref. 28.

Based on the typical results of the bolt shear tests shown in Fig. 25, the required form of the load-deformation (shear-deformation) relationship of the fastener is shown in Fig. 27. The relationship is essentially a linear one until inelastic deformations occur. Thereafter

it becomes non-linear. The ultimate shear strength is assumed to be approached in an asymptotic manner, and neglects the reduction in strength observed at final fracture.

No known analytical expressions have been developed for the elastic-inelastic load-deformation relationship of a fastener. For the elastic region a linear relationship is usually assumed such as

$$R = \bar{K}\triangle \tag{19}$$

The elastic constant $\bar{K}$ has usually been determined from experimental data. Reference 27 has given a solution for the coefficient $\bar{K}$ by assuming the fastener to be a fixed-end beam loaded as shown in Fig. 28. It was noted that such an analysis violated several basic assumptions underlying conventional beam theory.

The deflection caused by shear, bending and bearing was determined separately. Deflection was measured relative to a line passing through the centroids of the end cross sections of the fasteners, and shearing and bending deflections were found at the center of the span. The bolt bearing deformation was defined as a percentage of the bolt diameter. For shear it was found that

$$K_s = \frac{t + t'}{3G_b A_b} \tag{20}$$

For bending,

$$K_b = \frac{(t')^3 + 4t(t')^2 + 4t' t^2 + t^3}{192 EI_b} \tag{21}$$

For bearing,

$$K_{br} = \frac{2(t + t')}{E\ t\ t'} \tag{22}$$

The localized bearing effect of fastener on the plate was found to be the same as Eq. 22. Hence, the constant $\bar{K}$ in Eq. 19 was evaluated as

$$\bar{K} = \frac{2}{K_s + K_b + 2K_{br}} \tag{23}$$

where E = modulus of elasticity

G_b = shear modulus

A_b = fastener area $= \pi d^2/4$

I_b = moment of inertia $= \pi d^4/64$

t' = thickness of lap plates

t = thickness of main plate.

Reference 14 suggested a means of treating the load–deformation relationship for rivets. Basically, the load-deformation relationship was considered to be represented by two straight lines as illustrated in Fig. 29. The elastic slope was estimated by considering the rivet to be a simply supported beam as shown in Fig. 30. The displacement δ_1, between the main and lap plates was computed due to bending and shear. The bearing deformations in the plate and rivet were approximated. The total deformation was given by

$$\delta_1 = R\left[\frac{1.125(t')^3 + 3.75t(t')^2 + 5t't^2 + 2t^3}{11.78\ d^4E} + \frac{0.3(t+t')}{d^2E} + \frac{0.375}{dE} + \frac{1.3}{E}\left(\frac{1}{t'} + \frac{1}{t}\right)\right] \tag{24}$$

Hence, $\bar{K}$ was given by the bracketed term in Eq. 24. This was assumed to hold for large diameter rivets which were stiff and did not bend appreciably. For small diameter fasteners the deformation was influenced by large bending deformations. It was expressed as

$$\delta = \frac{R(3.7g + 6.8g^3)}{Ed} \tag{25}$$

where g was an empirical parameter. In order to obtain a coefficient giving the correct order of magnitude of the deformation, an approximate relationship was given as

$$\delta = \frac{R}{E}\left[\frac{6.7}{t'} + \frac{0.8}{t} + \frac{2.5}{d}\right] \tag{26}$$

The parameters relating load and deformation were determined empirically. However, it does take into account the geometrical properties of the fastener and connected material. The relationship is only valid below the limit of proportionality. The slope of the line representing the elastic behavior was assumed to be four times as great as the line representing the inelastic behavior.

Equations 23 and 24 were used to make an initial approximation of the elastic constant $\bar{K}$ in Eq. 19. This in turn was used to help evaluate the parameters for the analytical model developed.

2. Assumptions

The criteria in the choice of the analytical expression governing the load-deformation relationship of a bolt in double shear are

the boundary conditions and the known experimental data. A number of variables were known to influence the load-deformation relationship of the bolt control test. Among these are:

1. the diameter of the bolt;
2. the thickness of the lap plates;
3. the thickness of the main plate;
4. the type or grade of steel plates; and
5. the type of bolt.

Reference 28 discusses each of these variables in detail.

The following assumptions were made for the analytical relationship developed herein. They are based in part on the behavior observed in Fig. 25.

1. At zero loads the deformation should be zero.
2. For small values of deformation the relationship between load and deformation should be approximately linear.
3. As Δ approaches Δ_{ult}, the bolt force increases at a decreasing rate.
4. The deformation Δ contains the components due to shear, bending, and bearing of the fastener as well as the bearing deformation of the plates.

The following expression was selected because it satisfied these conditions and only one continuous function was necessary:

$$R = \tau\left[1 - \underline{e}^{-\mu\Delta}\right]^{\lambda} \tag{27}$$

where $0 < R < R_{ult}$ and $0 < \Delta < \Delta_{ult}$.

Δ = total deformation of bolt and bearing deformation of the connected material

τ, μ, λ = regression coefficients

$\underline{e}$ = base of natural logarithm.

Equation 27 satisfies the boundary condition that requires the load to be zero at a zero deformation.

If the function described by Eq. 27 is expanded in a Maclaurin's series there is obtained if is unity

$$f(\Delta) = \mu\tau\Delta - \mu^2\tau\frac{\Delta^2}{2!} + \ldots\tau\mu^n\Delta^n\frac{(-1)^{n+1}}{n!} \tag{28}$$

This series is convergent as long as $\mu\Delta<1$. For small values of this condition is satisfied and an approximate solution is obtained by considering only the first term. Hence,

$$R = \mu\tau\Delta \tag{29}$$

This is directly analogous to Eq. 19 and the expressions used in Refs. 14 and 29. It also shows that Eq. 27 satisfied assumption 2.

The equation satisfies the experimentally observed behavior shown in Fig. 25 as it allows the bolt force R to increase at a decreasing rate as the ultimate shear strength of the bolt is approached.

3. Evaluation of Parameters

The parameters τ, μ and λ were evaluated by regression analysis and the boundary conditions. Equation 27 was first linearized as

$$\log R = \log\tau + \lambda \log \left[1 - \underline{e}^{-\mu\Delta}\right] \tag{30}$$

The coefficients $\log\tau$ and λ were determined by the solution of the simultaneous least squares normal equations for the linear function given as Eq. 30. It was necessary to assume several values of μ for the analysis made on each type of control test specimen. Actual values of measured load and the corresponding deformation were used in the analysis. An initial estimate of μ could be determined using Eqs. 23, 24 and 29. A best fit was obtained when the squared residuals were minimized and the boundary condition $R = R_{ult}$ was satisfied. Hence, the coefficient τ was found to be

$$\tau = R_{ult} \tag{31}$$

The parameter μ was found to vary for the different fasteners investigated. For 7/8 in. A325 bolts tested in one-inch A7 steel plates, the value was approximately 18. For 7/8 in. A325 bolts tested in one-inch A440 steel plates, the value was approximately 23. This value appeared to be the same for bolts tested in plates loaded in tension as well as plates loaded in compression.

The parameter λ was found to be almost constant for the 7/8 in. fasteners and A7 or A440 connected material. It was evaluated as

being approximately

$$\lambda \sim 1 \tag{32}$$

The final relationship for load-deformation or shear-deformation was evaluated to be

$$R = R_{ult}\left(1 - e^{-\mu\Delta}\right)^{\lambda} \tag{33}$$

where R_{ult} = Ultimate shear strength.

The average values of R_{ult}, μ and λ are tabulated in Table 1 for the five lots of bolts that are compared with Eq. 33 in the next section.

The total deformation capacity Δ_{ult} for a given bolt and connected material is a function of the shear, bending, and bearing of the bolt and the bearing deformation of the plates. As might be expected this will vary with the type of calibration test, the type of connected steel, and the thickness of the gripped material. Values of Δ_{ult} are also tabulated in Table 1.

4. Comparison of Computed and Experimental Results for Single Bolts

The two types of control shear tests were described briefly in the previous articles. Additional information on the test methods and a detailed description of the test specimens is given in Ref. 28.

The test data for both types of control tests are plotted in Figs. 31 and 34. Usually three different specimens were tested for

each type test made for each bolt lot. Equation 33 has been compared with the test data in Figs. 31 to 34. The load-deformation data for 7/8 in. A325 bolts in A7 and A440 steel are given. The type of calibration test had little if any effect on the parameters μ and λ. The theoretical line is in all cases in excellent agreement with the test data.

The actual values of μ, R_{ult}, and λ for each bolt lot are given in Table 1. The exponent λ was affected only slightly by the variations in the connected material properties and the specimen geometry for 7/8 in. A325 bolts. The type of control test had little influence on the parameters μ and λ. Only the ultimate strength, R_{ult}, was affected as described earlier. Apparently the coefficient μ was most affected by the type of connected material.

It is believed that the parameters μ and λ can be related to the physical and geometrical properties of the plate and bolt. Hence, additional studies are desirable if a generalized expression is to be developed.

The total deformation capacity of the fasteners is less in the higher strength steels because the bearing deformation in the plate is less. However, as will be seen later, this disadvantage is offset by the more favorable redistribution of the joint load which occurs amongst the A325 fasteners when they are used in higher strength steels.

2.5 GENERAL SOLUTION OF THE EQUILIBRIUM AND COMPATIBILITY EQUATIONS

1. Assumptions in Theory

The solution of the general equilibrium and compatibility equations formulated in Art. 2.2 is accomplished by employing the load-deformation relationships developed in Arts. 2.3 and 2.4, relationships that are valid for the elastic and inelastic ranges.

The following assumptions were made to facilitate the solution:

1. The mechanical fasteners transmit all the applied load once major slip has occurred.
2. The frictional forces may be neglected in the region between slip and the ultimate load.
3. The analytical expressions developed in Arts. 2.3 and 2.4 are applicable to the component elements of the connection. (The load-deformation (stress-strain) relationships for each pitch are the same).
4. All fasteners are the same diameter.

2. General Load-Elongation Relationships

The functions $f\left[R_i\right]$, $f\left[R_{i+1}\right]$, $\Psi\left[Q_{i,i+1}\right]$ and $\emptyset\left[P_{i,i+1}\right]$ in Eq. 5 can be obtained from the analytical expressions developed in Arts. 2.3 and 2.4. These functions are as follows:

$$\Delta_i = f\left[R_i\right] \tag{34}$$

From Eq. 23 this expression can be determined as

$$\Delta_i = -\frac{1}{\mu} \ln \left(1 - \left[\frac{R_i}{R_{ult}} \right] \frac{1}{\lambda} \right) \tag{35}$$

where $0 < R_i < R_{ult}$.

Similarly

$$\Delta_{i+1} = -\frac{1}{\mu} \ln \left(1 - \left[\frac{R_{i+1}}{R_{ult}} \right] \frac{1}{\lambda} \right) \tag{36}$$

where $0 < R_{i+1} < R_{ult}$

The deformations in the main and lap plates can be determined from Eqs. 9 and 18. The deformation in the main plate has been defined as

$$e_{i,i+1} = \phi \left[P_{i,i+1} \right] \tag{37}$$

If the load $P_{i,i+1}$ is sufficiently small so that yielding does not occur on the net section, then Eq. 9 governs and

$$e_{i,i+1} = \epsilon p = \frac{P_{i,i+1}\, P}{A_g\, E} \tag{38}$$

where $P_{i,i+1}$ = load in main plate between point i and i+1

p = pitch

A_g = gross area of main plate

E = modulus of elasticity of main plate.

This equation is applicable when

$$0 < p_{i,i+1} < \sigma_y A_n$$

When $P_{i,i+1} > \sigma_y A_n$, then Eq. 18 governs. Hence Eq. 37 becomes

$$e_{i,i+1} = \frac{\sigma_y A_n p}{A_g E} + p \left\{ -(\sigma_u - \sigma_y)\left(\frac{g}{g-d}\right) \ln \left(1 - \left[\frac{P_{i,i+1} - \sigma_y A_n}{(\sigma_u - \sigma_y)} \right]^{\frac{2}{3}} \right) \right\} \quad (39)$$

where σ_y = yield point of main plate

σ_u = ultimate strength of main plate

S = gage (width of main plate gage strip)

d = hole diameter

A_n = net area of main plate.

Equation 39 is applicable to the region

$$\sigma_y A_n < P_{i,i+1} < \sigma_u A_n$$

In a similar manner the function for the lap plates

$$e'_{i,i+1} = \psi\left[Q_{i,i+1}\right] \quad (40)$$

becomes

$$e'_{i,i+1} = \frac{Q_{i,i+1}\, p}{A'_g\, E'} \quad (41)$$

where $Q_{i,i+1}$ = load in the lap plate between i and i+1

A'_g = gross area of the lap plate

p = pitch

E' = modulus of elasticity of lap plate

and $0 < Q_{i,i+1} < \sigma'_y A'_n$

when $Q_{i,i+1} > \sigma'_y A_n$ then

$$e'_{i,i+1} = \frac{\sigma_y A'_n p}{A'_g E'} + p \left\{ -(\sigma'_u - \sigma'_y)\left(\frac{g}{g-d}\right) \ln \left(1 - \left[\frac{Q_{i,i+1} - \sigma'_y A'_n}{(\sigma'_u - \sigma'_y) A'_n} \right]^{\frac{2}{3}} \right) \right\} \quad (42)$$

where σ'_y = yield point of lap plate

σ'_u = ultimate strength of lap plate

A'_n = net area of lap plate.

Equation 42 holds for

$$\sigma'_y A'_n < Q_{i,i+1} < \sigma'_u A'_n$$

Equations 38, 39, 41 and 42 can be expressed as functions of the initial gage load and the bolt forces by substituting Eqs. 1 and 2 for the lap plate force $Q_{i,i+1}$, and the main plate force $P_{i,i+1}$.

For the main plate the following expressions are obtained:

$$e_{i,i+1} = \frac{\left[P_G - \sum R_i \right] p}{A_g E} \quad (43)$$

when $0 < P_G - \sum R_i < \sigma_y A_n$

$$e_{i,i+1} = \frac{\sigma_y A_n p}{A_g E} + p \left\{ -(\sigma_u - \sigma_y)\left(\frac{g}{g-d}\right) \ln \left(1 - \left[\frac{P_G - \sum R_i - \sigma_y A_n}{(\sigma_u - \sigma_y) A_n} \right]^{\frac{2}{3}} \right) \right\} \quad (44)$$

when $\sigma_y A_n < P_G - \sum R_i < \sigma_u A_n$

For the lap plates the following alongations are obtained:

$$e'_{i,i+1} = \frac{\left[\sum R_i \right] p}{A'_g E'}$$

when $0 < \sum R_i < \sigma_y' A_n'$. In the inelastic regions, the elongations become:

$$e'_{i,i+1} = \frac{\sigma_y' A_n' p}{A_g' E'} + p \left\{ - (\sigma_u' - \sigma_y') \left(\frac{g}{g-d}\right) \ln \left(1 - \left[\frac{\sum R - \sigma_y' A_n'}{(\sigma_y' - \sigma_u') A_n'} \right]^{\frac{2}{3}} \right) \right\} \qquad (46)$$

where $\sigma_y' A_n' < P_G - \sum R_i < \sigma_u' A_n'$.

Equations 35, 36, 43, 44, 45 and 46 when substituted into Eq. 4 result in Eq. 6. These expressions allow a large number of variables to be evaluated. The strength and/or thickness of the plates can be varied. Also, the solution is applicable to hybrid joints. Different types and sizes of fasteners can also be accommodated.

3. Solution of Compatibility and Equilibrium Equations

The solution of the compatibility and equilibrium equations can now be made. If one observes the compatibility equation (Eq. 6) for i = 1, it is clear that three of the four terms are functions of R_1 alone. Hence, if R_1 is assumed or is known, R_2 can be solved for a given joint load. Once R_2 is known the succeeding value R_3 can be determined. In general then, each succeeding value of R_{i+1} can be determined once the value of R_i is known. All values of R_i are dependent on the originally assumed values of R_1 and P_G. A solution is valid only if the equilirbium equation (Eq. 7) is satisfied. If it is not, then a new value of R_1 or P_G must be chosen and the iteration repeated.

The following procedure was employed to obtain the solution to Eqs. 6 and 7. An initial value of R_1 and the corresponding deformation Δ_1 were selected as is shown graphically in Fig. 35. Next a "guess" was made of the gage load P_G which would correspond to the assumed bolt force R_1. With these known initial values, it is possible to compute the remaining bolt forces R_i. Figure 35 shows the relative location of these bolt forces on the load-deformation diagram. The equilibrium equation (Eq. 7) is checked and if it is not satisfied another guess is made for the gage load P_G and the process is repeated. This process continues until Eq. 7 is satisfied.

The solution of the equilibrium and compatibility equations just described would be most time consuming and laborious, especially for long joints with a large number of fasteners, were it not for the digital computer. Fortunately, it is ideally suited to the solution of complex problems which would be prohibitive by manual methods. This is particularly true when the solution must be obtained by iterative procedures.

A program was prepared in order that the solution of the equilibrium and compatibility equations could be obtained on the GE225, Lehigh University's high speed digital computer. This program is summarized by graphical representation in the form of a flow-chart in Fig. 36. All operations to be performed and all paths of processing are indicated in this manner.

This program constitutes an important part of the work presented in this report. Without it, literally years would be needed to

produce the numerical results that have been obtained. It will also enable extensive studies in the future on certain phases of the problem of the ultimate strength of mechanically fastened connections.

The program has been written in a manner that enables several joints to be analyzed. Also, if desired, it can accommodate different initial conditions of the end fasteners in the lap plate and of the joint that was discussed briefly in Art. 2.4.

Initial values are entered which are common to the joints for which a solution is desired. These parameters include β, μ, R_{ult}, R_1, Δ_1, and A_b. Thereafter, the data for a given joint is fed into the machine. This includes identification of the joint, $(\sigma_u - \sigma_y) A_n$, $(\sigma_u' - \sigma_y') A_n'$, $\frac{\sigma_y' A_n' p}{A_g' E'}$, $\frac{\sigma_y A_n p}{A_g E}$, $\sigma_y' A_n'$, $\sigma_y A_n$, $\frac{p}{A_g E}$, $\frac{p}{A_g' E'}$, $(\sigma_u - \sigma_y)(\frac{g}{g-d})$, $(\sigma_u' - \sigma_y')(\frac{g}{g-d})$, p, n, number of bolts subject to prying (from zero to two), number of bolts without prying and the initial load.

The solution is obtained by determining the deformations in terms of the initial values as described earlier. These operations are outlined in Fig. 36.

From the assumed initial values of the bolt force R_1 and the "trial" values of the load P_G, the succeeding bolt forces in the joint are computed. The equilibrium condition is tested and if it is satisfied within 0.1%, the solution is acceptable.

The program is written so that the solution converges from above. That is to say, the initial load value must be chosen so that

it is greater than the final value. The reason for this can be seen by examining the characteristics of Eq. 4. When solving for Δ_{i+1} the expression becomes

$$\Delta_{i+1} = \Delta_i + e'_{i,i+1} - e_{i,i+1} \tag{47}$$

If the initial value of joint load is greater than the true load, the main plate elongation $e_{i,i+1}$ is larger than the true elongation and each bolt force becomes smaller than the true bolt forces. Because of this, the equilibrium check produces a positive value. As the iteration process continues and the joint load is decreased, the equilibrium check will eventually be satisfied or a negative value will result. When the decrements of load are chosen sufficiently small, the solution can be obtained within any desired accuracy.

If the initially assumed gage load, P_G, is chosen too small, the main plate elongation will be less than the true elongation and the bolt deformation Δ_{i+1} will be greater than desired. As a result, the equilibrium check will indicate a negative value and the computation will stop.

There also exists an upper bound as to the maximum load that can be assumed. If a load is chosen such that $(P_{i,i+1} - \sigma_y A_n)/(\sigma_u - \sigma_y)(A_n)$ is greater than or equal to unity, Eq. 39 is violated because the natural log of zero is infinity. Physically this means that the ultimate strength of the plate material has been exceeded. It should be noted that solutions can be obtained for compact joints when the ultimate plate strength is exceeded. This results because the load acting on the first pitch is

$$P_{1,2} = P_G - R_1 \tag{48}$$

Hence, even though P_G exceeds the ultimate strength of the plate, a solution can be obtained if

$$(P_{1,2} - \sigma_y A_n)/(\sigma_u - \sigma_y)(A_n) < 1$$

The program can handle problems involving initial conditions in the fasteners which correspond to the unloading condition shown in Figs. 31 to 34 by the test data. Initial values of R_1 and Δ_1 corresponding to this condition can be used. Generally the end pitch deformations are sufficiently large so that Δ_2 is described by Eq. 33 as can be seen in Fig. 35. This feature is probably desirable if the solution of riveted connections is required. For high-strength bolts there is little deformation remaining between the ultimate load and fracture.

To use the program, one needs only to prepare parameter cards on which the data for the problem is given. This data is fed into the machine together with the language cards, which instruct the machine how to process the data. Answers are obtained in as little as a few seconds for compact joints. For the longer joints, the solution time is of the order of five to ten minutes and is dependent on the number of fasteners and the closeness of the initially assumed load to the correct load.

The program has been checked by comparing the solutions obtained on the GE225 to previous graphical solutions[7] and to experimental results. The comparison between the theoretical and experimental work is presented in Art. 4.

The output of the program yields the computed joint load P_G and the individual fastener forces R_i. In addition, the bolt deformation Δ_i is provided. It is also possible to predict the total joint deformation.

3. APPLICATION OF THEORY TO IMPORTANT PARAMETERS

All the hypothetical studies described in this article are based on minimum strength plate and fasteners. Recent studies on the shear strength of high-strength bolts[28] have shown that the minimum shear strength can be approximated by

$$\tau_{min} = \frac{\sigma_{min}}{\sigma_u} \tau_u \tag{49}$$

where τ_u is the double shear strength of a single fastener tested in plates subjected to tensile loads. The tensile strength σ_u was determined from standard 0.505 in. cylindrical coupons. Using the results of these tests gave the most consistent relationships between shear and tensile strength. When shear strength is compared to the tensile strength based on the threaded portion, considerable scatter results as the tensile strength varies with the "stress area" and the type of threads. Because the shear failures always occur in the shank, a more logical relationship results when the tensile strength of the shank is used.

The minimum ultimate shear strength for all sizes A325 bolts was taken as

$$\tau_{min} = 73.5 \text{ ksi} \tag{50}$$

Table 2 contains the bolt parameters used in this article based on these assumptions and on the average values of μ, λ and Δ_{ult}

that were given in Art. 2.4 and Ref. 28.

The individual plate elements were all assumed to be one-inch thick. All joints were assumed to be built up of several one-inch plies. The ultimate strength of the material was varied depending on the (g/(g-d)) value from the minimum specified because of the "reinforcement" effect that was observed in the calibration tests of the plates described in Art. 2.3. This behavior is shown in Fig. 13. The ratio of the ultimate strength of the material from the plate calibration tests is compared with the ultimate strength given by standard laboratory coupon tests. The effect is seen to be greater with the A440 steel.

For the purposes of this analysis, the ultimate strength was assumed to vary linearly with increasing values of g/(g-d).

$$\frac{\sigma_u}{(\sigma_u)_{coup}} = \rho + \omega \left[\frac{g}{g-d}\right] \tag{51}$$

where σ_u = ultimate strength of plate with hole

$(\sigma_u)_{coup}$ = tensile strength given by standard bar coupons

The coefficients ρ and ω were evaluated from the data given in Fig. 13. For minimum strength material, the following relationships give the desired plate ultimate:

$$\text{A7:} \quad \sigma_u = 60(0.9 + 0.1\ g/g-d) \tag{52}$$

$$\text{A440:} \quad \sigma_u = 67(0.8 + 0.2\ g/g-d) \tag{53}$$

The static yield point was selected to be 29 ksi for A7 steel and 43 ksi for A440 steel.

3.1 EFFECT OF JOINT LENGTH

The theoretical[4,7] and experimental[3,4,6] results of previous investigations have shown that joint length was an important parameter which influenced the ultimate strength of the joint. In both A7 and A440 long steel joints connected with A325 bolts, one or more of the bolts at the dead end of the lap plate (Row no. 1 in Fig. 2) unbuttoned due to the larger bolt deformations and the prying action of the lap plates.

The joint length is a function of the fastener pitch (spacing). In this article a constant pitch is used. Article 3.3 further explores the effect of varying the pitch and ascertains what influence this has on the ultimate strength with increasing joint length.

Prior to this study the existing theoretical studies were limited in scope. Solutions were available for A7 joints with three to ten fasteners in a line and for A440 joints with four, seven, ten, thirteen and sixteen fasteners in a line respectively. Hence, the effect of joint length was not adequately ascertained theoretically. In addition, none of the theoretical studies were made using minimum strength material. The available studies had been correlated with the experimental phases. These results were arbitrarily reduced by multiplying

the average shear strength by the ratio of the minimum shear strength to the shear strength of a single fastener having the same properties as the fasteners in the test joints. This procedure was applied to approximate minimum conditions.

Hence, solutions were desirable for longer joints which were fabricated of minimum strength materials for both A7 and A440 steels.

In this phase of the study, the ratio between the bolt shear area and the net tensile area was maintained constant. For A7 steel joints the net tensile area was always 10% greater than the bolt shear area. For A440 steel joints, the bolt shear area and the net tensile area were equal. This was done because previous experimental bolted connections were proportioned in this manner[3,4,6]. These studies have shown that a balanced design would result for compact joints for these ratios; that is to say, both plate and bolt had equal opportunity to fail at the ultimate load of the joint.

The following geometrical properties were also assumed; For joints having up to twelve 7/8-in. A325 fasteners in a line, the thickness of the gripped material was taken as four inches. Joints having more than twelve fasteners in a line were assumed to have eight inches of gripped material. The main plate area was taken equal to the area of the lap plates. The pitch was maintained constant at 3.5 inches. Only one gage strip was considered.

The results of these theoretical studies of the influence of joint length are summarized in Fig. 37. The average fastener shear

stress is plotted as a function of the joint length. In comparison with the short or "compact" joints the longer joints show a decrease in the average shear strength. For the A7 steel joints the decrease was greater for joints having three to ten fasteners in a line that for the A440 steel joints of similar length. For both A7 and A440 steel joints, the decrease in the average shear strength with increasing joint length was at a decreasing rate. For more than ten fasteners in a line the curves are approximately parallel with the average shear strength of fasteners in A7 steel joints about 6 ksi less than the A440 steel joints.

Both of the theoretical curves in Fig. 37 were based on the behavior of a bolt subjected to shear by plates loaded in tension. Not all bolts in a joint are subjected to the prying action which is experienced by the end rows. As will be pointed out in Art. 4, the agreement between the theoretical solution considering this prying action and the experimental results was best for the compact joints. For the longer joints, the experimental strength was slightly greater than the value predicted by this method.

The reasons for the improved performance of the A325 bolt when used with higher strength steels and for the decrease in joint strength with increased length is best illustrated in Figs. 38 to 42. Here, the computed bolt shear stress in each row at two different stages is shown for joints of equal length and the same number of A325 fasteners. The comparisons are made for joints having four, ten, sixteen, twenty

and twenty-five fasteners in a line. The upper set in each figure is for A440 steel and the lower set is for A7 steel.

The two different stages of joint behavior described are (1) when yielding first occurs in the gross section of the plate material, and (2) when the ultimate strength of the end fasteners is reached and one or more bolts have failed by shearing. Each of these stages occurs after slip has taken place and the fasteners are in bearing. Also shown is the proportional limit of the bolt.

Figure 38 shows the bolt forces in a short joint and clearly indicates that almost complete redistribution of bolt forces has taken place in both the A7 and A440 steel joints since all fasteners are carrying approximately an equal share of the load at ultimate. An additional comparison of the bolt forces in the short A7 steel joint is made in Fig. 43. The hypothetical load-deformation curve of a single fastener is shown and the locations are indicated where the bolts in a four-fastener joint are acting when the total load is at ultimate. The interior bolts are well into the inelastic region.

In Figs. 39 to 42, it can be seen that the fasteners near the center of the A7 steel joints are carrying less than half the forces carried by the end fasteners at ultimate. The higher yield strength of the A440 steel has allowed a better redistribution to occur because inelastic deformations occur in all bolts while the plate material is still elastic and relatively rigid. With increasing joint length, the higher yield strength steel effected a better redistribution of the bolt forces. This was true for ten, sixteen, twenty and twenty-five fasteners in a line.

In the lower yield point A7 steel, the results of Figs. 39 to 42 show that inelastic deformations occurred nearly simultaneously in the plate and end fasteners. The inelastic plate deformations caused the end fasteners to continue to pick up load at a faster rate and did not allow redistribution to occur as well as in the higher yield point steel. It can be noted that, except for four fasteners in a line, the interior fasteners in the A7 steel joints showed little change in load carrying ability from the onset of major yielding until an end bolt failed. The interior fasteners in the joints were nearly uniformly loaded over about one-third to one-half of the total number of fasteners. The end fasteners making up the rest of the joint showed a rapid increase in load as the ends of the joint were approached. This is simply an indication of the relative magnitude of the strain in the main and the lap plates. Near the center of the joint the strains in the main and lap plates are about the same; but near the ends of the joint the strain in one plate becomes successively greater than in the other.

3.2 EFFECT OF VARIATION IN FASTENER DIAMETER

In the main, the experimental and theoretical work has been conducted on 7/8-in. fasteners. Reference 3 contained test data on one compact joint connected with 1-in. bolts and one compact joint connected by 1-1/8 in. bolts. Is the relationship between the average shear strength and joint length the same for all A325 bolts?

To ascertain the influence of changing the fastener diameter, analytical studies were performed on "hypothetical" A7 steel joints because the effect of joint length was found to be most severe when the A325 bolts connected this type of material (see Art. 3.1).

In this study the fastener spacing and the ratio of the shear area to the net tension area were maintained constant and a 3.5 inch pitch was used for bolts of different diameters. For the 7/8 in. bolts, the pitch was four diameters. For the 1-1/8 in. bolts, the pitch just exceeded three diameters. The net tension area was always 10% greater than the bolt shear area. The ultimate shear strength for all size bolts was taken as 73.5 ksi as indicated earlier.

The results of this study are summarized in Fig. 44 where the average shear strength is expressed as a function of the joint length. There is no truly significant difference between the curves for the 7/8 in., 1-in., and 1-1/8 in. bolts. The strength decreases slightly as the diameter decreases.

Thus, it can be seen that the average bolt shear strength is not appreciably affected by changing the fastener diameter. This is not to say that the same number of fasteners carry the same load regardless of diameter. For a given joint length the difference in joint load will be directly proportional to the bolt shear area. Because of this, an increase in fastener diameter will provide an improvement in average shear strength for a given load. The joint will be shorter with an

increase in bolt diameter in proportion to the areas of the fasteners used. A more complete redistribution will occur with a resulting increase in the joint strength.

Figure 45 shows the computed bolt shear stress for A7 steel joints with ten fasteners in a line. The upper set is for 7/8-in. fasteners and the lower set is for 1-1/8 in. fasteners. The distribution of stress in the two sizes of fasteners for a joint of equal length do not differ significantly.

Data are not currently available on the behavior of 1-in. and 1-1/8 in. single fasteners in A440 steel. Because of this, analytical studies were not performed. However, it seems reasonable to assume that similar results will be obtained for various sizes of A325 fasteners in A440 steel joints.

3.3 EFFECT OF PITCH

The pitch of fasteners is the distance along the line of principal stress between centers of adjacent fasteners. This distance undoubtedly plays an important role in the performance of the fasteners.

Most of the available test data[3,4,6] are for a pitch of 3.5-in. (4 bolt diameters). In Ref. 6 one specimen was tested with a different pitch. In this specimen, the minimum pitch spacing stipulated by most specifications was used, namely 3 bolt diameters. This yielded a pitch of 2.625-in. for 7/8-in. bolts.

A number of observations were made on this test in Ref. 6. A comparison of the test data with the data for pitches of four diameters showed that the average shear stress at failure was approximately the same as a joint having fewer fasteners but the same length. By decreasing the pitch, a shorter joint was achieved which was better able to redistribute the bolt forces and resulted in an increase in load carrying capacity. Hence, it appeared that the joint length, not the number of fasteners, was the most important variable insofar as the average shear strength was concerned.

An analytical study of ten "hypothetical" joints was made in Ref. 30; the theoretical solution given in Ref. 7 was used to ascertain the effect of varying the pitch. The hypothetical joints were A7 steel plates fastened with A141 steel rivets or A325 bolts. The bolted joints had nine fasteners in a line, and the riveted joint thirteen fasteners in a line. This study showed that for a given number of fasteners in a line, the ultimate strength of the connection decreased as the pitch was increased. This was true for both riveted and bolted connections.

Because the pitch is an important variable insofar as joint strength is concerned, it is desirable to see what influence it had over a wide range of joint length. Also, were the tentative conclusions reached in Ref. 6 correct? Was joint length the important variable and not the number of fasteners, per se?

To determine the effect of the fastener pitch, analytical studies were made for joints with fastener spacings of three diameters,

four diameters and seven diameters. Most of the studies reported herein are for a fastener spacing of four diameters. This allowed a comparison for a shorter and longer fastener spacing. The fasteners were assumed to be 7/8-in. A325 bolts.

The results of these studies are summarized in Figs. 46 and 47 for A7 and A440 steel respectively. Although the joints with greater pitch are somewhat stronger, the results show clearly that joint length is the most important variable for both A7 and A440 steel. There is little if any significant difference between the average shear strength for pitches of 3 or 4 diameters. For the longer pitch (7 diameters), the compact joints with up to six fasteners in a line behaved almost identically to other compact joints with the same number of fasteners but with a shorter pitch. With few fasteners in a line and a pitch of seven diameters, the joint load was redistributed, and the decrease in the average shear strength was not significant until after five or six fasteners in a line. In other words, the pitch had little influence on compact joints. With increasing joint length, the curves converged so that once again only joint length affected the ability of the fasteners to redistribute their loads.

As pointed out in Ref. 6, one should be careful not to construe this to mean that the carrying capacity of a connection with n bolts in line is equal to that of the same length connection with m bolts in line. Only the average shear strength is the same. For joints of the same length the load carrying capacity is directly proportional to the shear area of the connection in question.

3.4 EFFECT OF VARIATION IN RELATIVE PROPORTIONS OF SHEAR AND TENSILE AREAS

The relationship between the shear area and net tensile area has frequently been used in the past to describe the design requirements of mechanically fastened joints. This relationship has evolved from the so-called "tension-shear" ratio, the ratio of the average tensile stress on the net section of the plate to the average shear stress on the mechanical fasteners. The desirable ratio has been considered to be that which causes the ultimate load of the fasteners in shear to equal the ultimate load of the plate in tension. In turn, this has been classified as "balanced design" at ultimate load.

As pointed out in the introduction, tests were conducted on short compact joints of A7 steel connected with A325 bolts and a "tension-shear" ratio of 1.0 to 1.10 was selected to establish "balanced design"[3]. Subsequent tests of A440 steel joints connected by A325 bolts yielded a "balanced design" when the "tension-shear" ratio was 1.0 to 1.0[4].

The analyses described in Arts. 3.1, 3.2 and 3.3 have clearly shown that the "balanced design" concept has no meaning with increasing joint length because the bolts unbutton before the plate material can attain its full ultimate strength. The type of connected material had no noticeable effect on the behavior of the A325 bolt in compact joints.

In Ref. 7 the effect of varying the tension-shear ratio was investigated for a few specimens. It was shown that the ultimate load-

carrying capacity of a connection with eight fasteners in a line increased with an increase in the area of the connected material.

The results of tests on bolted lap joints with varying ratios of net tensile and bolt shear area have also indicated an increase in shear strength[6]. The pilot test series for the A440 steel joints showed similar results[4]. As the plate area at the net section was increased from 95 to 110% of the bolt shear area, the bolt shear stress at ultimate increased.

On the other hand, as the net plate area is decreased relative to the bolt shear area, the joints invariably fail by tearing of the plate. This has been illustrated in tests of A7 and A440 steel joints connected by A325 bolts. Because of this, the ultimate strength of the fasteners is not attained. Hence, a need exists for additional information on the effect of varying the proportions of the tension and shear areas.

For the analytical studies, both A7 and A440 steel connections were considered. The fastener diameter was selected as 7/8-in. and the pitch as four diameters. For the A7 steel joints, the net plate area was varied from 75 to 130 per cent of the bolt shear area. For the A440 steel joints, the net plate area was varied from 90 to 120 per cent of the bolt shear area.

The results of these studies are summarized in Figs. 48 and 49 for A7 and A440 steel joints, respectively. Also shown is the

limiting condition which is reached if the net plate areas were infinitely greater than the bolt shear area. Under this condition the plate material would be perfectly rigid and each fastener would deform the same amount and would carry an equal share of the load.

In Fig. 48, the curves for the ratio of net plate area to the bolt shear area of 1.0 to 1.10, 1.0 to 1.0, and 1.0 to 0.75 are shown for the case of bolt failure only. For the shorter joints, plate failure will occur and the shear strength of the bolts will not be achieved. Only with an increase in joint length do the accumulated differential strains between the main plate and lap plate become critical and cause a bolt failure before the plate can tear. This phenomenon has been observed in a number of tests[18]. A similar condition exists for A440 steel joints for the ratio of the net plate area to the bolt shear area of 1.0 to 0.90. A bolt failure would not be expected to occur until there were seven fasteners in a line (Fig. 49).

Both Figs. 48 and 49 show that with an increase in the net plate area, the average shear strength of the fasteners for the longer joints is greater. The decrease in the average shear strength of the fasteners is not as great with an increase in the plate area. In Fig. 48, the decrease in the bolt shear strength starts to occur at four fasteners in a line when the ratio of net plate area to the bolt shear area was 1.0 to 1.10; at four fasteners when the ratio was 1.0 to 1.20; at five fasteners when the ratio was 1.0 to 1.30. For the A440 steel

joints shown in Fig. 49, the decrease started at four fasteners in a line when the ratio was 1.0 to 1.0; at five fasteners when the ratio was 1.0 to 1.10; and at six fasteners when the ratio was 1.0 to 1.20.

4. COMPARISON OF THEORY WITH TESTS

The test results reported in Refs. 3, 4 and 6 afford an opportunity to test the validity of the theory when applied to determine the ultimate strength of A7 and A440 steel joints. The validity of the assumptions made can also be verified.

4.1 ANALYSIS OF TEST JOINTS

For the analyses reported herein, the actual bolt and plate properties were substituted into Eqs. 9, 18, and 33. The mechanical properties had been determined from tests on bolts from the same lot and steel plate from the same heat that was used in the test joints. Measured dimensions were also used.

It was thought desirable to check the ultimate strengths that would be obtained from the two different shear-deformation relationships. The data for one shear-deformation relationship was obtained from tests in which the plate material is loaded in tension and the high-strength bolts subjected to double shear as shown in Fig. 24a. In the other shear test the bolts are subjected to double shear by applying a compression load to the plates as shown in Fig. 24b.

Observations made during the joint tests reported in Refs. 4 and 6 had indicated that the prying action was present near the ends

of the lap plates where a clear separation of the plates was noted near the ultimate loads as is illustrated in Fig. 26. In the interior of the joints this behavior was not as noticeable.

In addition to the different behavior of the fasteners noted during the calibration tests and joint tests, an inspection of Figs. 31 to 34, shows that after having reached its ultimate strength, the bolt begins to unload very rapidly. Additional deformation can be achieved in a few instances before complete rupture. Because of this, it may be possible in some joints for further redistribution to take place before an unbuttoning failure is observed.

Because of these observations, several different analyses were made and these are compared with the experimental results in Table 3 for the A7 steel joints and Table 4 for the A440 steel joints. The following initial values and conditions were used (they are called "Methods" in Tables 3 and 4):

Method 1. All bolts are assumed to behave the same as a single bolt loaded in a tension jig. The maximum load and deformation in the end fasteners of the joint corresponds to the ultimate load and deformation of a single fastener in a tension jig.

Method 2. All bolts are assumed to behave the same as a single bolt loaded in a tension jig. The failure load and deformation of the end fasteners of the joint corresponds to the rupture load and deformation of a single fastener in a tension jig.

Method 3. All bolts are assumed to behave the same as a single bolt loaded in a compression jig. The maximum load and deformation of the end fasteners of the joint corresponds to the ultimate load and deformation of a single fastener in a compression jig.

Method 4. The bolts in the end two rows at the end of the lap plates of the joint are assumed to behave the same as a single bolt loaded in a tension jig and the remaining bolts in the joint are assumed to behave the same as a single bolt loaded in a compression jig. The maximum load and deformation of the end fastener at the lap plate end corresponds to the ultimate load and deformation of a single fastener tested in a tension jig.

Method 5. The bolts in the end two rows at the end of the lap plate of the joint are assumed to behave the same as a single bolt loaded in a tension jig and the remaining jolts in the joint by the compression jig loading. The failure load and deformation at the lap plate end fastener corresponds to the rupture load and a deformation of a single fastener tested in a tension jig.

The predicted ultimate strength in kips for each of the five analyses is given in Tables 3 and 4, along with the experimental results. Also given is the ratio of the computed ultimate strength to the observed ultimate strength for Methods 1 and 3. These two methods incorporate the two basic types of shear test of a single bolt. Method 1 utilizes the tension jig and Method 3 uses the compression jig.

It can be seen that there is good agreement between "Method 1" and the experimental results. For the A7 steel joints (Table 3), Method 1 gave the best agreement up to nine fasteners in a line. For the A440 steel joints, Method 1 gave the best agreement with the test results for up to ten fasteners in line. For more than ten fasteners in a line, the theoretical results were slightly less than the experimental.

The greatest difference between the theoretical and experimental results of A440 steel joints was approximately 4% for Method 1 as can be seen in Fig. 50. Here, the average bolt shear strength is plotted as a function of joint length. The theoretical solutions were based on the analysis designated as Method 1 and utilized the measured bolt and plate properties. Two different lots of bolts were used in the test series to accommodate the change in grip. This together with the change in geometry accounts for the discontinuity at a joint length of approximately 37 inches.

The objective of Method 2 was to see whether or not the additional deformation between the ultimate load and rupture load of a single bolt would allow further redistribution to occur in a joint. For the A7 steel joints with less than nine fasteners in line, the ultimate joint load computed using Method 2 (with the end fasteners at rupture load and deformation) was less than that computed using Method 1 (with the end fasteners at their ultimate load and corresponding deformation). This was also true for A440 steel joints with less than nine fasteners in a line. Clearly, no additional redistribution was possible

for these joints. In the longer joints, the additional deformation enabled further redistribution to occur. However, the increase in load was only one percent. For practical purposes, Methods 1 and 2 are not significantly different.

Method 3 is based upon the results obtained using the shear deformation relationship given by the compression test of a single fastener. As expected, the results predict a higher strength in most instances. For the A7 steel joints (Table 3), the computed strength was slightly greater than the experimental strength for up to nine fasteners in a line. For A7 steel joints with ten to thirteen fasteners in a line, the computed strength was within 1% of the observed failure load. For the A7 steel joint with sixteen fasteners in a line, the computed strength was approximately 3% greater than the experimental results. For the A440 joints, the computed strength was up to 11% greater for all but the longest joint with sixteen fasteners in a line (Table 4). For the longer joints, Method 3 yields better results because the prying action of the lap plates has less effect since more of the fasteners are being subjected to shear without the prying action present.

Methods 4 and 5 utilize both types of shear deformation relationships. Because of the prying action, the bolts in the end two rows at the ends of the lap plate of the joint were assumed to be represented by a single bolt tested in a tension jig. The remaining bolts in the joint were assumed to behave the same as a single bolt tested in a compression jig. The compression jig test simulates the action of the

fasteners away from the dead end of the lap plate where the prying action is minimized[28].

For the compact (shorter) joints, Methods 4 and 5 (Table 3 and 4) predicted ultimate strengths which were slightly higher than the experimental results. For the longer joints, the predicted ultimate strengths were not significantly different than the strength obtained with Methods 1, 2, and 3.

The comparisons in Tables 3 and 4 can be summarized as follows: For compact joints, the shear-deformation relationship of a single bolt loaded by plates in tension gives the best agreement with the experimental results. This appears reasonable because the double shear test of a single fastener by plates loaded in tension is much the same as the compact joint test. For longer joints, the prying action at the end of the lap plates due to the bearing condition near the shear planes does not extend into the interior of the joint. As a result, the interior fasteners have a greater shear strength as is evident from the tests of single fasteners (Fig. 25). Better agreement between the computed ultimate strength and the experimental results is obtained for longer joints if this effect is taken into account (Methods 3, 4, 5). Regardless of this slight difference, the computed results given by Method 1 were always within four percent of the experimental strength.

Method 3 (compression) yielded ultimate strengths which were somewhat higher than the observed failure load for joints with up to ten fasteners in a line. For A7 steel joints this difference was only slightly

greater (2%). For the A440 steel joints the differences varied from 4 to 11%. For the longer joints this method gave the best agreement.

A comparison between the theory and experimental results is made in Fig. 51 for Methods 1 and 3. Here, the average bolt shear strength is plotted as a function of joint length. The comparison is made for the A440 steel joints. Both methods used the measured bolt and plate properties. It is readily apparent that Method 3 predicted too great a strength for the shorter joints. For the longer joints Method 3 agreed best with the experimental results. However, the differences between Methods 1 and 3 are small for the longer joints.

Method 1 was selected for the hypothetical studies in this report because it agreed well with the test results (within 7%). The computed strengths were also lower than the experimental results when the differences were greatest. It should be noted, however, that the tension jig control test is more difficult to conduct and is also the more costly. The compression jig control test gave the best agreement for the longer joints. The control test is relatively simple to do and is less costly than the tension jig test.

4.2 INFLUENCE OF MATERIAL PROPERTIES

Two additional analyses were made and compared with the experimental results. One analysis was made using minimum strength bolts and the measured properties of the plate material used in the

experimental studies. The ultimate strength of the A440 steel plate was about 13% greater than the minimum strength specified by ASTM A440. The results of this study is shown in Fig. 52. The effect of decreasing the bolt strength is readily apparent when comparing the theoretical curve with the curve which used the measured bolt properties. The reduction in bolt strength was most noticeable for the compact joint.

The second analysis was based on minimum strength bolts and plates as described in Art. 3. The decrease in the ultimate strength of the plate caused a further decrease in the shear strength of the joints as can be seen in Fig. 52. The effect was most noticeable for joints with four to ten fasteners in a line (length of 10 to 30 inches). Thereafter, the curves were approximately parallel.

Obviously, both the ultimate strength and yield point of the A440 steel are instrumental in effecting a better redistribution of the fasteners forces. Similar results can be expected with variations in the yield point and ultimate strength of A7 steel.

5. SUMMARY AND CONCLUSIONS

In this dissertation, a general theoretical solution for the load partition in double-lap plate splices was developed. This solution is applicable to the region from major joint slip to the ultimate load. It is based on the observed behavior of plates with holes and of high-strength bolts in shear. This solution required the development of analytical expressions for the "stress-strain" relationship of plates with holes and for the shear-deformation relationship of high-strength bolts. Necessarily, both expressions are applicable to the elastic and inelastic regions.

The theoretical solution of load partition and ultimate strength has been verified by comparing the theoretical results with the results of eight large A7 steel bolted joints and seven large A440 steel bolted joints. In all cases the theory and tests results were in good agreement. The greatest difference between the theoretical and experimental results was approximately 4%.

The theory has been used in a study of the factors that might influence the behavior of bolted splices. Among the variables studied were joint length, pitch, fastener diameter, and variations in the relative proportions of the bolt shear area and the net tensile area. The behavior of joints up to 90 inches long was investigated (up to twenty-five fasteners in line).

Specific findings are summarized as follows:

(1) A theoretical solution for the influence of joint length on the shear strength of bolted double-lap tension splices was developed. It predicted a decrease in strength for increasing length that was confirmed experimentally in tests of A7 and A440 steel connections (within about 4%).

(2) It was shown that the decrease in average ultimate shear strength was greater for A7 than for A440 steel joints connected with A325 bolts (Fig. 37).

(3) The fastener pitch influenced the average shear strength only insofar as it influenced the joint length. With few fasteners in line, the joint load was redistributed regardless of the fastener pitch, and the decrease in the average shear strength was not significant. With an increase in joint length, the total length was the most important variable, not the number of fasteners (Figs. 46 and 47).

(4) The average shear strength as a function of joint length was not significantly affected by changing the fastener diameter (Fig. 44).

(5) The study of varying the relative proportions of the bolt shear area and the net tensile area showed that with an increase in the net plate area, the average shear strength of the fasteners for the longer joints was increased (Figs. 48 and 49).

(6) As the plate area of the shorter joints was decreased, the joints invariably failed by a tearing of the plate. As the joint length increased, the end fasteners would fail due to unbuttoning. A theoretical solution was developed for the "plate failure" boundary.

(7) The "balanced design" concept was shown to have little meaning. A joint can be in balance only for a specific length and specific ratio of the bolt shear area and net tensile area.

(8) Both the yield point and ultimate tensile strength are shown to influence the load partition and ultimate strength of bolted double-lap tension splices (Figs. 37 and 52).

(9) A digital computer program was developed for the solution of bolted splice plate problems in order to make practicable what otherwise would be too tedious.

6. NOMENCLATURE

1. SYMBOLS

A_b	fastener area = $\pi d^2/4$
A'_g	gross area of lap plate
A'_n	net area of lap plate
A_g	gross area of main plate
A_n	net area of main plate
d	hole diameter
E	modulus of elasticity
$e'_{i,i+1}$	elongation of the lap plate between bolts i and i+1
$e_{i,i+1}$	elongation of the main plate between bolts i and i+1
G_b	bolt shear modulus
I_b	fastener moment of inertia = $\pi d^4/64$
i	row of bolts or holes, i = 1, 2, 3, n
K	plate coefficient
$\bar{K}$	bolt constant
K_b	bolt bending coefficient
K_{br}	bolt bearing coefficient
K_s	bolt shear coefficient
n	number of bolts in a line
P	total load on joint
P_G	load on gage strip
$P_{i,i+1}$	load per gage strip in the main plate between bolts i and i+1

p	pitch; the longitudinal spacing of the bolts
$Q_{i,i+1}$	load in the lap plates between bolts i and i+1
R	total bolt shear force
R_i	force on bolt i
R_{ult}	ultimate shear strength of the fastener in double shear, kips
t'	thickness of one lap plate
t	thickness of main plate
α	plate coefficient; $= (\sigma_u - \sigma_y)\left(\frac{g}{g-d}\right)$
β	plate coefficient
γ	plate coefficient
τ	bolt parameter = R_{ult}
Δ	total deformation of bolt and bearing deformation of the connected material
Δ_i	deformation of bolt i
Δ_{ult}	bolt deformation at ultimate load (R_{ult})
ϵ	strain
ϵ_y	yield strain
ϵ_{ult}	ultimate strain
λ	bolt parameter
μ	bolt parameter
ρ	plate parameter
σ	tensile stress
σ_u	tensile stress (ultimate), ultimate tensile strength of main plate
σ_y	yield point, static yield stress of main plate

σ_u ultimate strength of lap plate

σ_y static yield stress of lap plate

$\cup$ plate parameter

2. GLOSSARY

Gage	The transverse spacing of the fasteners.
Gage strip	A width of plate equal to the gage with the fasteners centered.
Grip	The thickness of the plate material in the connection.
Pitch	The longitudinal spacing of the bolts.
Prying Action	The tendency for the lap plate free ends to bend out due to the bearing condition.
Unbuttoning	The sequential failure of fasteners which progresses from the ends of a joint inward.

TABLE 1

SUMMARY OF TEST RESULTS AND ANALYSIS OF A325 BOLTS

Bolt Lot	Type Connected Material	Type Test Jig	Ultimate Strength R_{ult}, kips	Bolt Parameters μ	λ	Ultimate Deformation, Δ_{ult}, in.
8A	A440	Tension	98.6	23	1	0.187
8A	A440	Compression	102.3	23	1	0.200
8B	A440	Tension	92.5	25	0.95	0.200
8B	A440	Compression	104.0	22	1	0.239
H	A440	Tension	95.2	22	1	0.220
H	A440	Compression	103.0	22	1	0.236
C	A7	Tension	98.5	18	1	0.238
C	A7	Compression	106.9	18	1	0.291
D	A7	Tension	101.8	18	1	0.279
D	A7	Compression	102.5	18	1	0.300

TABLE 2

HYPOTHETICAL BOLT PROPERTIES

Bolt Diameter	Type Connected Material	$R_{ult} = 73.5A_b$	μ	λ	Δ_{ult}
7/8	A7	88.5	18	1	0.27
7/8	A440	88.5	23	1	0.22
1	A7	115.2	14.5	0.55	0.27
1-1/8	A7	146	10	0.55	0.32

TABLE 3

COMPARISON OF THEORETICAL AND EXPERIMENTAL ULTIMATE LOADS - A7 STEEL JOINTS

Joint	Load at Failure Kips	COMPUTED ULTIMATE STRENGTH, KIPS						
		Method 1	Computed / Observed	Method 2	Method 3	Computed / Observed	Method 4	Method 5
D71	1126	1123	0.997	1118	1142	1.014	1132	1119
D81	1282	1232	0.961	1232	1252	0.977	1233	1232
D91	1358	1365	1.005	1370	1389	1.023	1366	1370
D101	1506	1445	0.959	1451	1470	0.976	1446	1452
D10	1544	1434	0.929	1441	1550	1.004	1444	1452
D13A	1988	1823	0.917	1839	1969	0.990	1840	1855
D13	1854	1724	0.930	1736	1858	1.002	1737	1750
D16	2085	1997	0.958	2014	2146	1.029	2012	2030

TABLE 4

COMPARISON OF THEORETICAL AND EXPERIMENTAL ULTIMATE LOADS - A440 STEEL JOINTS

Joint	Load at Failure Kips	COMPUTED ULTIMATE STRENGTH, KIPS						
		Method 1	Computed / Observed	Method 2	Method 3	Computed / Observed	Method 4	Method 5
E41	728	730	1.003	699	800	1.099	768	738
E41f	727	730	1.003	699	800	1.099	768	738
E41g	767	767	1.000	757	798	1.040	779	770
E71	1188	1209	1.018	1193	1320	1.111	1239	1225
E101	1610	1604	0.996	1596	1720	1.068	1620	16[illegible]5
E131	2125	2062	0.970	2074	2155	1.014	2091	2[illegible]06
E161	2545	2425	0.953	2446	2526	0.993	2456	2478

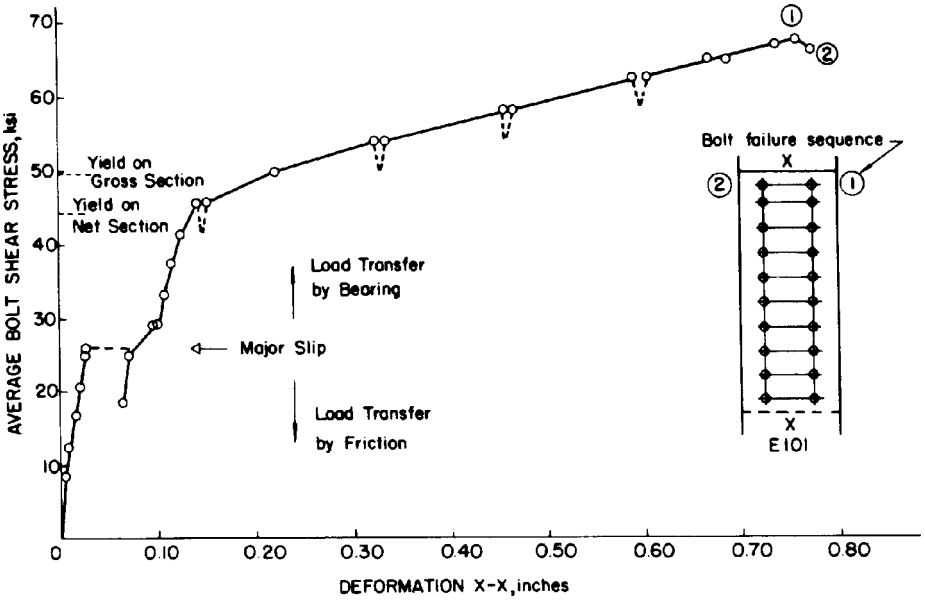

Fig. 1 Typical Load Deformation Curve

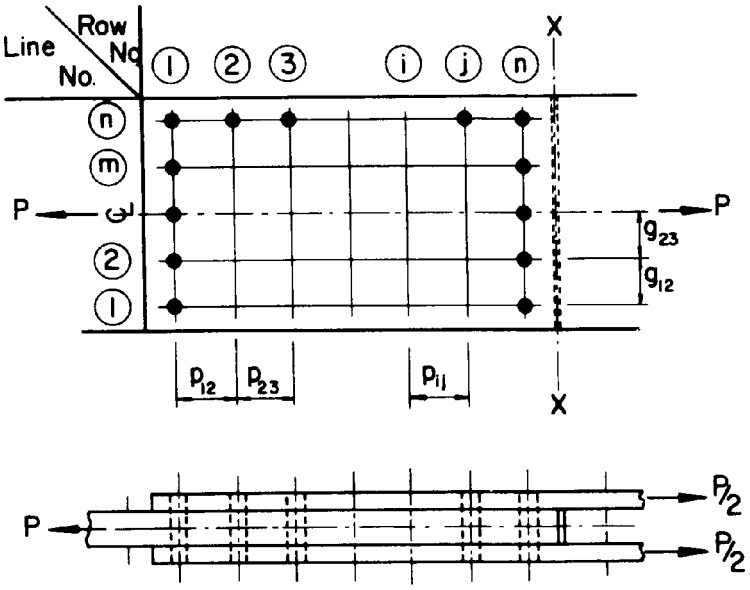

Fig. 2 Joint Geometry

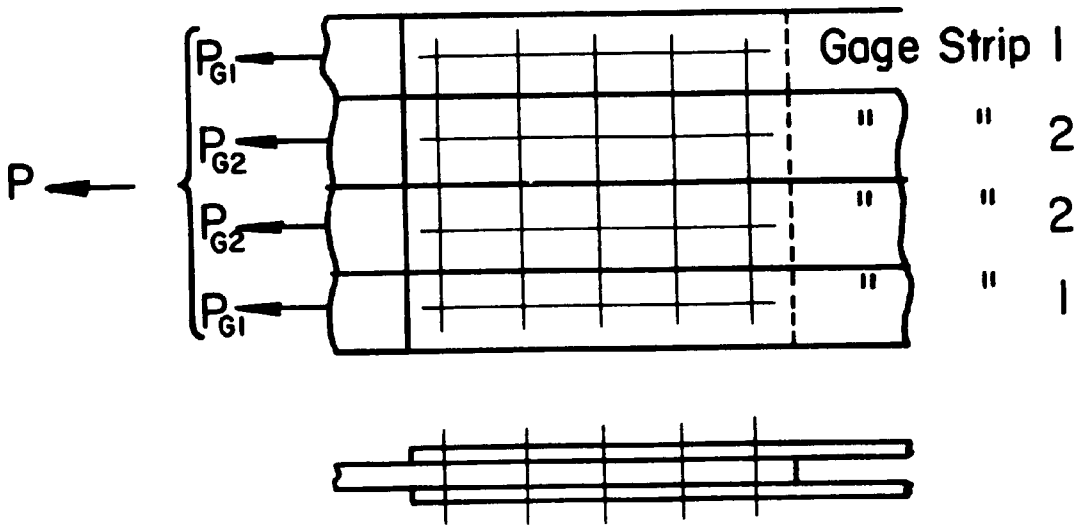

Fig. 3 Division of Joint into Gage Strips

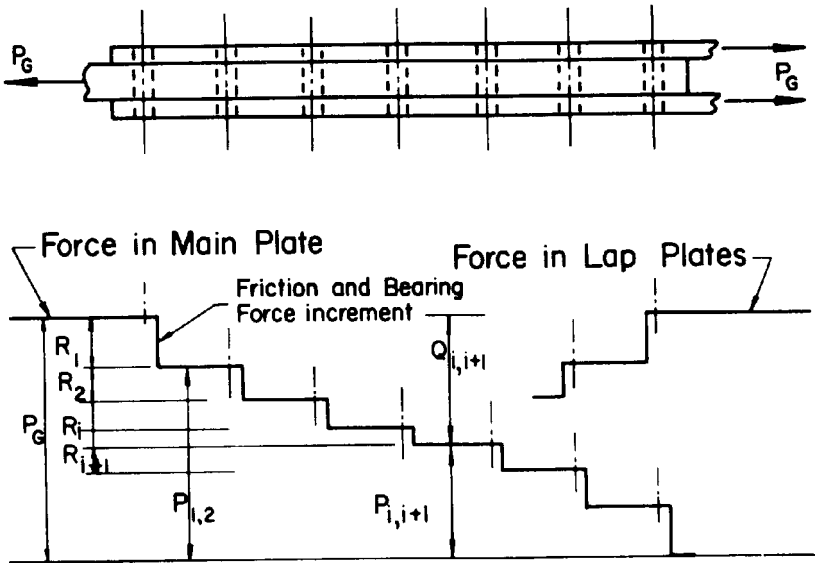

a. Idealized Load Transfer Diagram

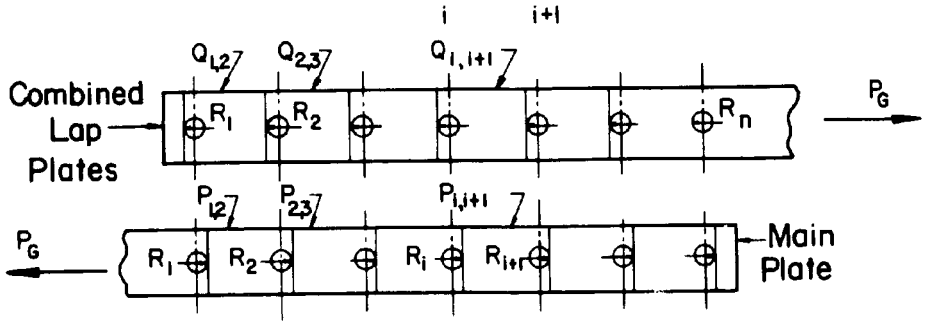

b. Force Zones

Fig. 4 Idealized Load Transfer

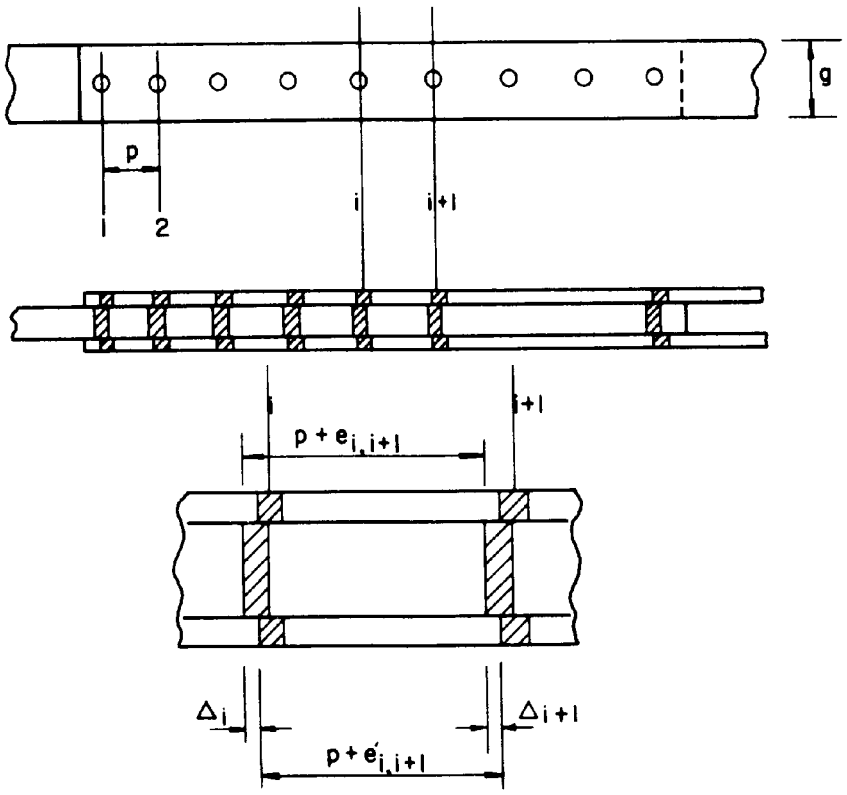

Fig. 5 Deformations in Bolts and Plates

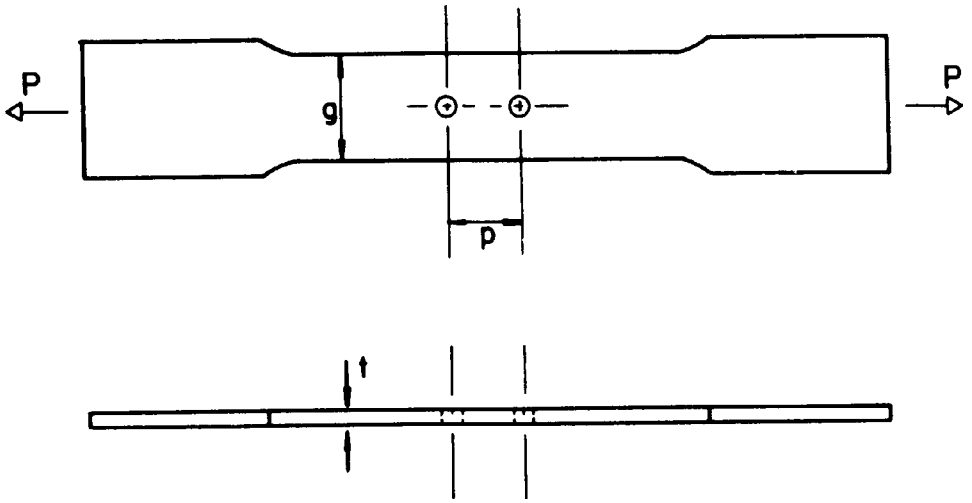

Fig. 6 Schematic of Plate Calibration Coupon

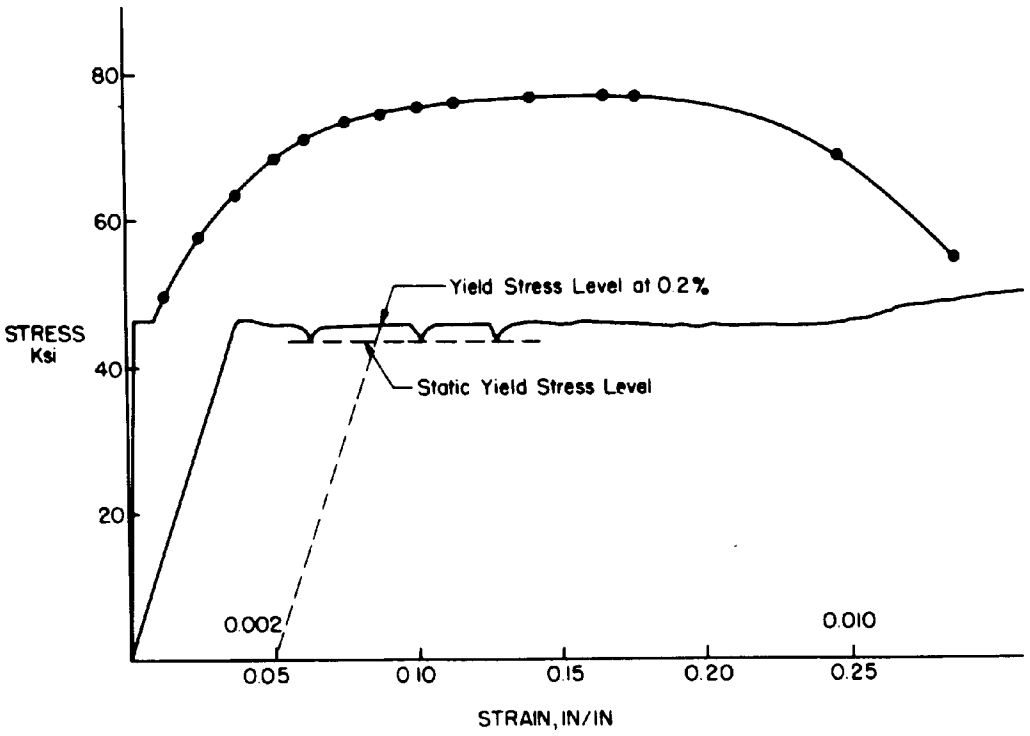

Fig. 7 Typical Stress-Strain Diagram for Standard Bar Coupon - A440 Steel

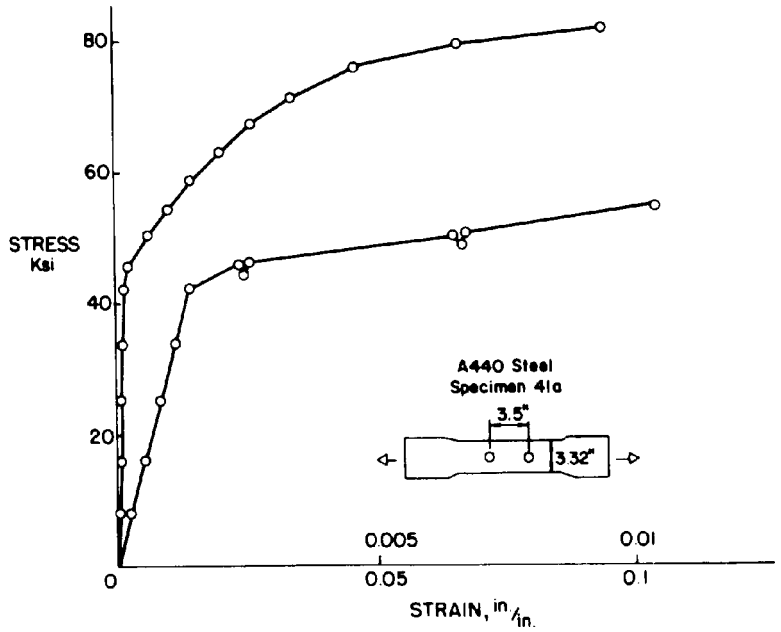

Fig. 8 Typical Stress-Strain Diagram for Plate Calibration Coupon - A440 Steel

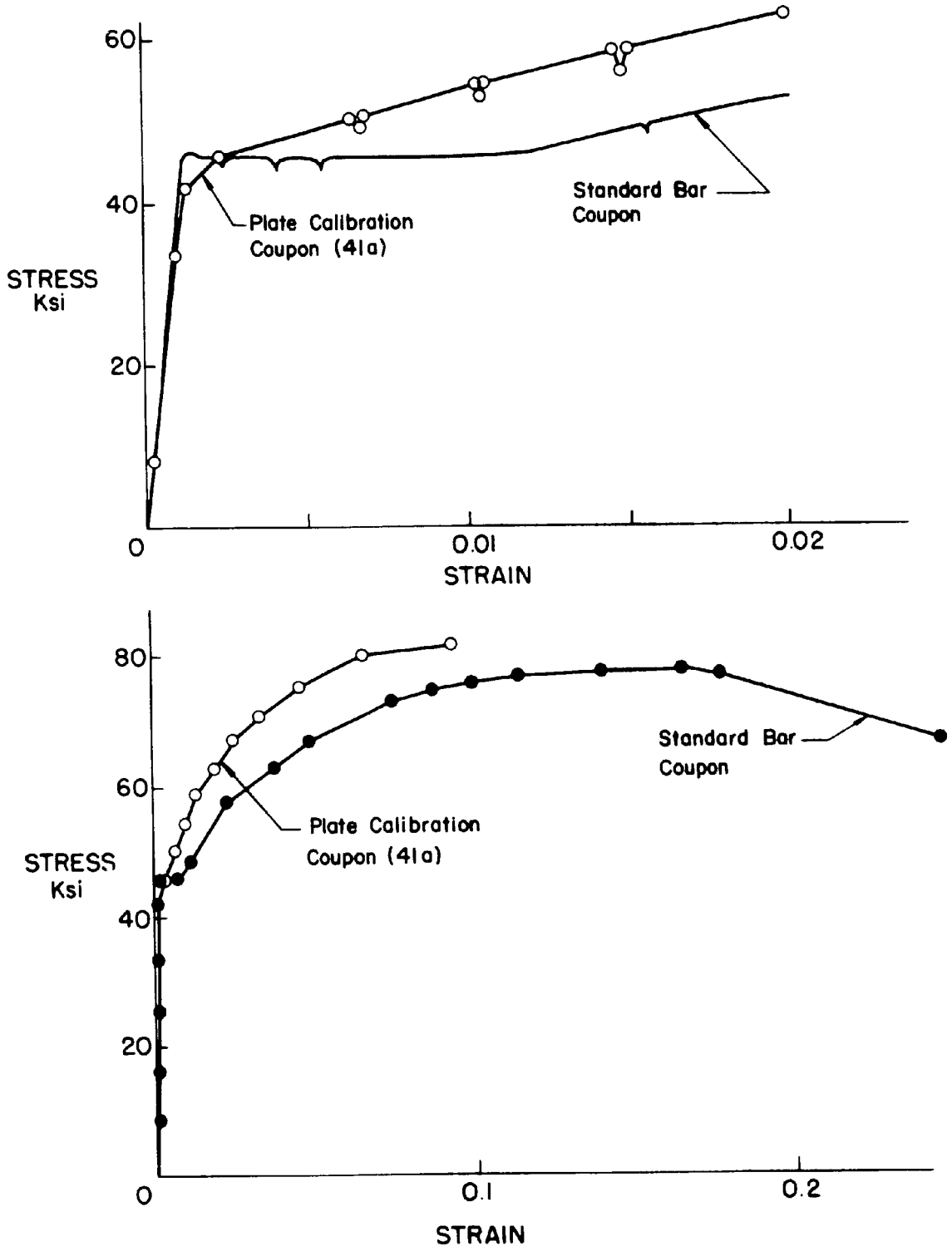

Fig. 9 Comparison of Standard Bar and Plate Calibration Coupons - A440 Steel

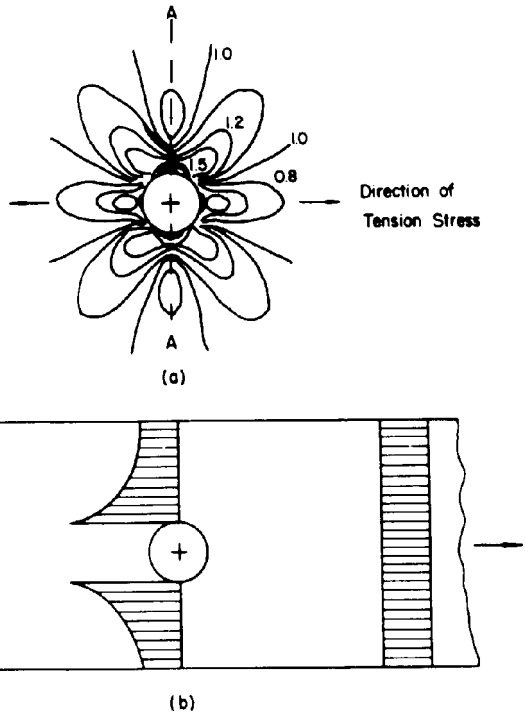

Fig. 10 Stress Concentration in an Elastic Plate with Hole in Tension

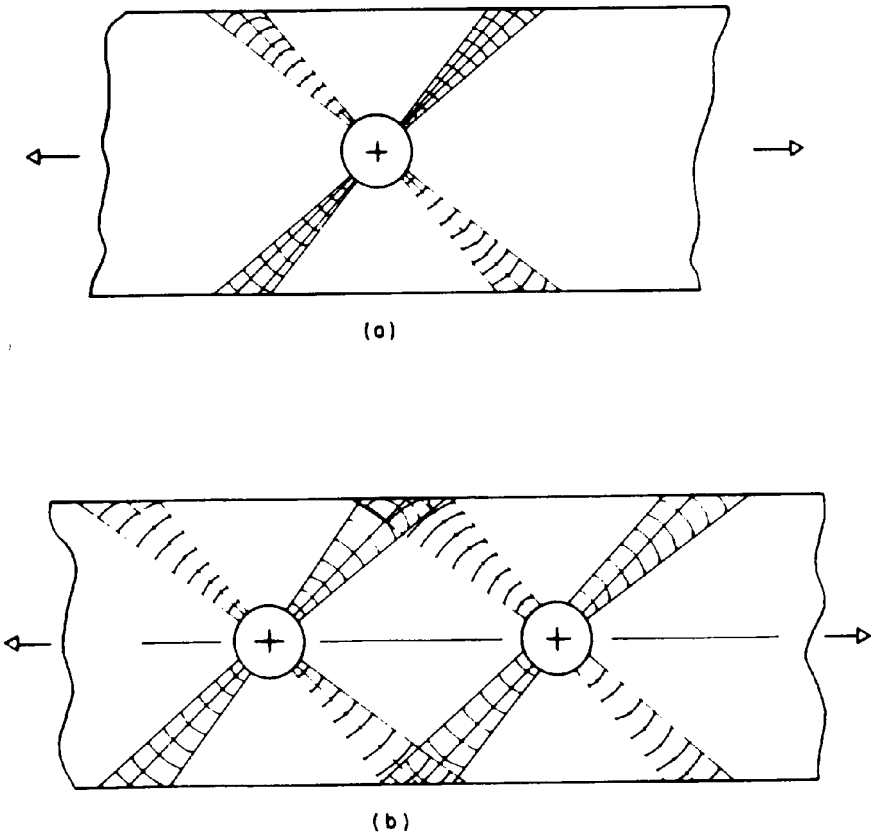

Fig. 11 Slip Lines on the Plate Calibration Coupon

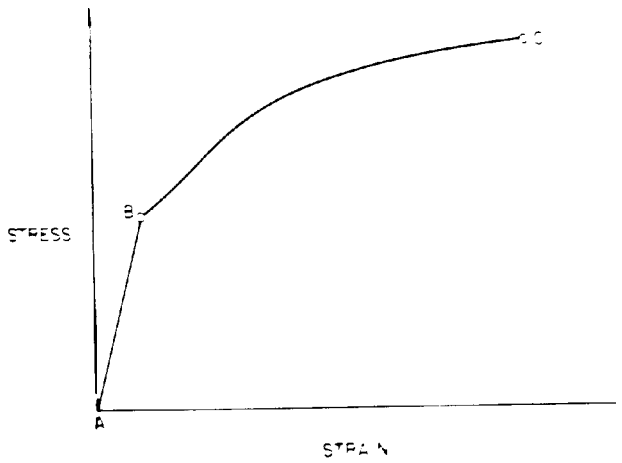

Fig. 12 Idealized Stress-Strain Relationship

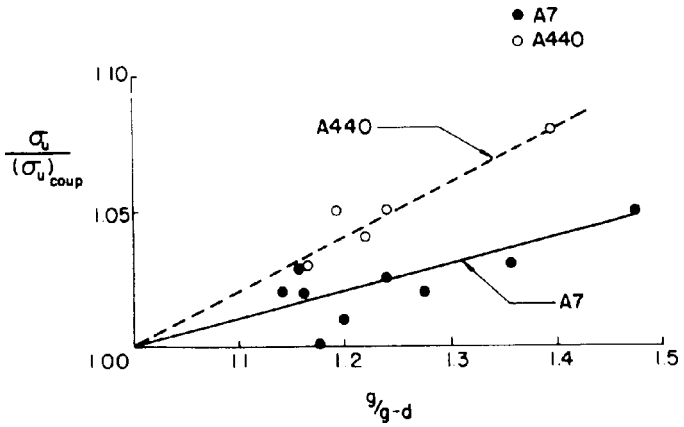

Fig. 13 Effect of Gage on Ultimate Strength of Plate Calibration Coupon

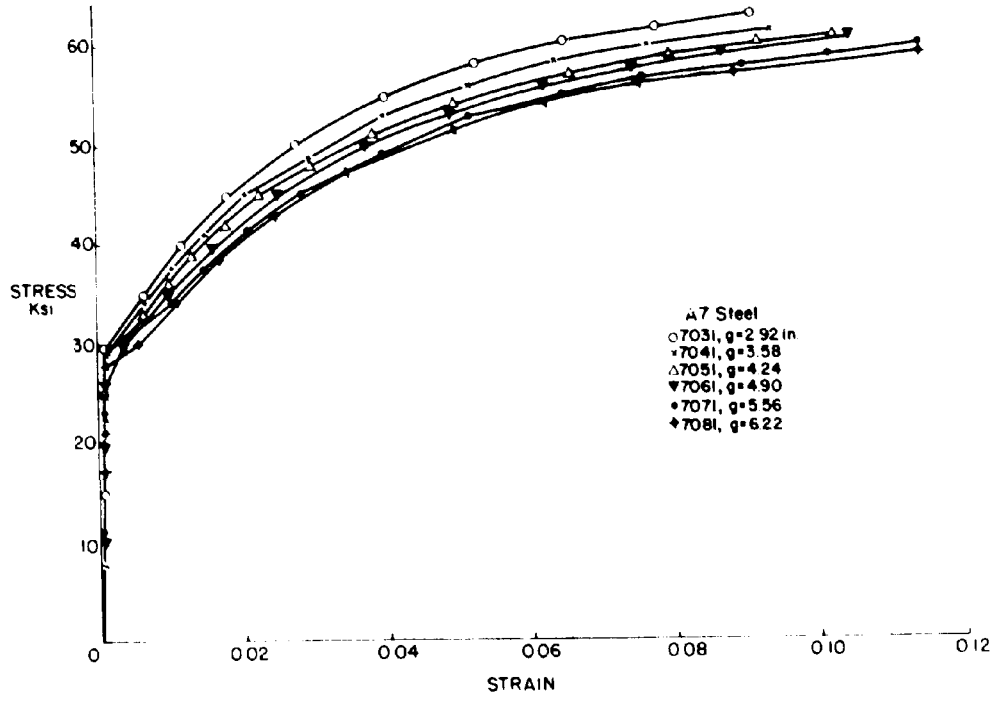

Fig. 14 Results for A7 Steel Plate Calibration Tests

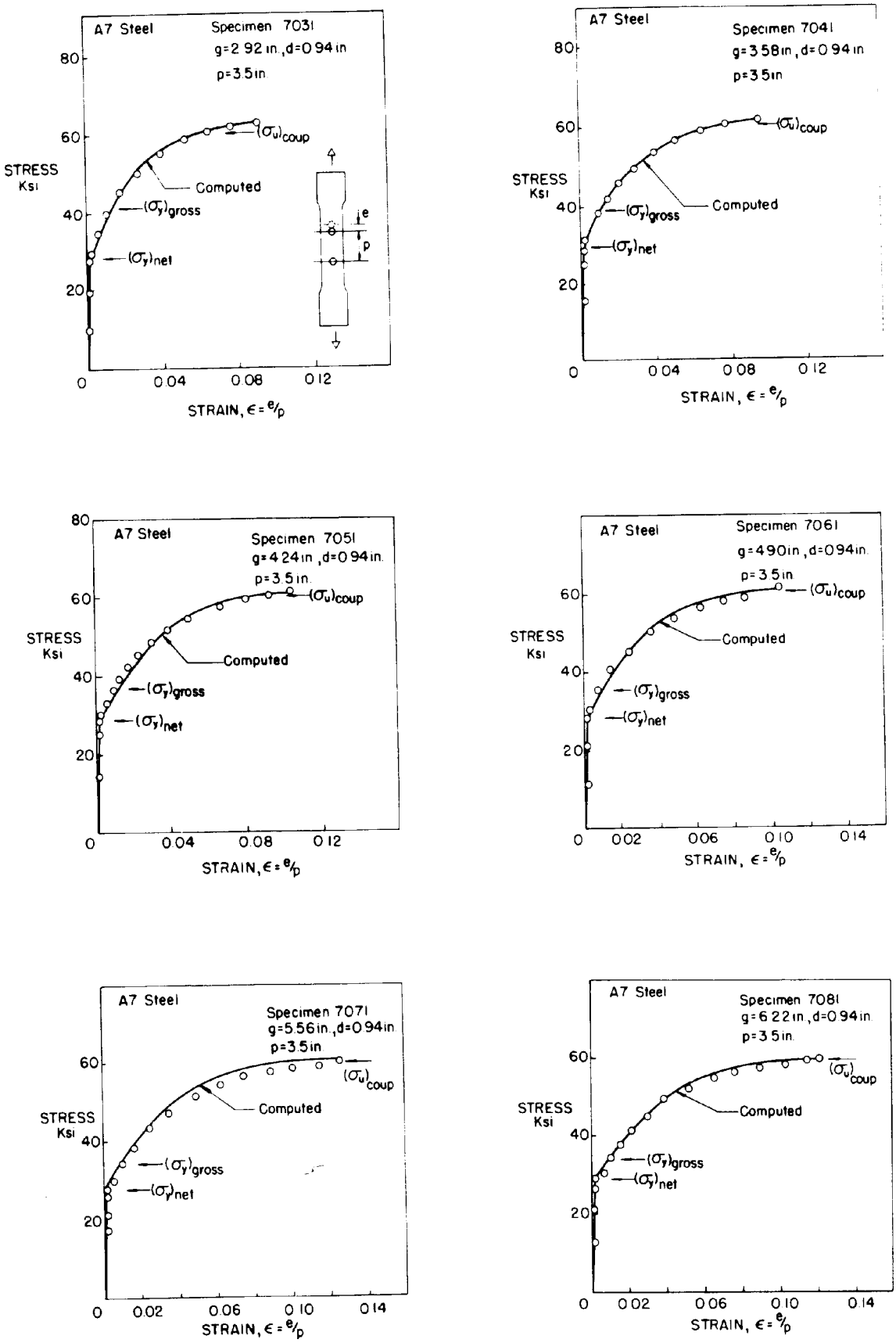

Fig. 15 Comparison Between Theory and Tests - A7 Steel

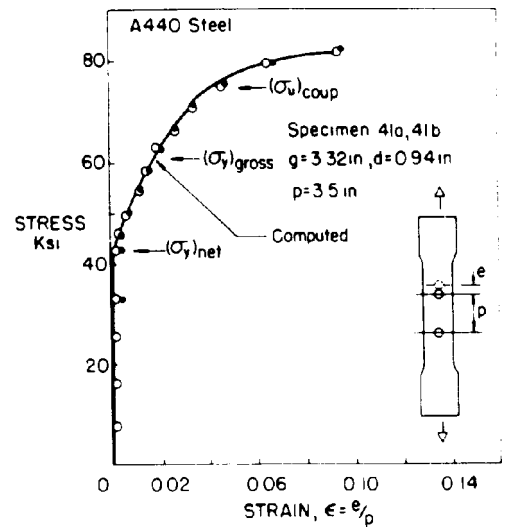

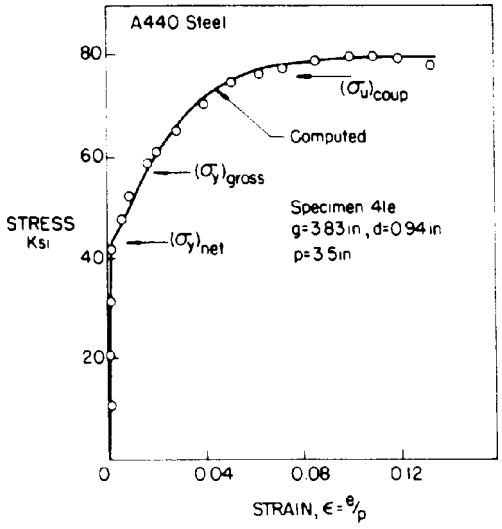

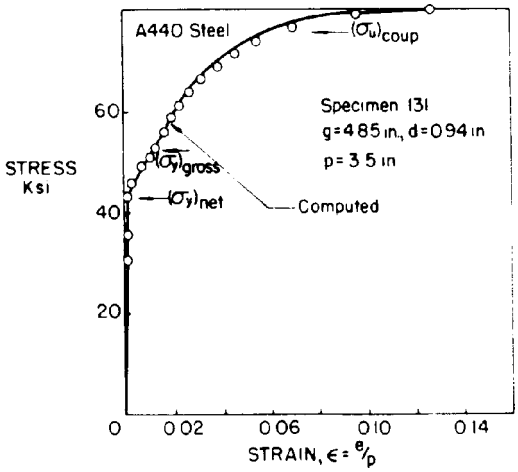

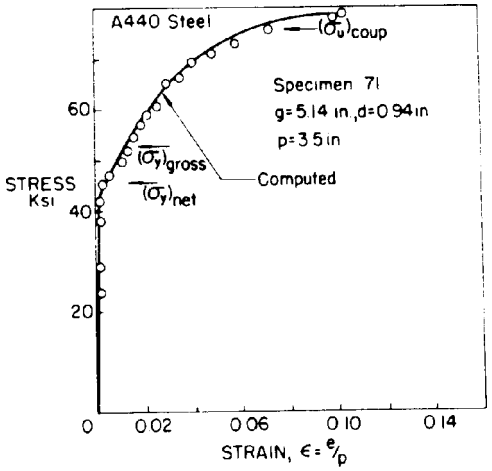

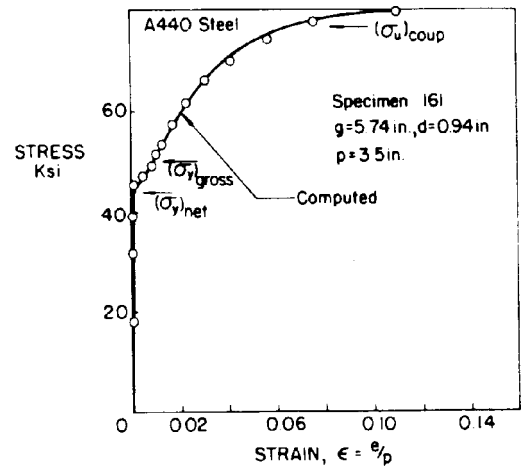

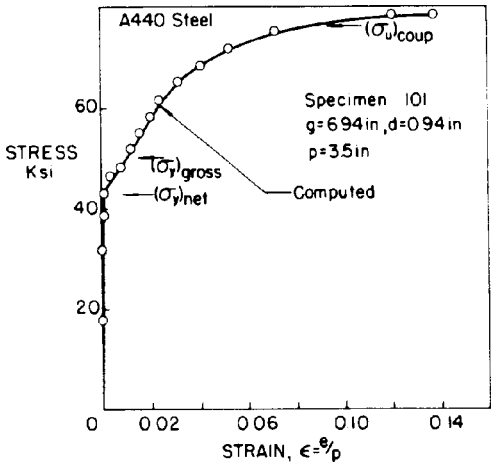

Fig. 16 Comparison Between Theory and Tests - A440 Steel

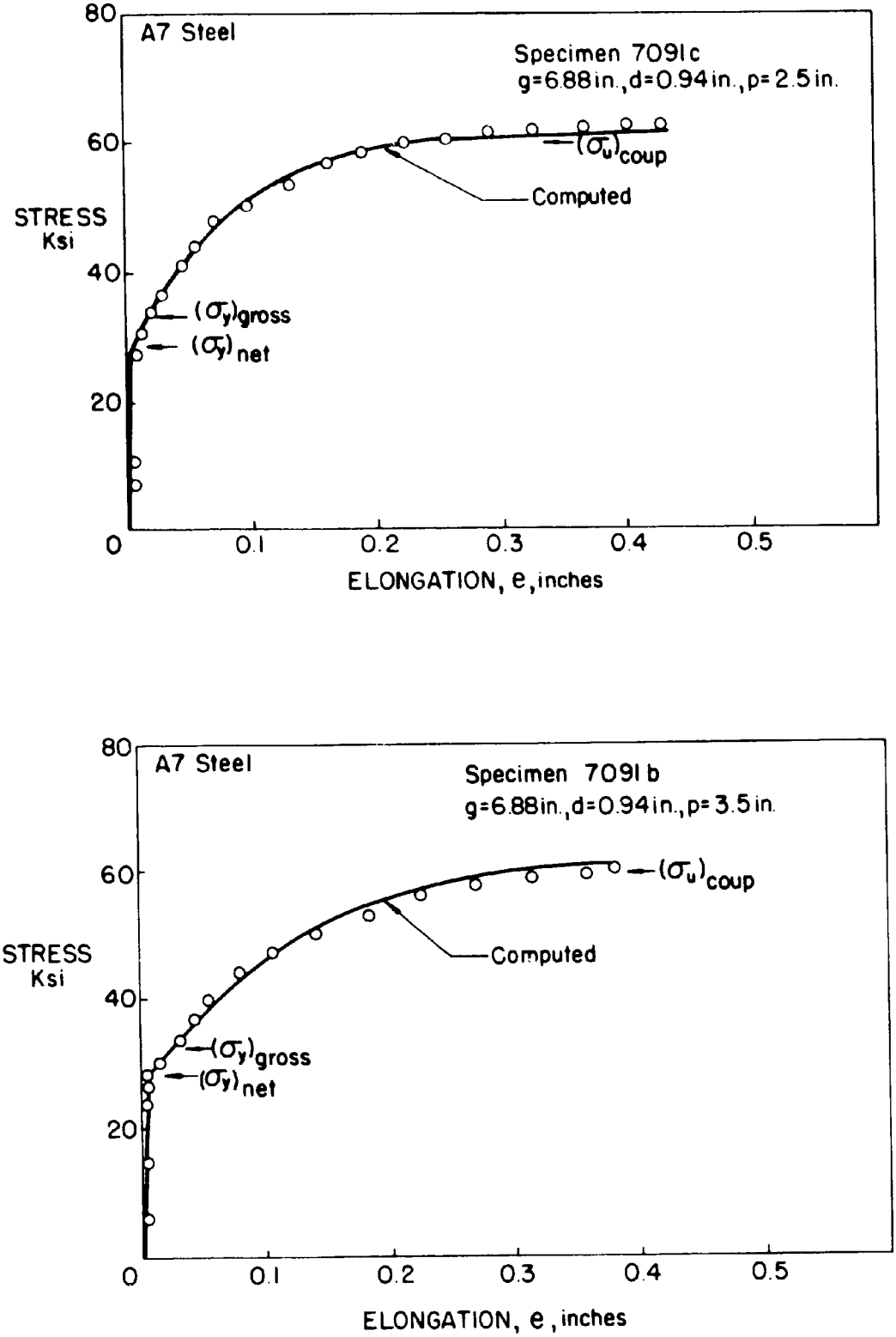

Fig. 17 Effect of Pitch; p = 2.5 in. and 3.5 in.

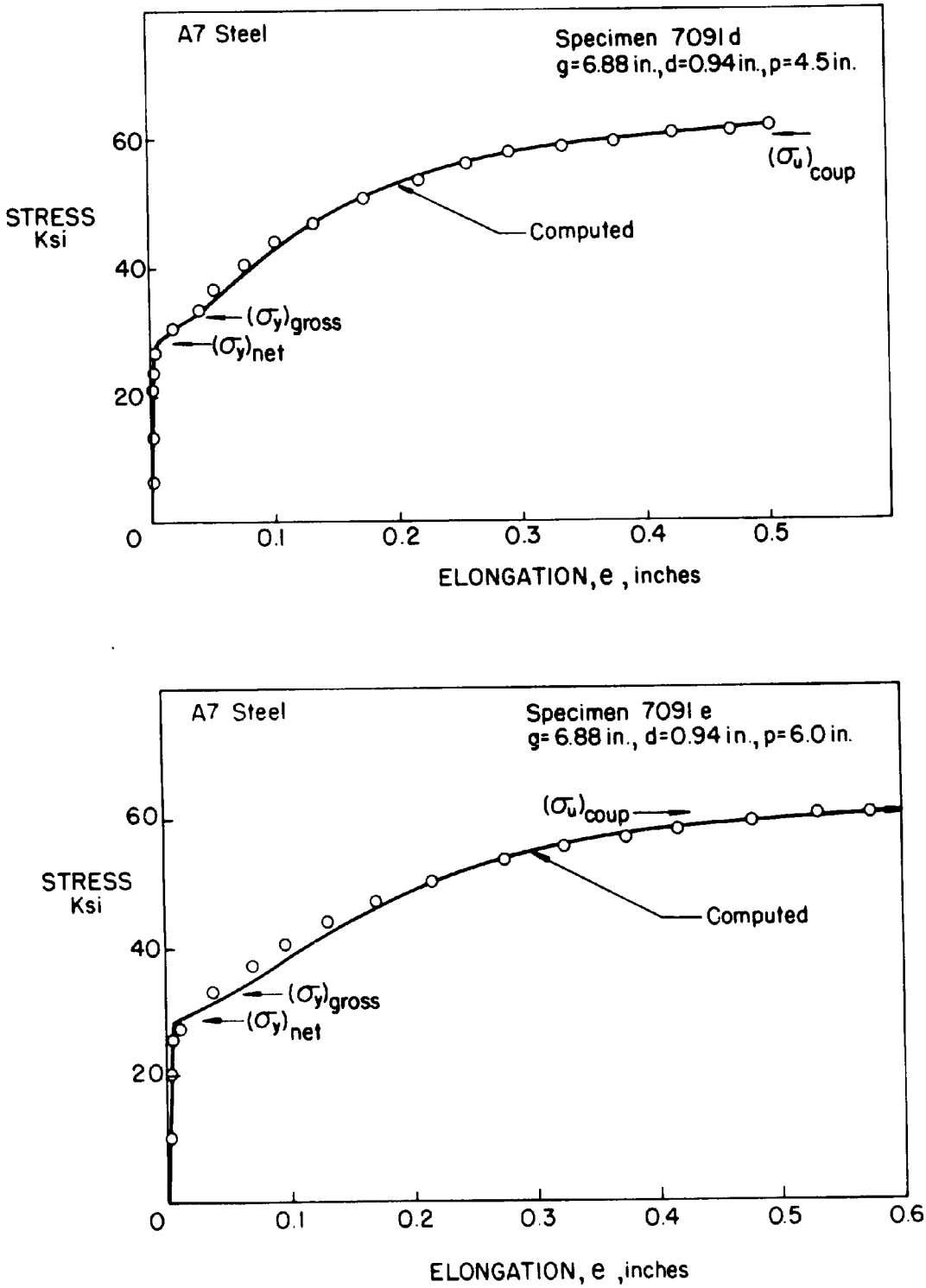

Fig. 18 Effect of Pitch; p = 4.5 in. and 6.0 in.

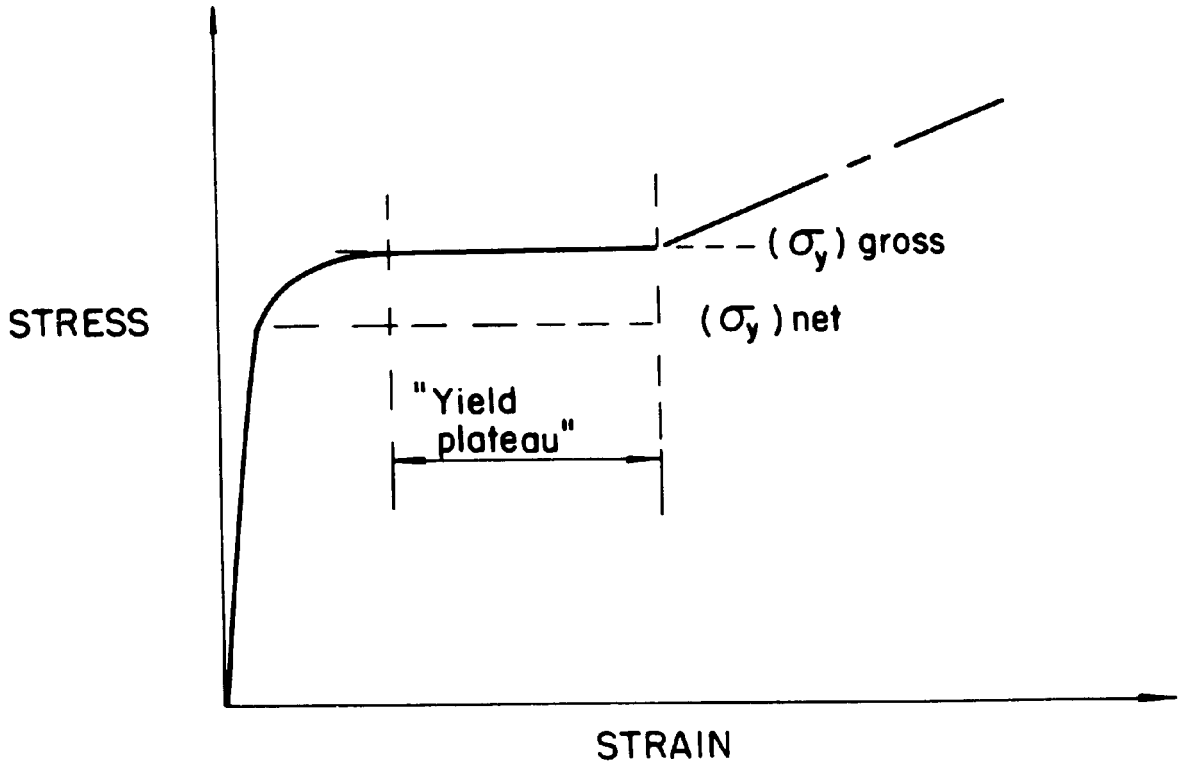

Fig. 19 Schematic Stress-Strain Diagram

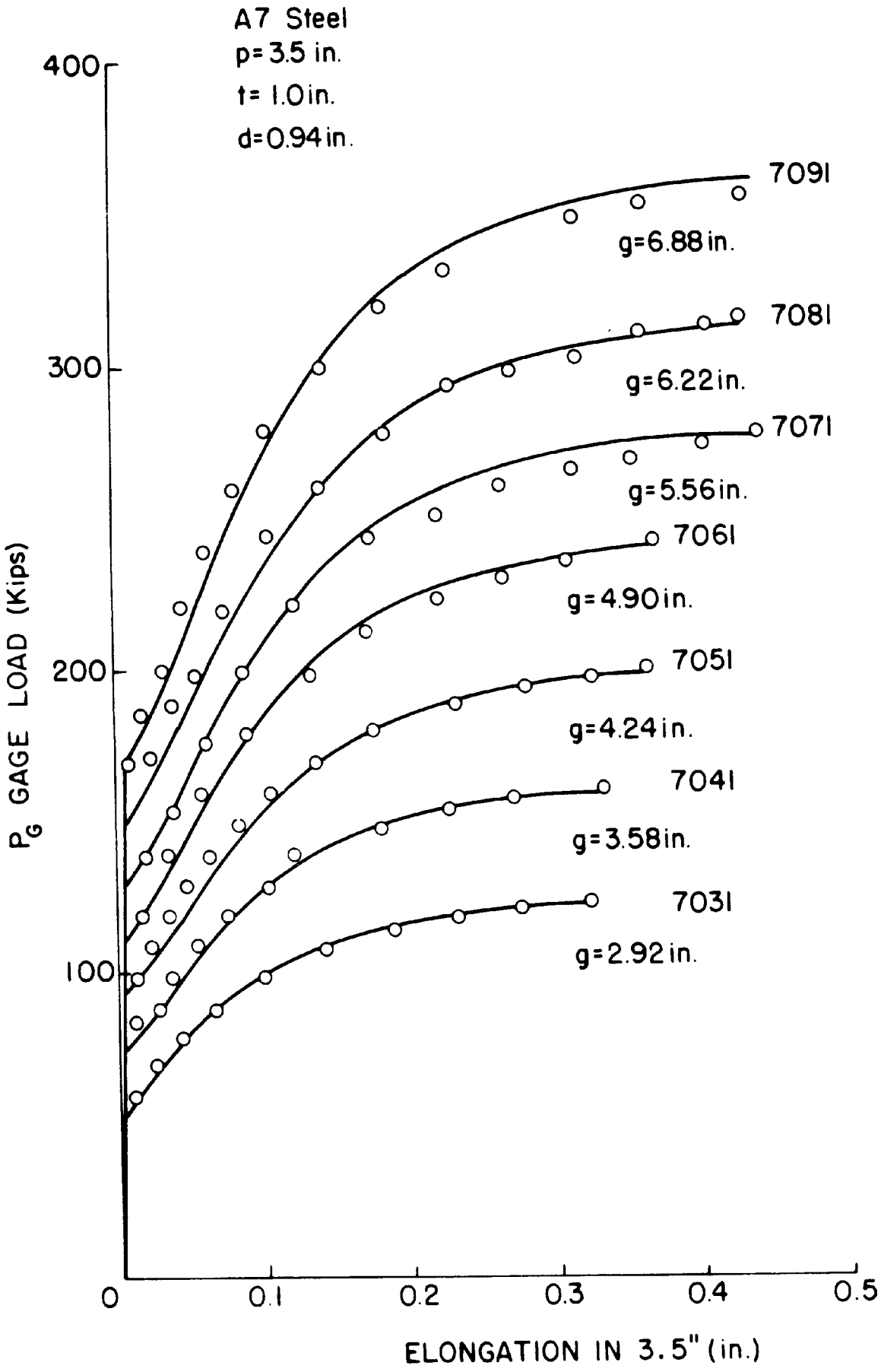

Fig. 20 Summary of Plate Calibration Tests for A7 Steel Plate

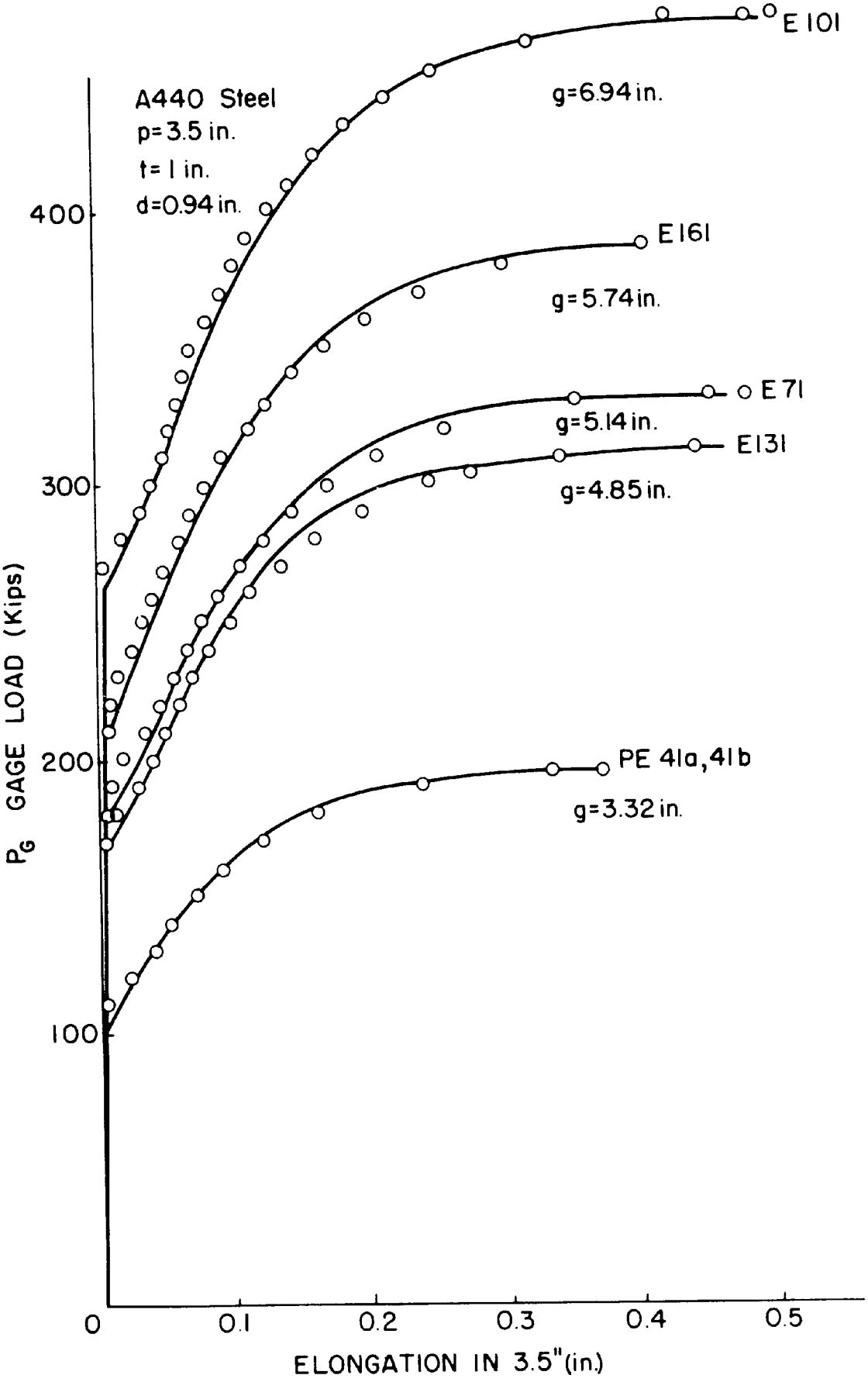

Fig. 21 Summary of Plate Calibration Tests for A440 Steel Plate

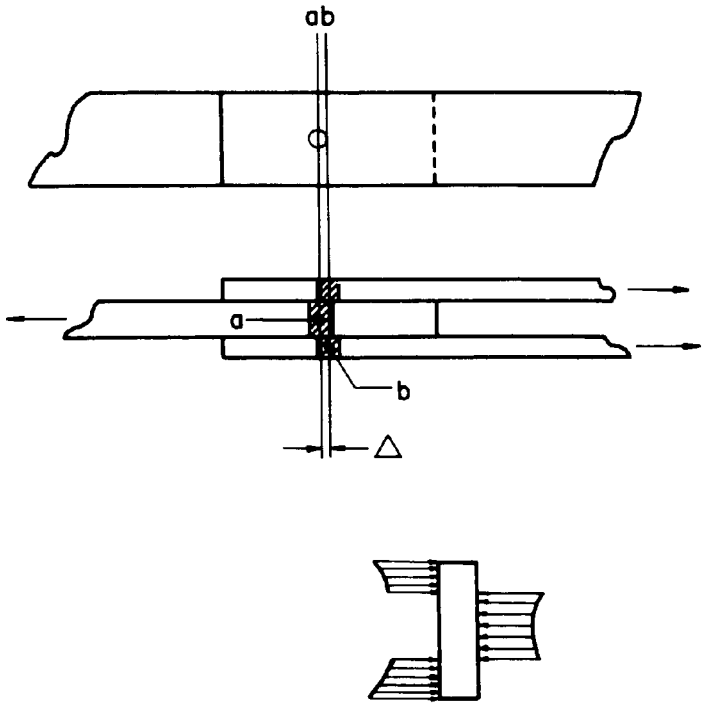

Fig. 22 Deformation of a Single Bolt

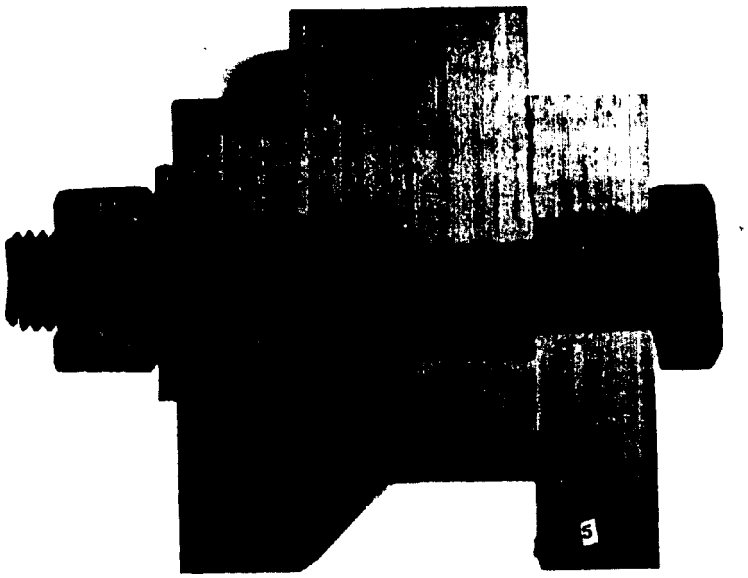

Fig. 23 Sawed Section of a Single Bolt

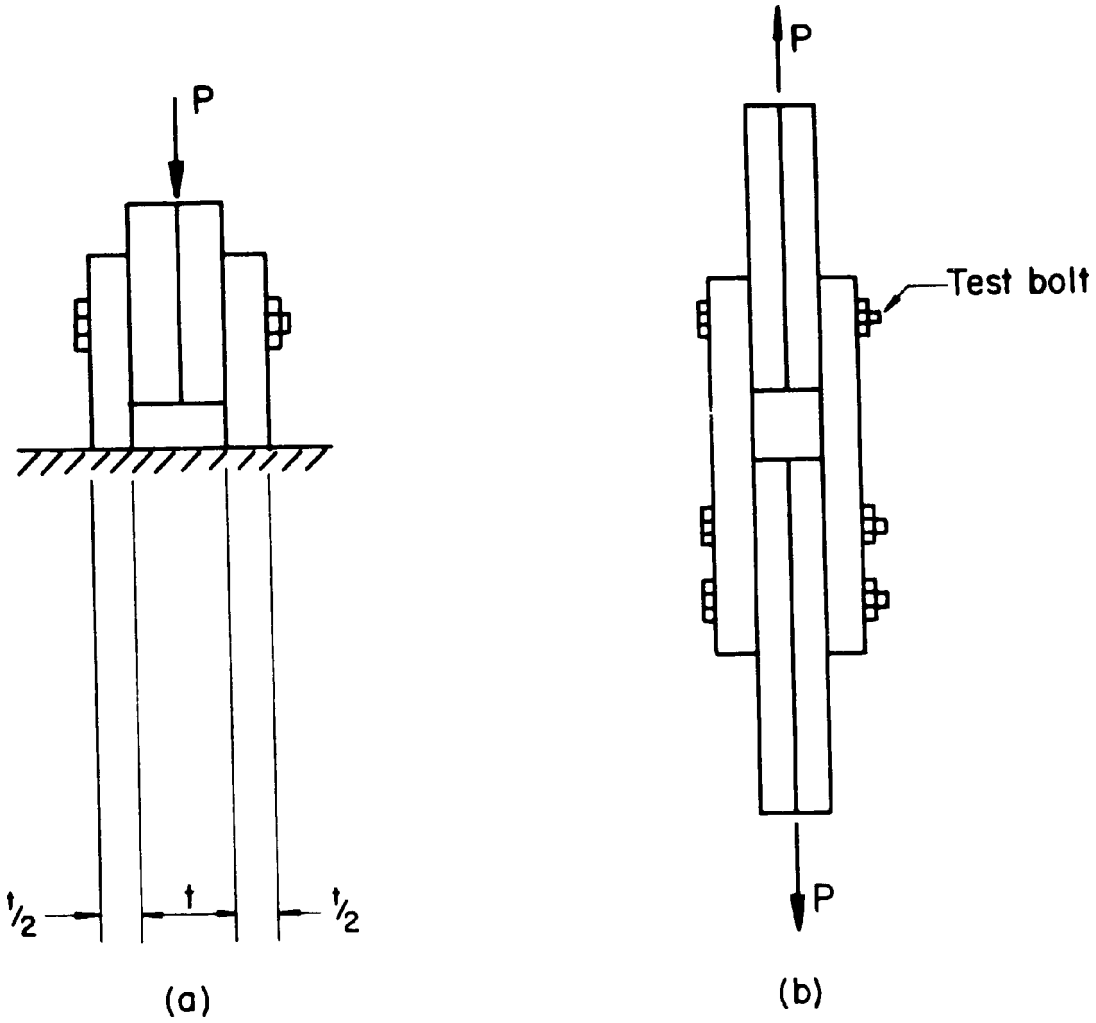

Fig. 24 Testing Jigs for Single Bolts

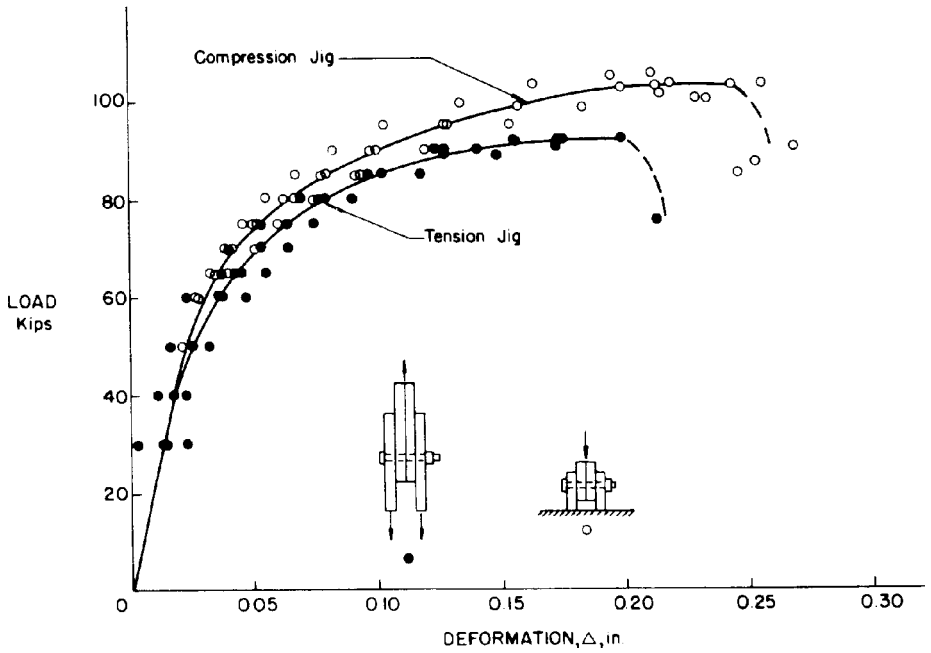

Fig. 25 Typical Load-Deformation Data for A325 Bolts Connecting A440 Steel

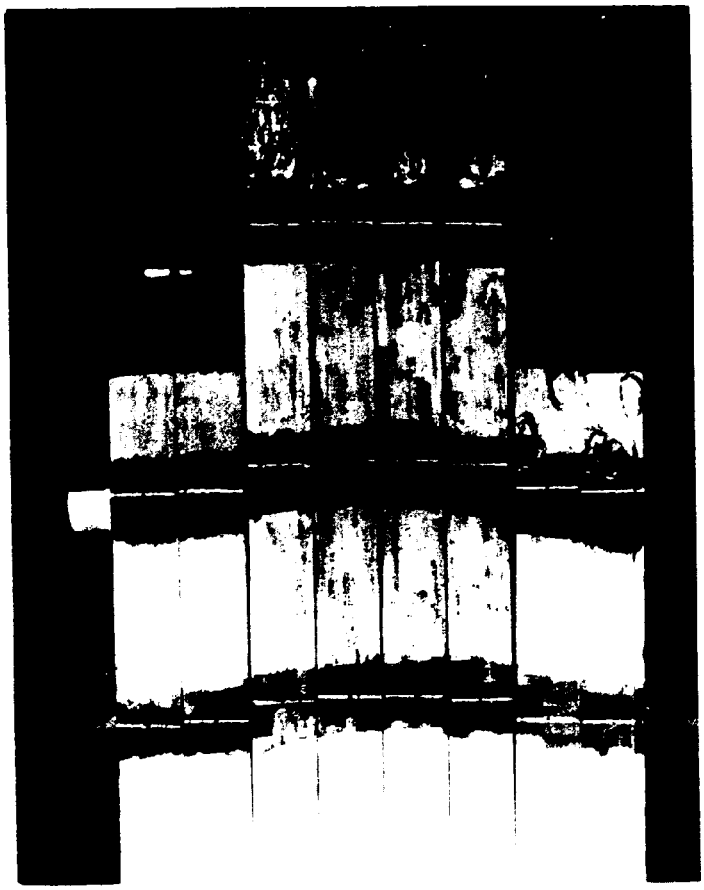

Fig. 26 A Long Joint with Lap Plate Prying

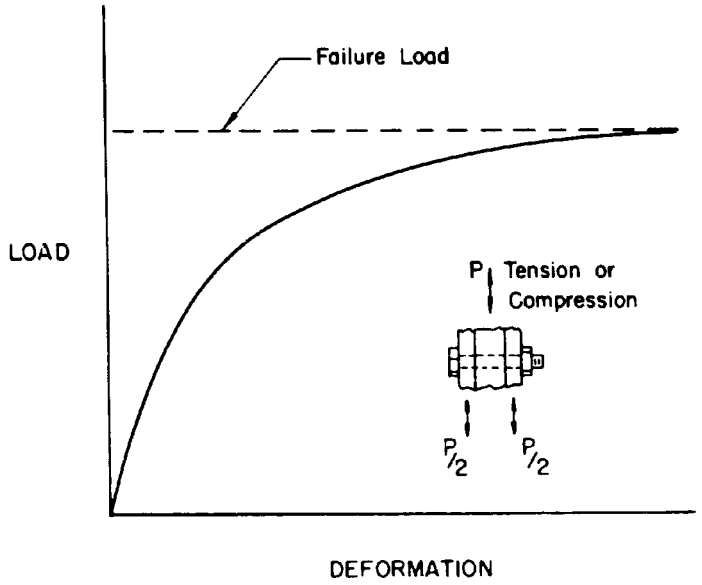

Fig. 27 Idealized Load-Deformation Relationship for Single Bolt

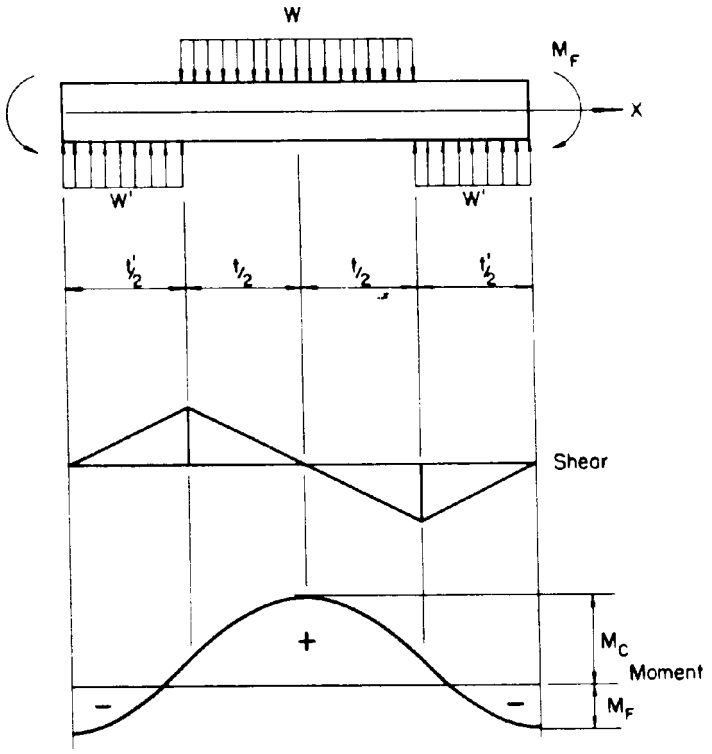

Fig. 28 Assumed Loading on Bolt for Elastic Analysis of Bolt Parameters (Ref. 29)

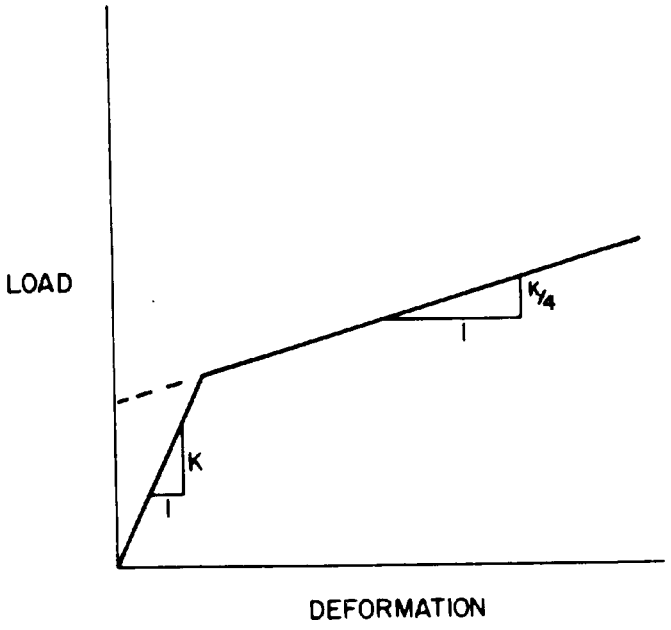

Fig. 29 Idealized Load-Deformation Relationship used in Ref. 14

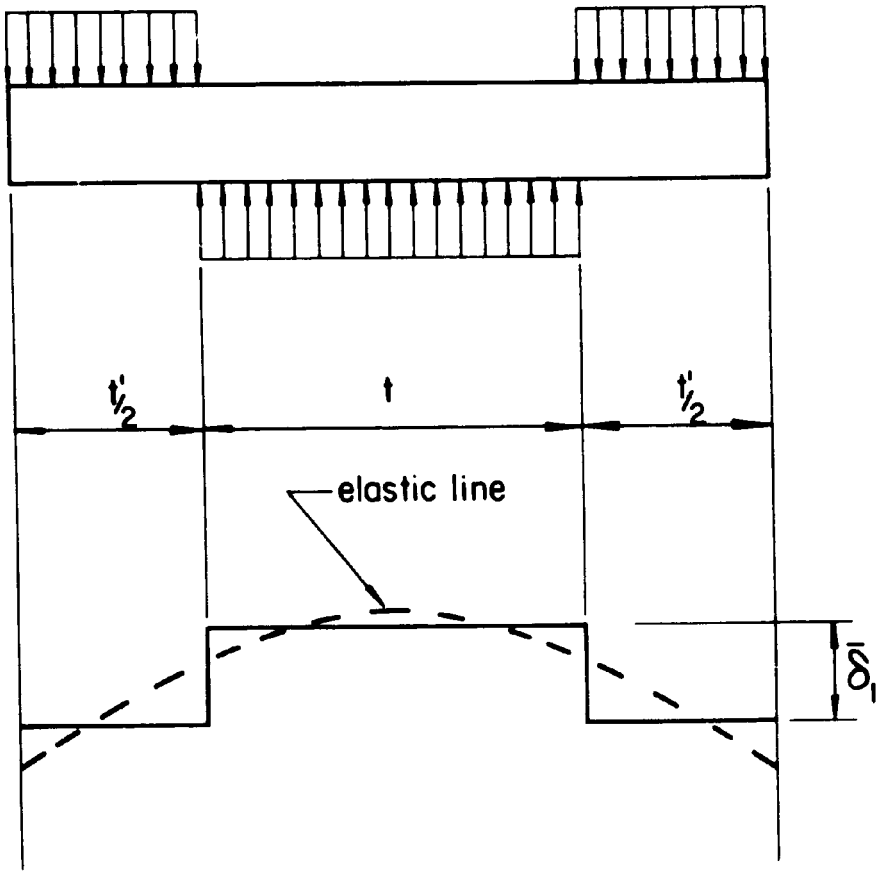

Fig. 30 Assumed Loading on Bolt or Rivet (Ref. 14)

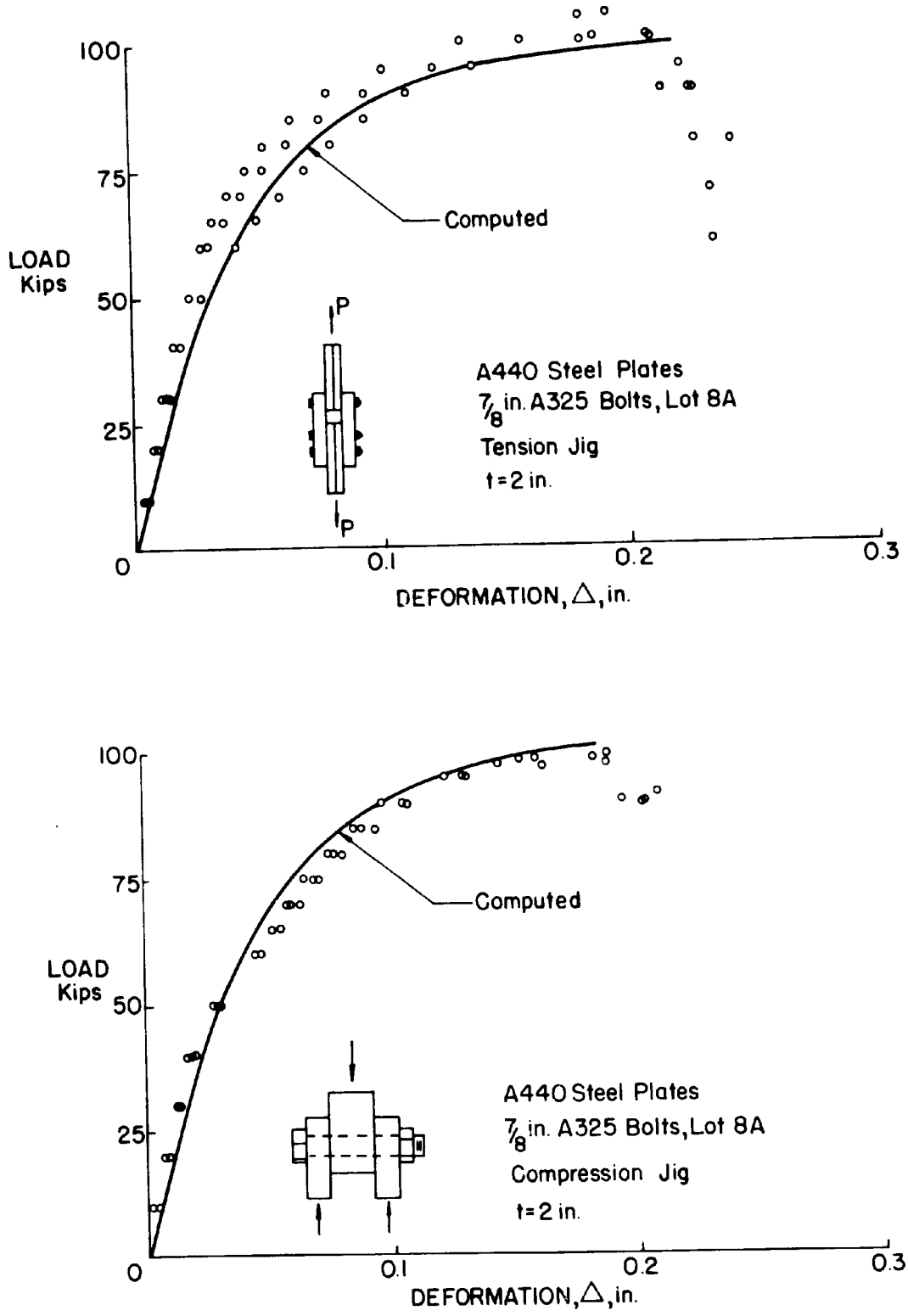

Fig. 31 Load-Deformation Relationships for A325 Bolts in A440 Steel - Lot 8A

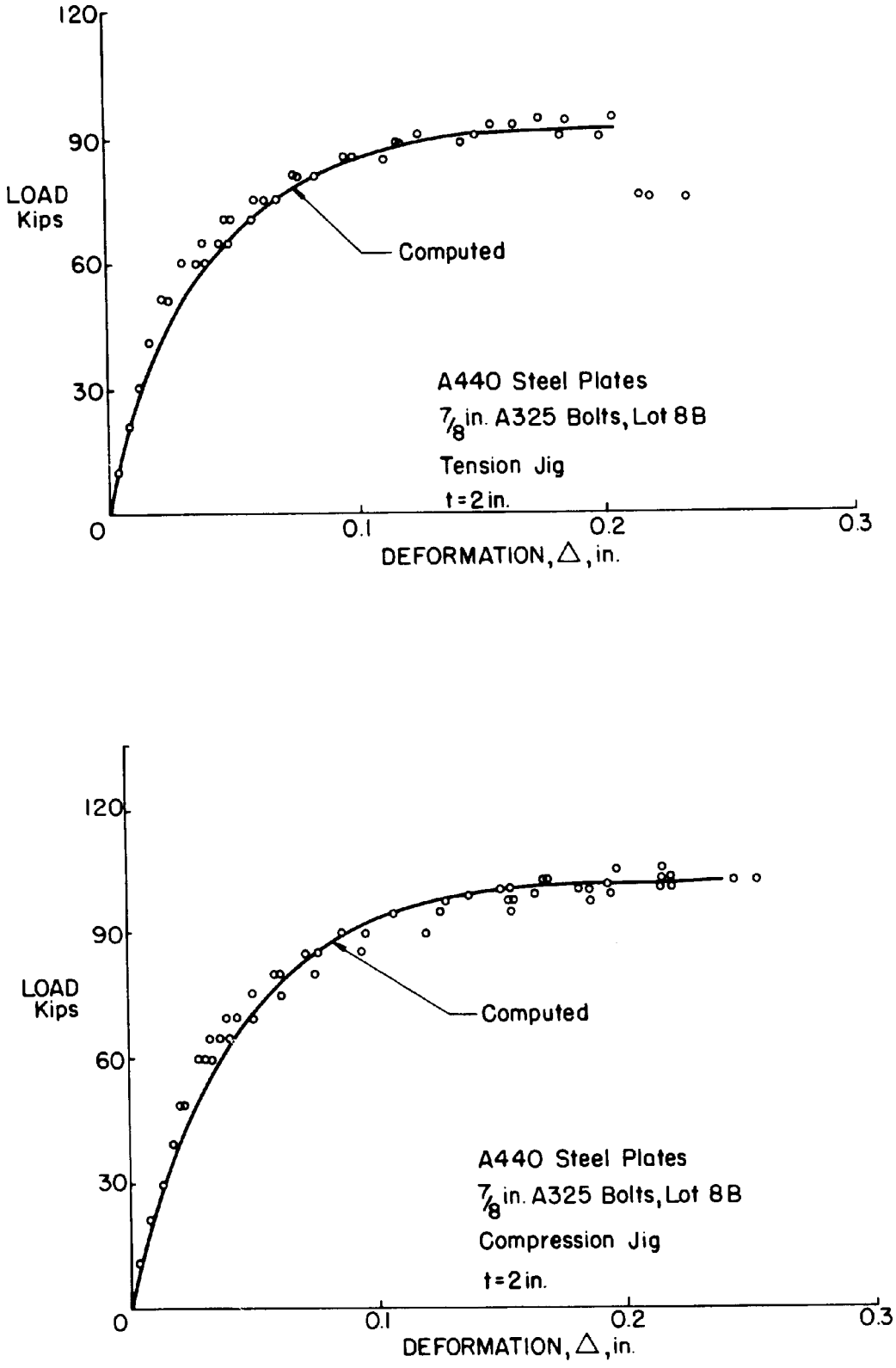

Fig. 32 Load-Deformation Relationships for A325 Bolts in A440 Steel - Lot 8B

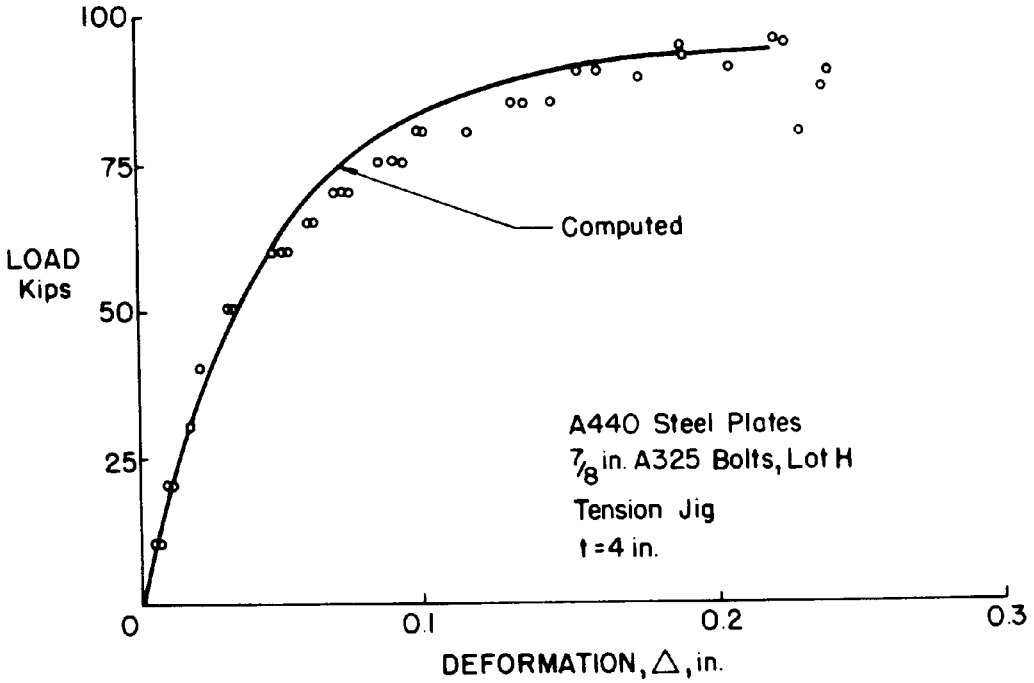

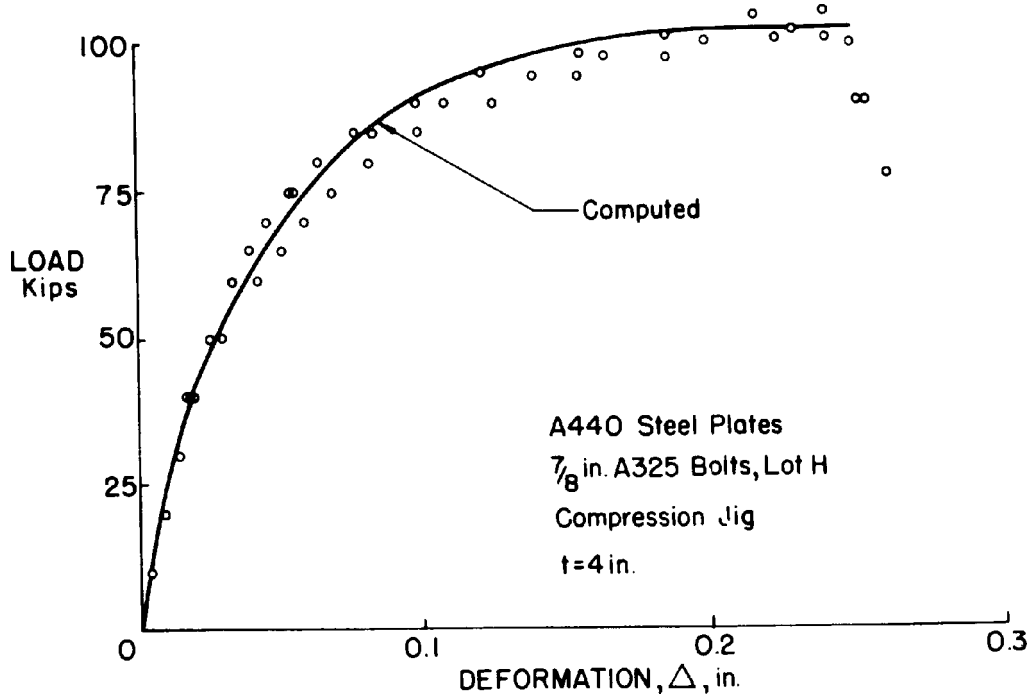

Fig. 33 Load-Deformation Relationships for A325 Bolts in A440 Steel - Lot H

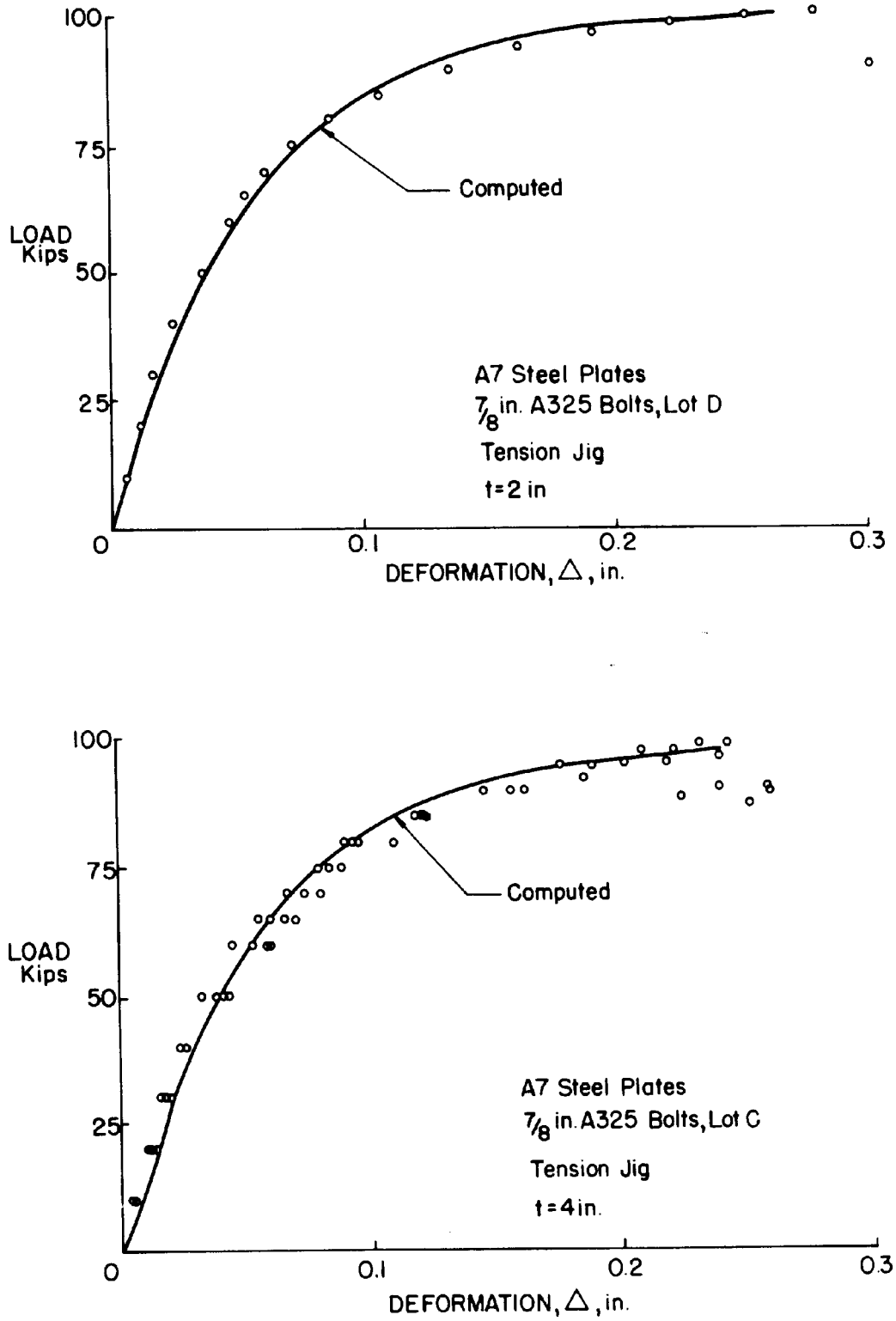

Fig. 34 Load-Deformation Relationships for A325 Bolts in A7 Steel-Lot C, D

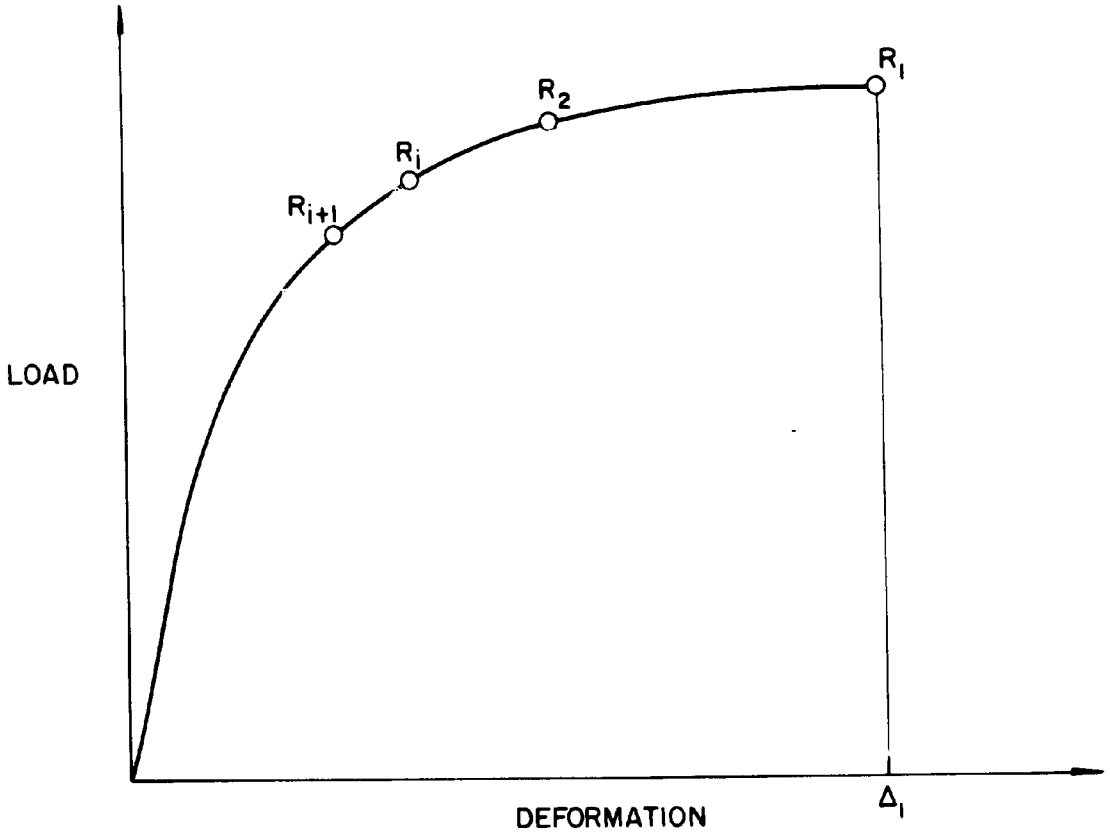

Fig. 35 Location of Bolt Forces on Load-Deformation Curve

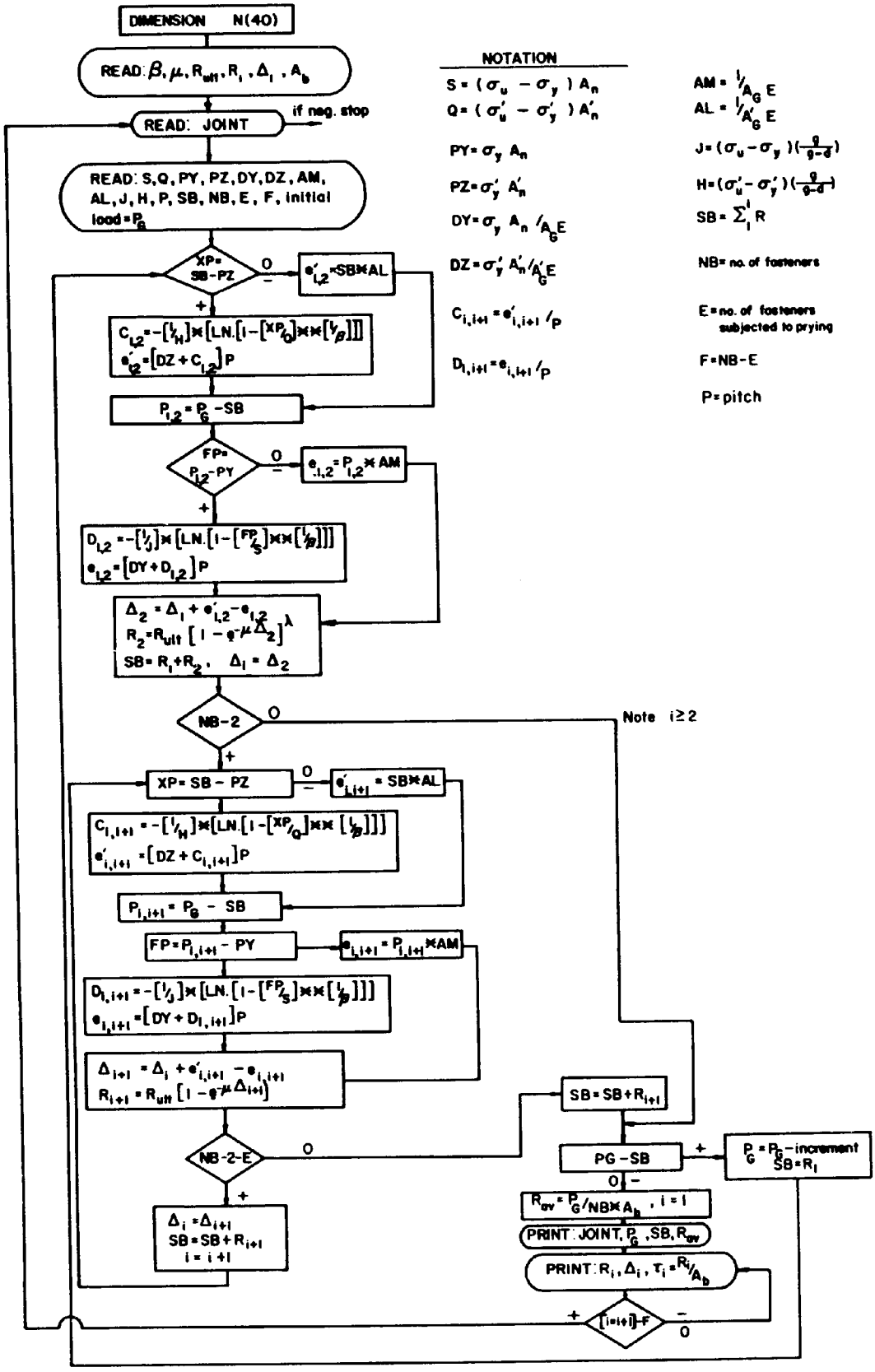

Fig. 36 Flow Diagram for Load Partition Computations

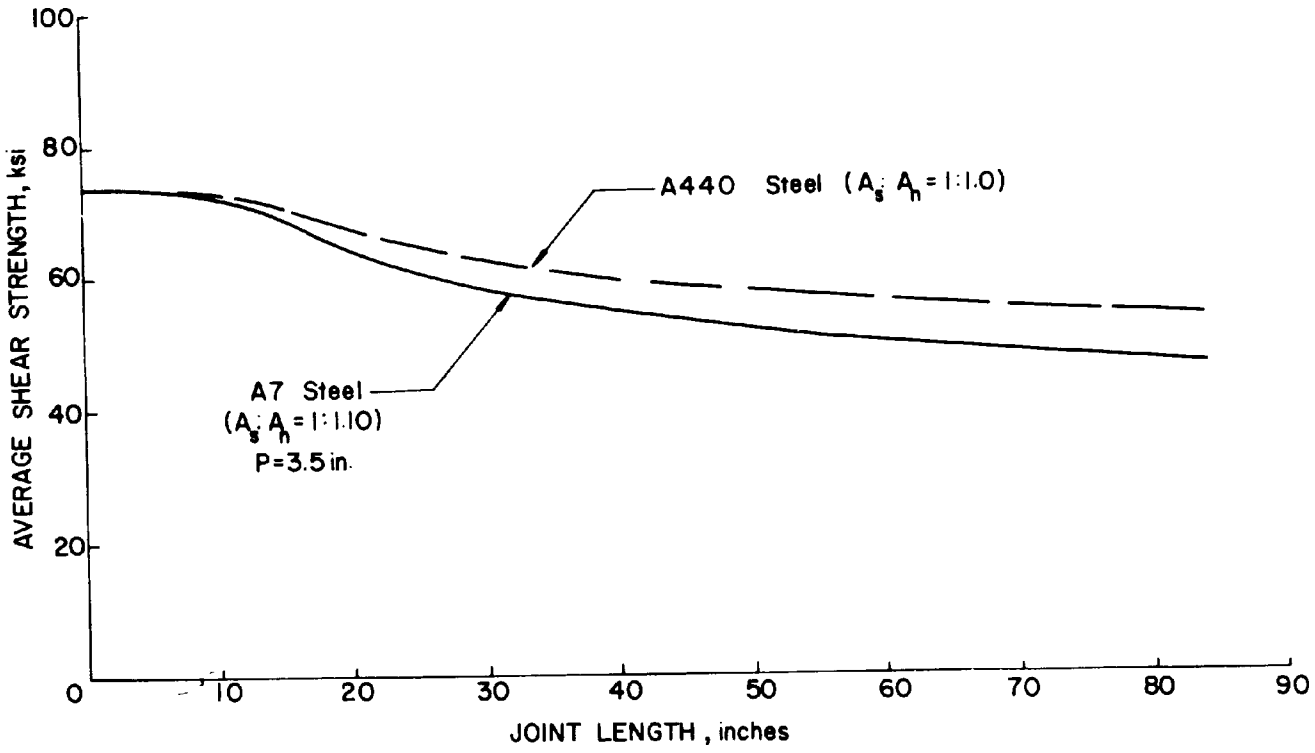

Fig. 37 Effect of Joint Length on Ultimate Strength for "Balanced Design"

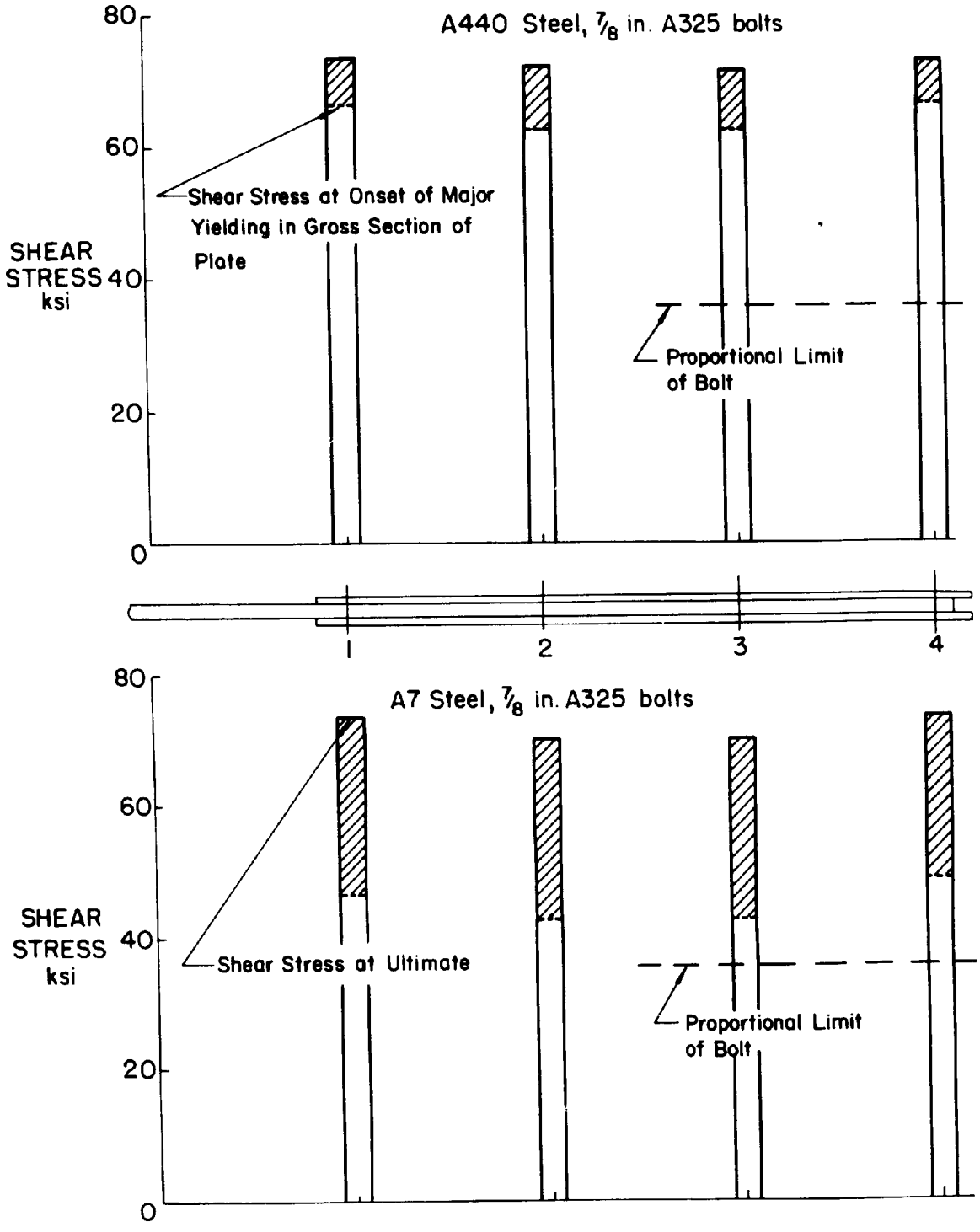

Fig. 38 Load Partition in Joints with Four Fasteners in Line

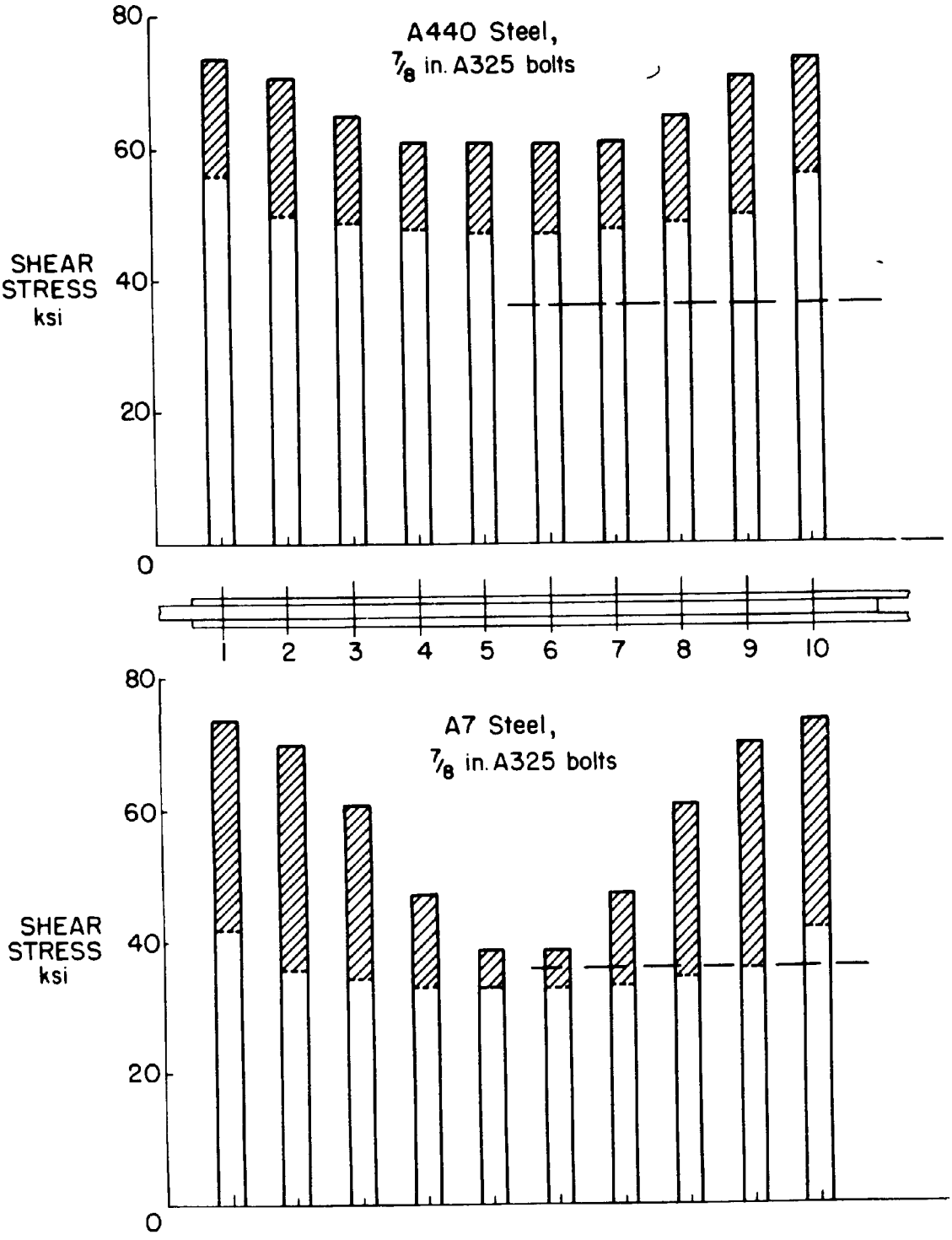

Fig. 39 Load Partition in Joints with Ten Fasteners in Line

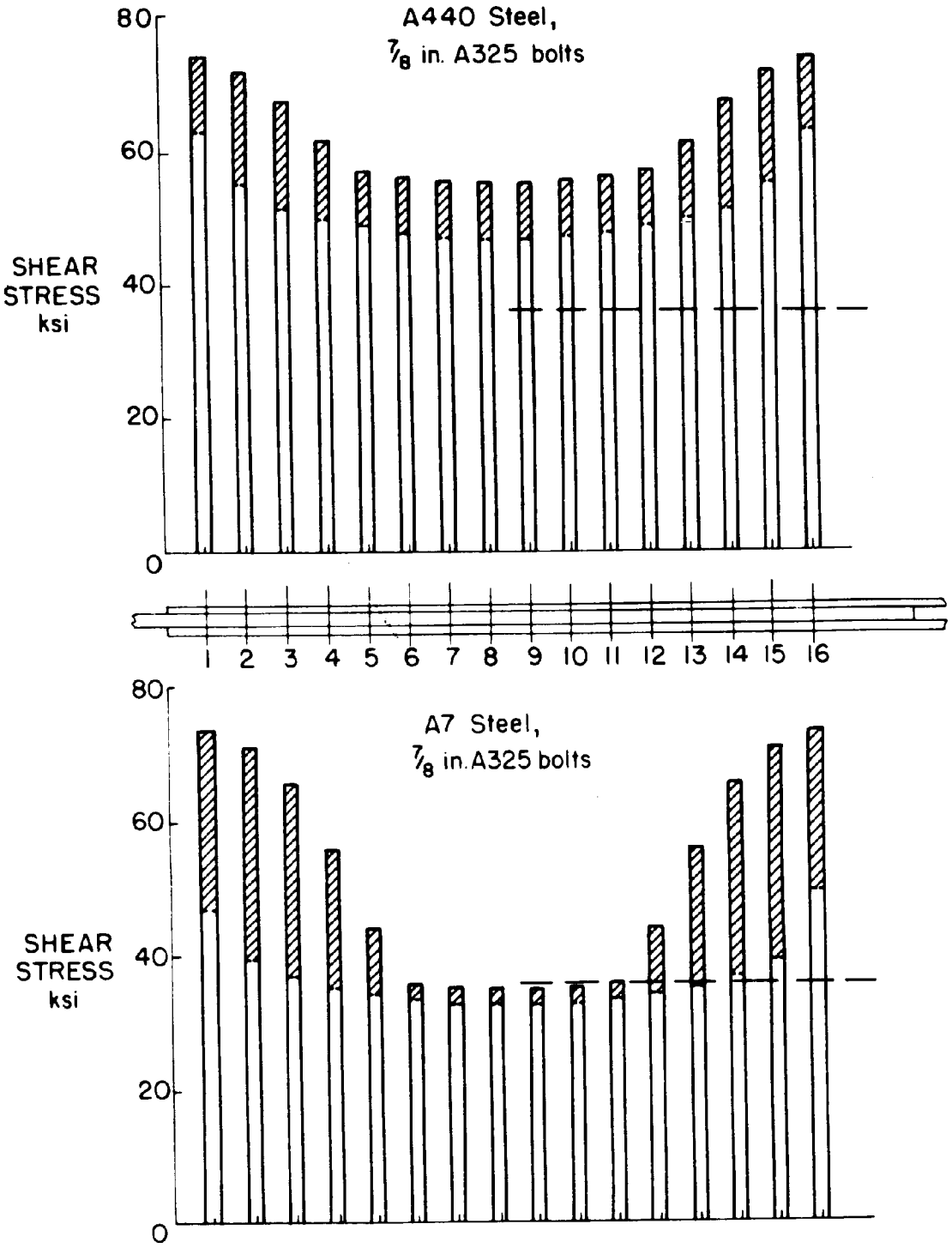

Fig. 40 Load Partition in Joints with Sixteen Fasteners in Line

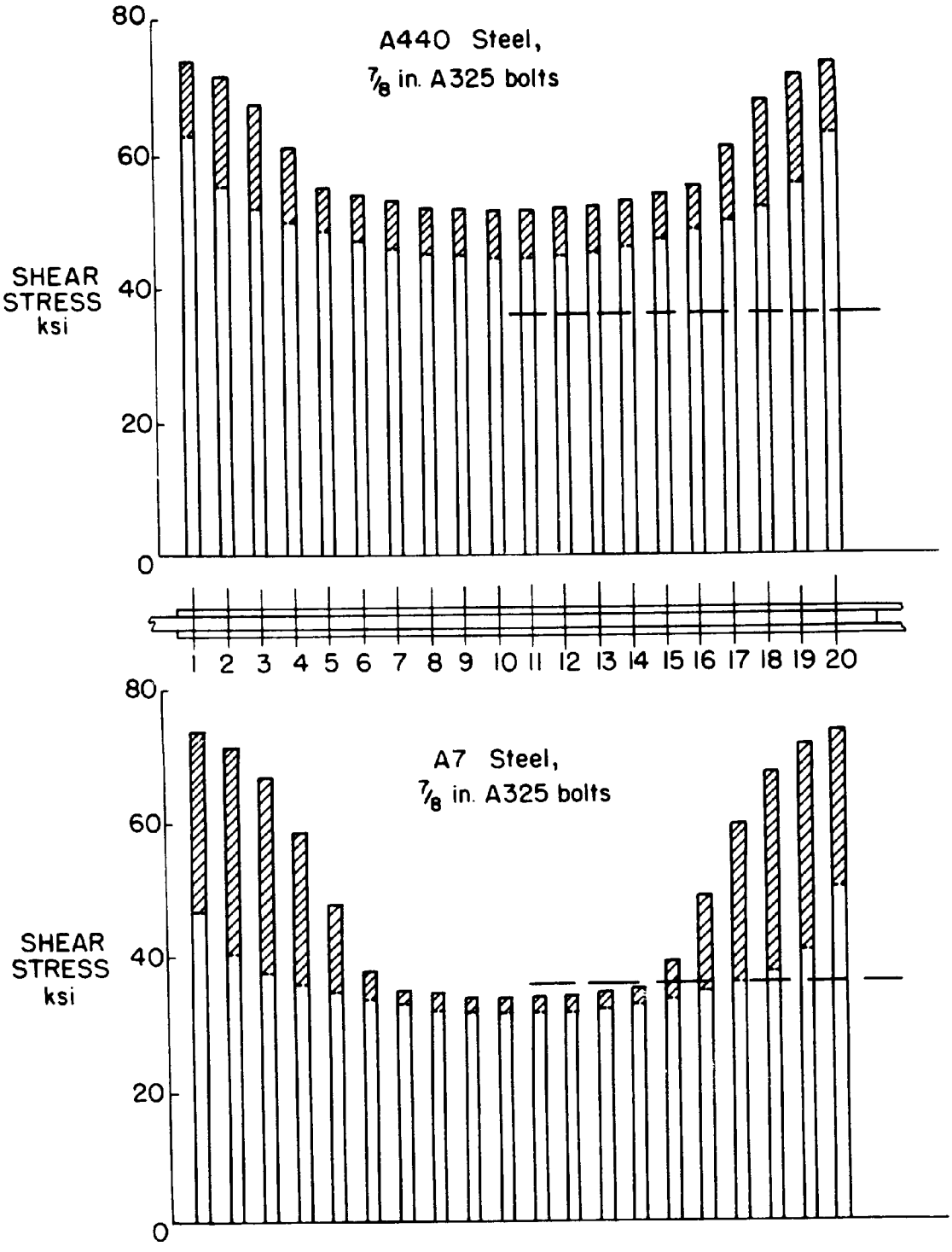

Fig. 41 Load Partition in Joints with Twenty Fasteners in Line

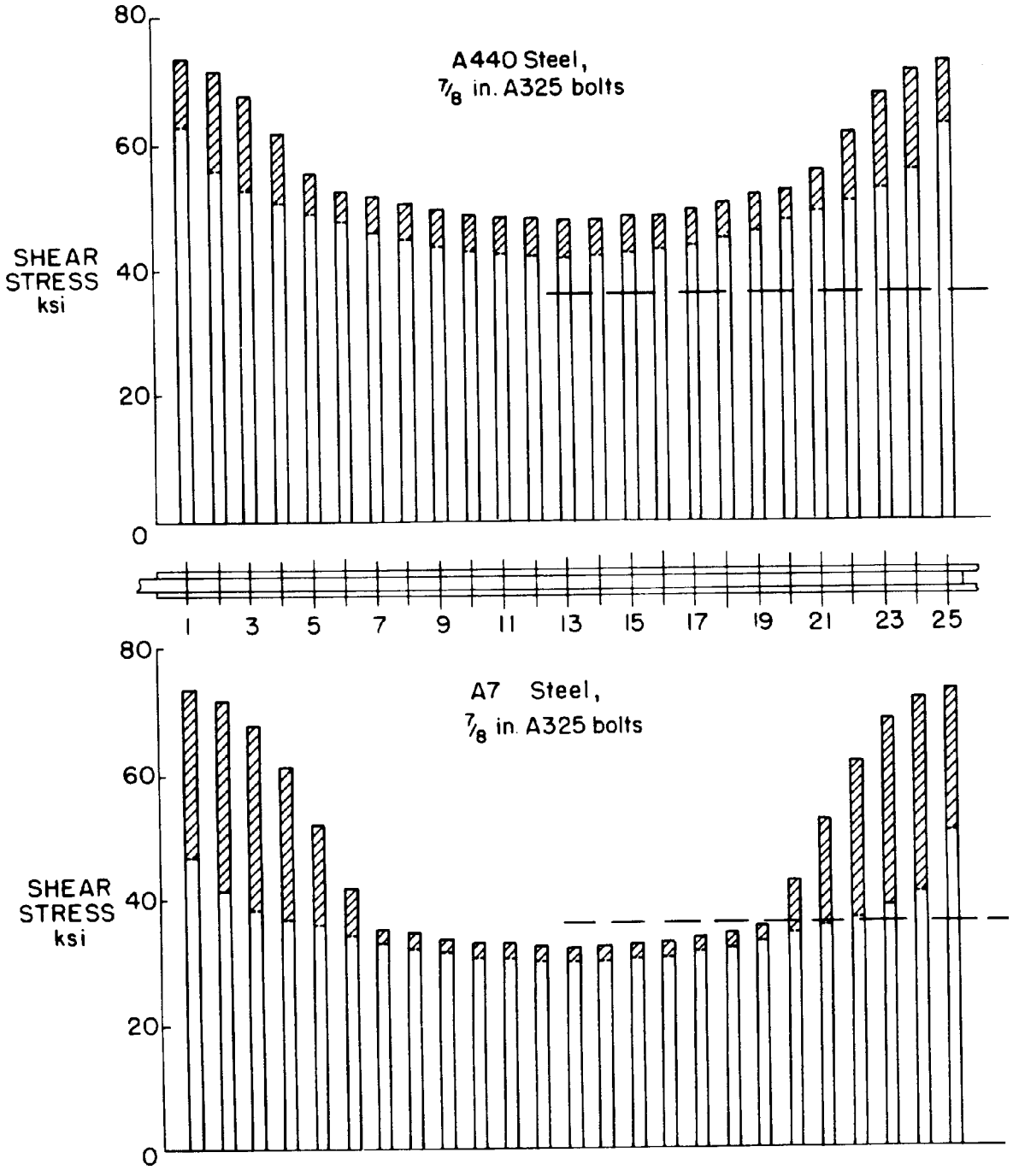

Fig. 42 Load Partition in Joints with Twenty-Five Fasteners in Line

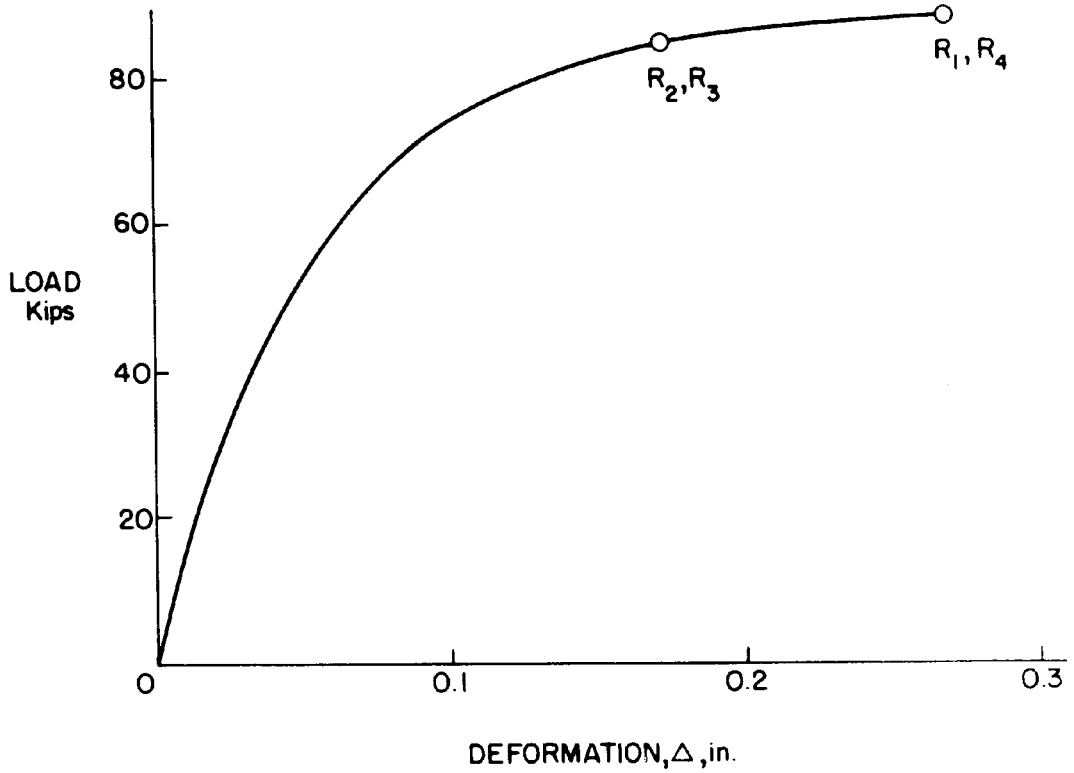

Fig. 43 Position of Individual Bolts on the Load-Deformation Curve

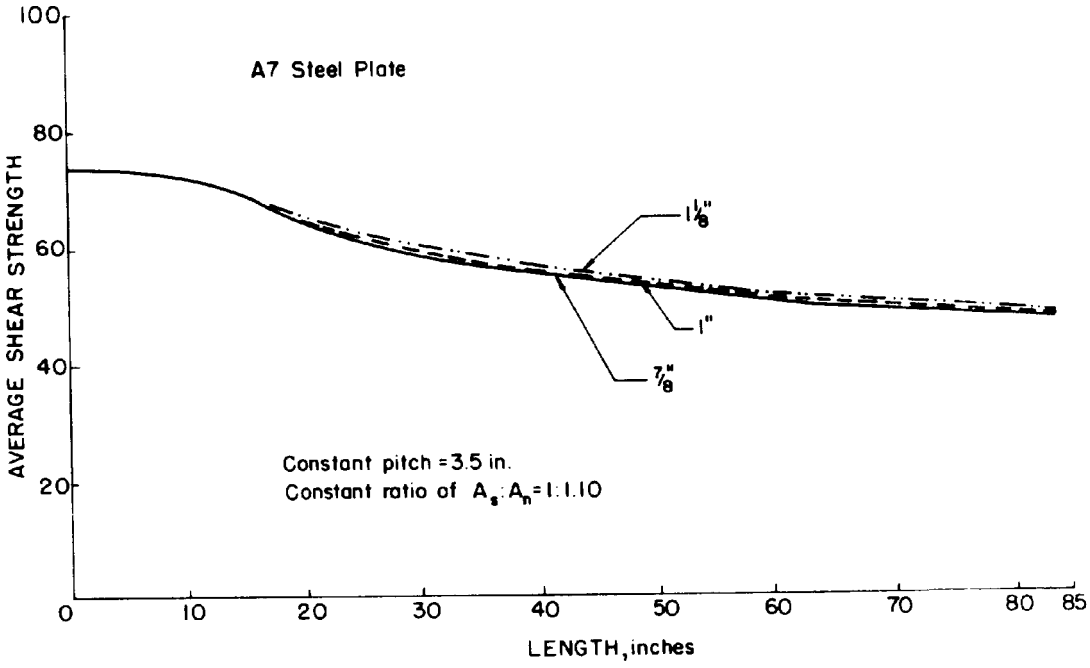

Fig. 44 Effect of Diameter of A325 Bolts on Ultimate Strength

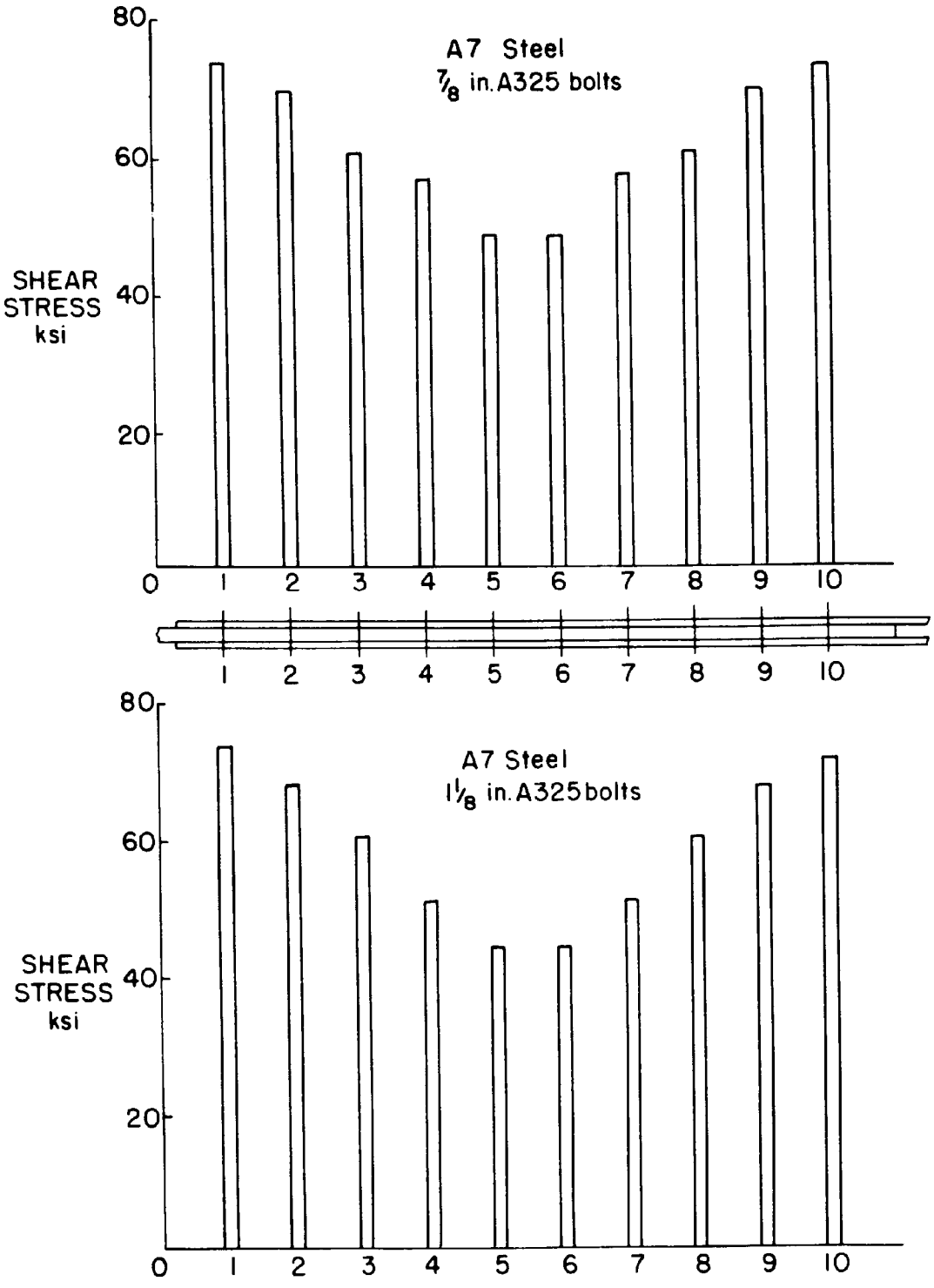

Fig. 45 Load Partition in Joints with Ten 7/8-in. and Ten 1/8-in. Bolts

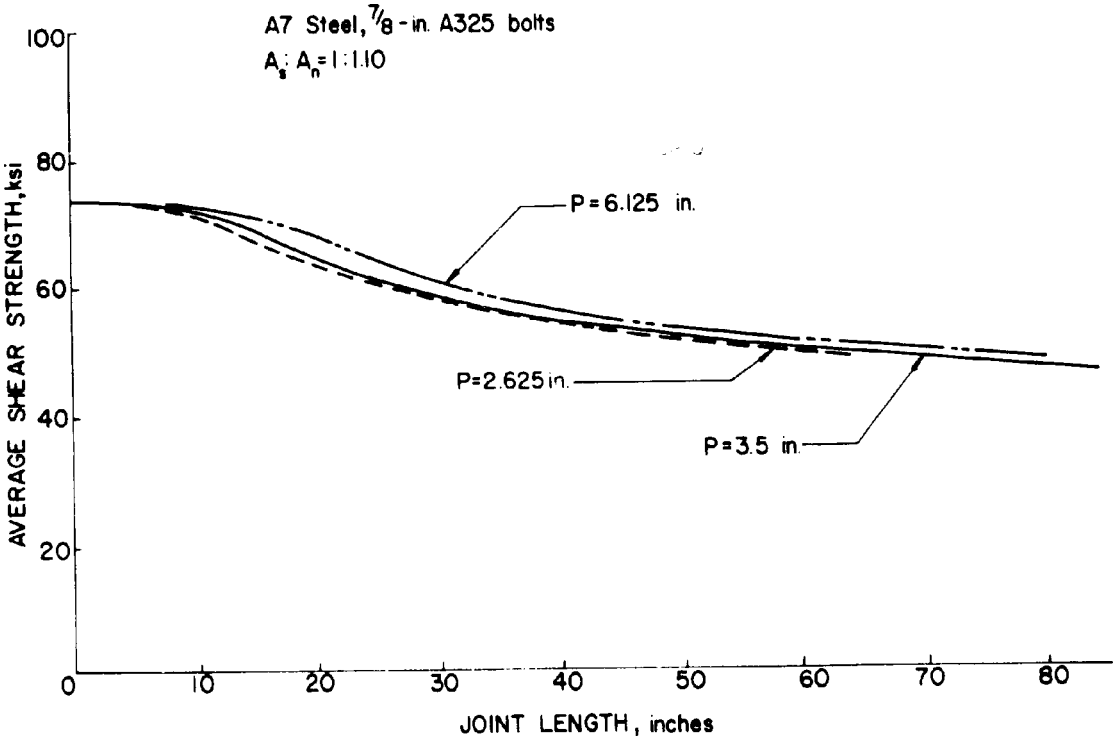

Fig. 46 Effect of Pitch on the Ultimate Strength of A7 Steel Joints

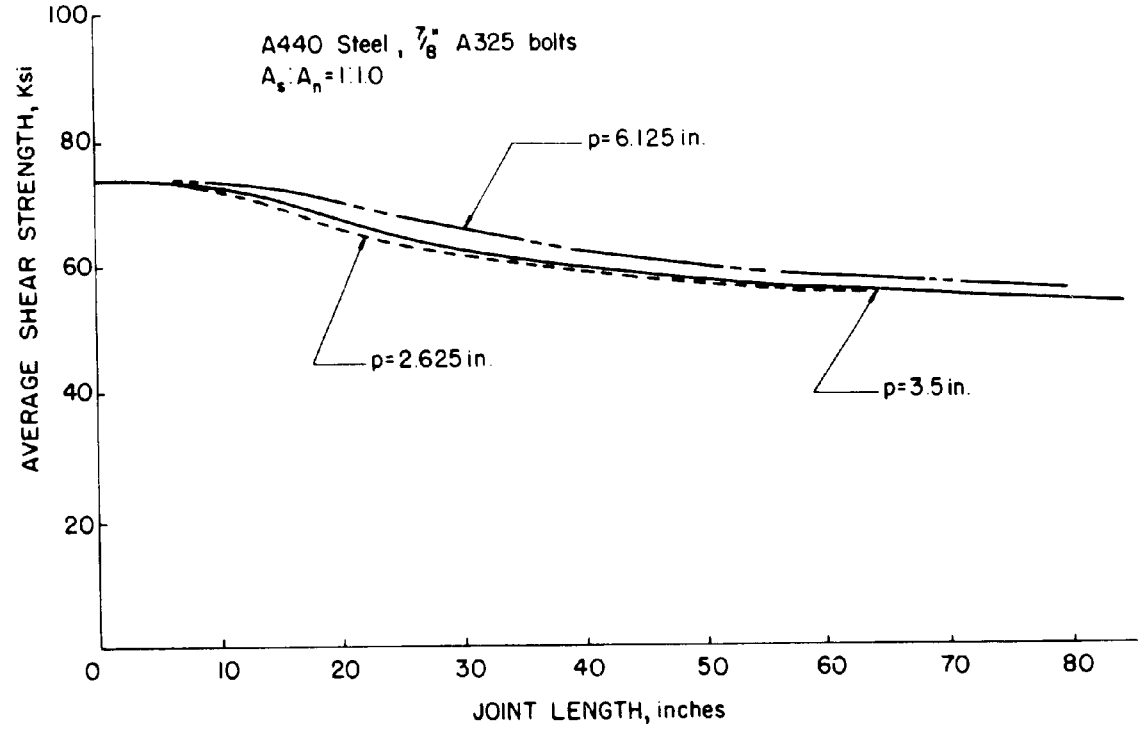

Fig. 47 Effect of Pitch on the Ultimate Strength of A440 Steel Joints

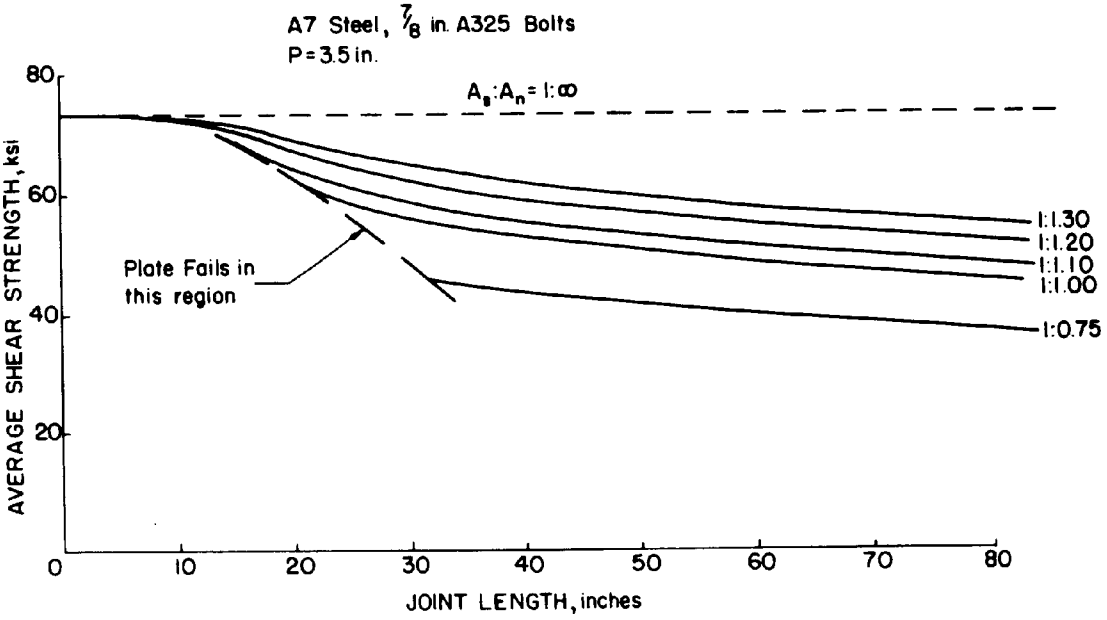

Fig. 48 Effect of Variation in the Relative Proportions of the Bolt Shear Area and the Net Tension Area - A7 Steel

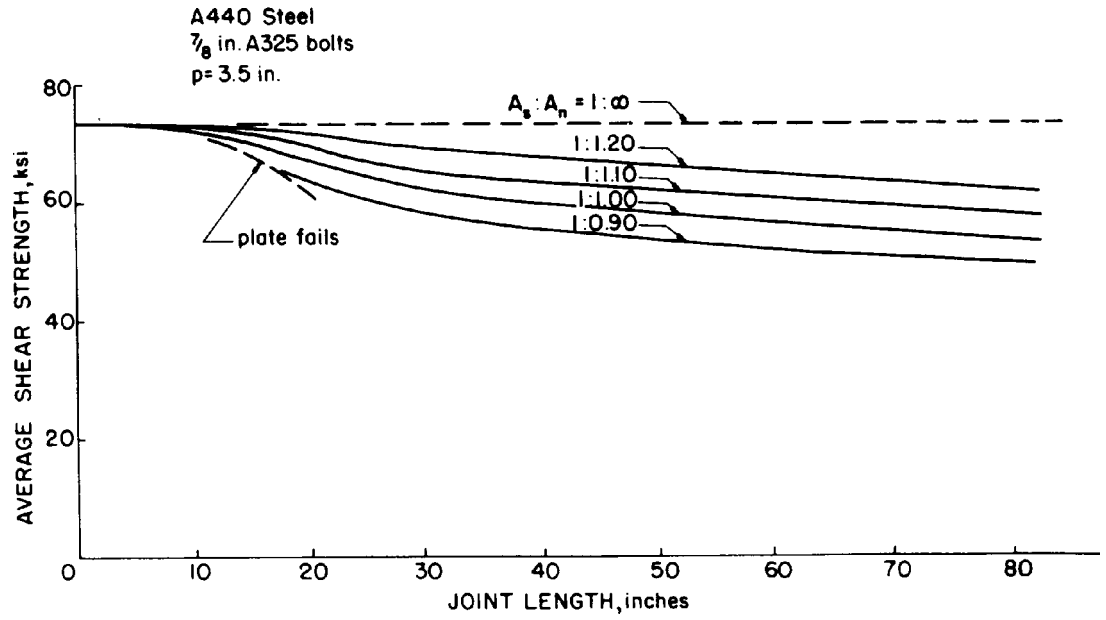

Fig. 49 Effect of Variation in the Relative Proportions of the Bolt Shear Area and the Net Tension Area - A440 Steel

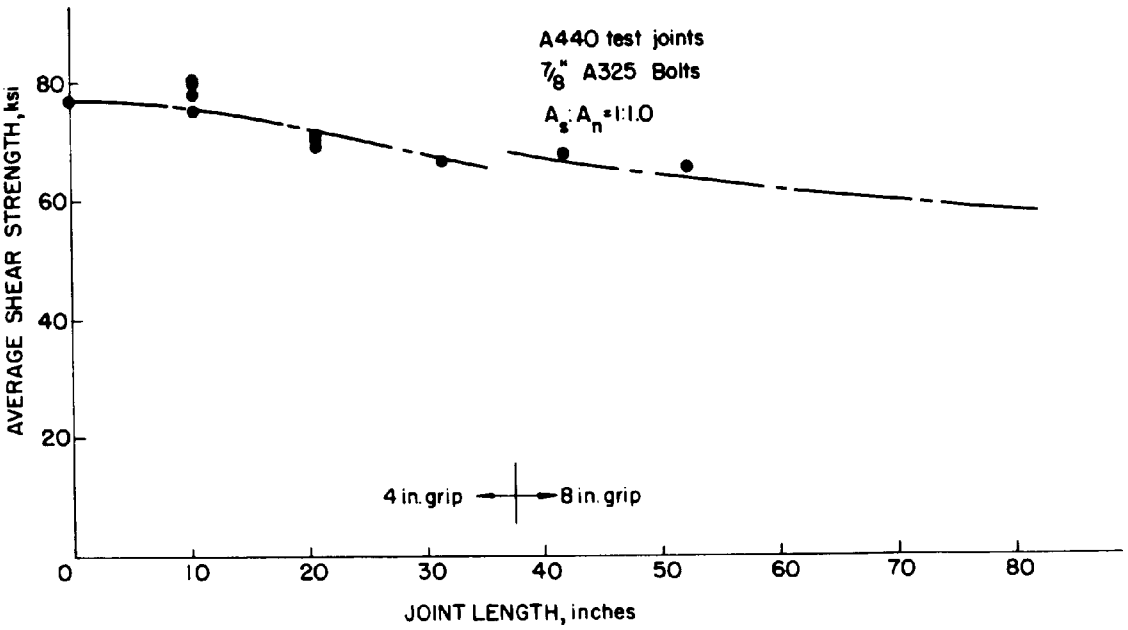

Fig. 50 Comparison of Computed Ultimate Strength with Test Results - A440 Steel

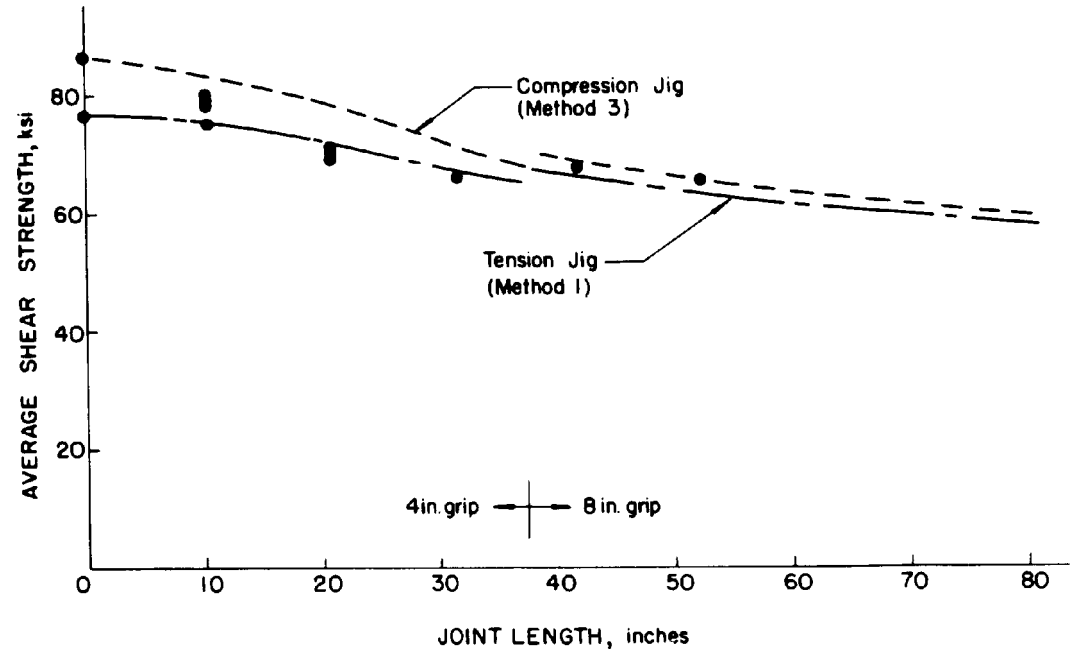

Fig. 51 Comparison of Methods 1 and 3 with Experimental Results

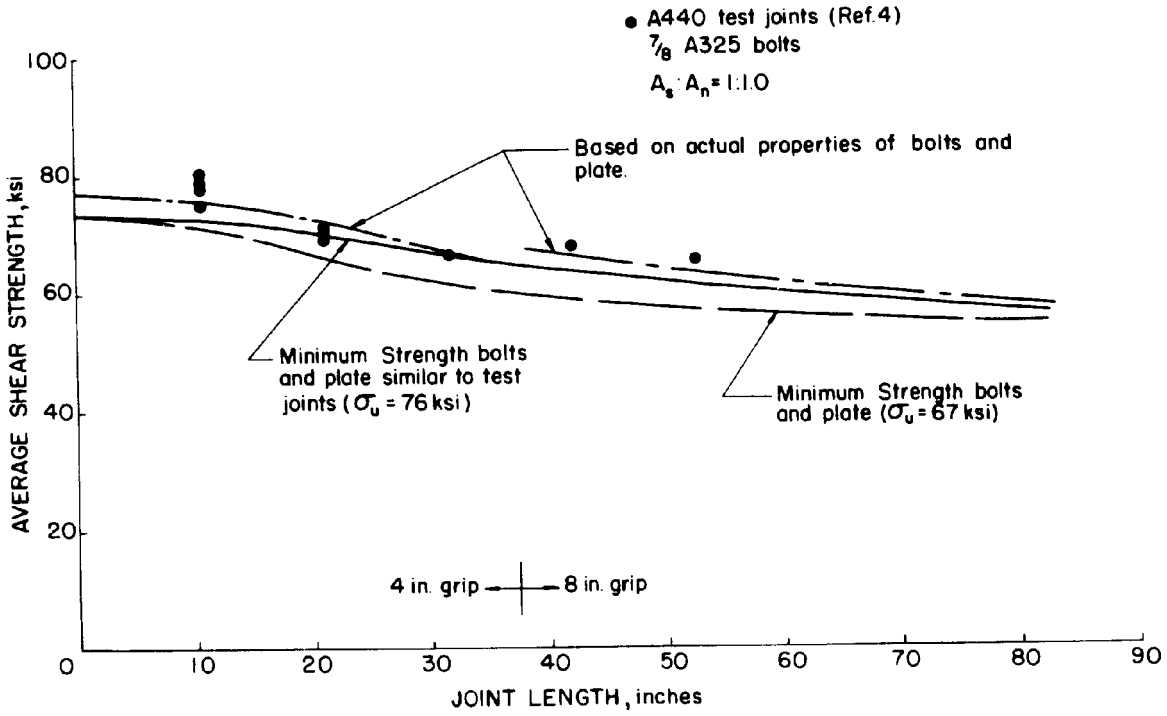

Fig. 52 Influence of Variation in Material Properties on the Ultimate Strength

8. REFERENCES

1. Davis, R. E., Woodruff, G. B. and Davis, H. E.
TENSION TESTS OF LARGE RIVETED JOINTS, Transactions ASCE, Vol. 105, p. 1193, (1940).

2. SPECIFICATIONS FOR ASSEMBLY OF STRUCTURAL JOINTS USING HIGH STRENGTH BOLTS, (1951), Research Council on Riveted and Bolted Structural Joints of the Engineering Foundation.

3. Foreman, R. T. and Rumpf, J. L.
STATIC TENSION TESTS OF COMPACT BOLTED JOINTS, Transactions ASCE, Vol. 126, Part II, p. 228, (1961).

4. Fisher, J. W., Ramseier, P. O. and Beedle, L. S.
TESTS OF A440 STEEL JOINTS FASTENED WITH A325 BOLTS, Publications IABSE, Vol. 23, (1963).

5. Fisher, J. W., and Beedle, L. S.
CRITERIA FOR DESIGNING BOLTED JOINTS (BEARING-TYPE), Fritz Laboratory Report 288.7, Lehigh University, (1963).

6. Bendigo, R. A., Hansen, R. M. and Rumpf, J. L.
LONG BOLTED JOINTS, Journal of the Structural Division, ASCE, Vol. 89, SI6, (1963).

7. Rumpf, J. L.
THE ULTIMATE SIRENGTH OF BOLTED CONNECTIONS, Ph.D. Dissertation, Lehigh University, (1960).

8. Steinhardt, O. and Mohler, K.
VERSUCHE ZUR ANWENDUNG VORGESPANNTER SCHRAUBEN IM STAHLBAU, II Teil, Stahlbau-Verlags-Gmblt., Cologne, (1959).

9. Wallaert, J. J. and Fisher, J. W.
HISTORY OF INTERNAL TENSION IN BOLTS CONNECTING LARGE JOINTS, Fritz Laboratory Report 288.13, Lehigh University (1964).

10. Arnovlevic, I.
INANSPRUNCHNAHME DER ANSCHLUSSNIETEN ELASTISCHER STABE, Zeitschrift fur Architekten und Ingenieure, Vol. 14, Heft, 2, p. 89, (1909).

11. Batho, C.
THE PARTITION OF LOAD IN RIVETED JOINTS, Journal of the Franklin Institute, Vol. 182, p. 553, (1916).

12. Bleich, F.
THEORIE UND BERECHNUNG DER EISERNEN BRUCKER, Julius Springer, Berlin, (1921).

13. Hrennikoff, A.
THE WORK OF RIVETS IN RIVETED JOINTS, Transactions, ASCE, Vol. 99, pp. 437-489, (1934).

14. Vogt, F.
LOAD DISTRIBUTION IN BOLTED OR RIVETED STRUCTURAL JOINTS IN LIGHT-ALLOY STRUCTURES, U.S. NACA Tech. Memo No. 1135, (1947).

15. Francis, A. J.
THE BEHAVIOR OF ALUMINUM ALLOY RIVETED JOINTS, The Aluminum Development Association, Research Report No. 15, London, (1953).

16. DeJonge, A. E. R.
RIVETED JOINTS: A CRITICAL REVIEW OF THE LITERATURE COVERING THEIR DEVELOPMENT, ASME, New York, (1945).

17. Wyly, L. T., Treaner, H. E. and LeRoy, H. E.
DEMONSTRATION TEST OF AN A242 HIGH STRENGTH STEEL SPECIMEN CONNECTED BY A325 and A354 BD BOLTS, AISC Proceedings, (1957).

18. Vasarhelyi, D. D., Benno, S. Y., Madison, R. B., Lu, Z. A. and Vasishth, U. C.
EFFECTS OF FABRICATION TECHNIQUES, Transactions ASCE, Vol. 126, Part II, (1961).

19. Baud, R. V., Wahl, A. M. and Nadai, A.
STRESS DISTRIBUTION OF PLASTIC FLOW IN AN ELASTIC PLATE WITH A CIRCULAR HOLE, Mechanical Engineering, p. 187, (March 1930).

20. Nadai, A.
THEORY OF FLOW AND FRACTURE OF SOLIDS, Vol. 1, 2nd Ed., McGraw-Hill, 1950, p. 299.

21. Hollomon, J. H.
TENSILE DEFORMATION, Transactions, AIME (Iron and Steel Division), Vol. 162, 1945.

22. Homquist, J. L. and Nadai, A.
A THEORETICAL AND EXPERIMENTAL APPROACH TO THE PROBLEM OF COLLAPSE OF DEEP-WELL CASING, American Petroleum Institute (Drilling and Producing Practice), (1939 meeting, Chicago), pp. 392-420.

23. Ramberg, W. and Osgood, W. R.
DESCRIPTION OF STRESS-STRAIN CURVES BY THREE PARAMETERS NACA T.N. 902, 1943.

24. Schutz, F. W.
THE EFFICIENCY OF RIVETED STRUCTURAL JOINTS, Ph.D. Dissertation, University of Illinois, 1952.

25. Munse, W. H. and Chesson, E., Jr.
RIVETED AND BOLTED JOINTS: NET SECTION DESIGN, Journal of the Structural Division, ASCE, Vol. 89, No. ST1, 1963.

26. Schenker, L., Salmon, C. G., and Johnston, B. G.
STRUCTURAL STEEL CONNECTIONS, AFSWP Report No. 352, University of Michigan, June 1954.

27. Coker, E. G.
THE DISTRIBUTION OF STRESS DUE TO A RIVET IN A PLATE, Trans. Inst. of Naval Arch., Vol. 55, p. 207, (1913).

28. Wallaert, J. J.
THE SHEAR STRENGTH OF A325 AND ALLOY STEEL STRUCTURAL BOLTS, MS Thesis, Lehigh University, 1964.

29. Tate, M. B. and Rosenfeld, S. J.
PRELIMINARY INVESTIGATION OF THE LOADS CARRIED BY INDIVIDUAL BOLTS IN BOLTED JOINTS, NACA T.N. 1050, (1946).

30. Hansen, R. M.
THE EFFECT OF FASTENER PITCH IN LONG STRUCTURAL JOINTS, MS Thesis, Lehigh University, 1961.

9. V I T A

John William Fisher was born in Ancell, Missouri, on February 15, 1931. He is the first child of Nevan A. and Nettie M. Fisher. He attended secondary schools in Honolulu, T.H. and Illmo, Missouri, graduating from Illmo-Fornfelt Consolidated High Schoolin 1948. After attending Southeast Missouri State College for one year and Marion College, Marion, Indiana for one semester, he entered the United States Army. Upon release from active duty in December 1953 he entered Washington University, St. Louis, Missouri from which he received the Bachelor of Science degree in Civil Engineering in 1956. At that institution he became a member of the American Society of Civil Engineers and Tau Beta Pi. He was co-recipient of the St. Louis Section, ASCE Student Award and received Final Honors from the engineering faculty.

After being employed during the summer of 1956 by McDonnell Aircraft Corporation, he entered Lehigh University and was employed as a Research Assistant at Fritz Engineering Laboratory until June 1958. At Lehigh University he became an Associate Member of The Society of the Sigma Xi in May 1957. He was awarded the Master of Science degree in June 1958. From July 1958 until August 1961 he was employed by the National Academy of Sciences as Assistant Bridge Research Engineer for the American Association of State Highway Officials Road Test in Ottawa, Illinois.

He returned to Lehigh University in September 1961 as a Research Associate and began work on his doctoral program. He was elected a member

of The Society of the Sigma Xi in April 1962. He has acted as supervisor for the "Large Bolted Connections" Project since returning to Lehigh in 1961.

The author is a Registered Professional Engineer in Illinois. He is the author or co-author of fourteen articles in technical publications of the American Welding Society, Welding Research Council, Highway Research Board, American Society of Civil Engineers, Prestressed Concrete Institute, and the Swiss Society of Civil Engineers.

In September of 1962 he was selected by the National Academy of Science to attend the NATO Advanced Course on the Use of Computers in Civil Engineering held at the Laboratorio Nacional de Engenharia Civil in Lisbon, Portugal.